



HAL
open science

Flavour tagged time-dependent angular analysis of the $B_{\bar{s}} \rightarrow J/\psi\phi$ decay and extraction of $\Delta\Gamma$ and the weak phase $\phi_{\bar{s}}$ in ATLAS

G. Aad, S. Abdel Khalek, A. Bassalat, C. Becot, S. Binet, C. Bourdarios, D. Charfeddine, J.B. de Vivie de Regie, L. Duflot, M. Escalier, et al.

► To cite this version:

G. Aad, S. Abdel Khalek, A. Bassalat, C. Becot, S. Binet, et al.. Flavour tagged time-dependent angular analysis of the $B_{\bar{s}} \rightarrow J/\psi\phi$ decay and extraction of $\Delta\Gamma$ and the weak phase $\phi_{\bar{s}}$ in ATLAS. *Physical Review D*, 2014, 90, pp.052007. 10.1103/PhysRevD.90.052007. in2p3-01022705

HAL Id: in2p3-01022705

<https://in2p3.hal.science/in2p3-01022705v1>

Submitted on 3 Jun 2021

HAL is a multi-disciplinary open access archive for the deposit and dissemination of scientific research documents, whether they are published or not. The documents may come from teaching and research institutions in France or abroad, or from public or private research centers.

L'archive ouverte pluridisciplinaire **HAL**, est destinée au dépôt et à la diffusion de documents scientifiques de niveau recherche, publiés ou non, émanant des établissements d'enseignement et de recherche français ou étrangers, des laboratoires publics ou privés.

Flavor tagged time-dependent angular analysis of the $B_s^0 \rightarrow J/\psi\phi$ decay and extraction of $\Delta\Gamma_s$ and the weak phase ϕ_s in ATLAS

G. Aad *et al.**

(ATLAS Collaboration)

(Received 8 July 2014; published 23 September 2014)

A measurement of the $B_s^0 \rightarrow J/\psi\phi$ decay parameters, updated to include flavor tagging is reported using 4.9 fb^{-1} of integrated luminosity collected by the ATLAS detector from $\sqrt{s} = 7 \text{ TeV}$ pp collisions recorded in 2011 at the LHC. The values measured for the physical parameters are

$$\begin{aligned}\phi_s &= 0.12 \pm 0.25(\text{stat}) \pm 0.05(\text{syst}) \text{ rad} \\ \Delta\Gamma_s &= 0.053 \pm 0.021(\text{stat}) \pm 0.010(\text{syst}) \text{ ps}^{-1} \\ \Gamma_s &= 0.677 \pm 0.007(\text{stat}) \pm 0.004(\text{syst}) \text{ ps}^{-1} \\ |A_{\parallel}(0)|^2 &= 0.220 \pm 0.008(\text{stat}) \pm 0.009(\text{syst}) \\ |A_0(0)|^2 &= 0.529 \pm 0.006(\text{stat}) \pm 0.012(\text{syst}) \\ \delta_{\perp} &= 3.89 \pm 0.47(\text{stat}) \pm 0.11(\text{syst}) \text{ rad}\end{aligned}$$

where the parameter $\Delta\Gamma_s$ is constrained to be positive. The S -wave contribution was measured and found to be compatible with zero. Results for ϕ_s and $\Delta\Gamma_s$ are also presented as 68% and 95% likelihood contours, which show agreement with the Standard Model expectations.

DOI: 10.1103/PhysRevD.90.052007

PACS numbers: 14.40.Nd

I. INTRODUCTION

New phenomena beyond the predictions of the Standard Model (SM) may alter CP violation in B -decays. A channel that is expected to be sensitive to new physics contributions is the decay $B_s^0 \rightarrow J/\psi\phi$. CP violation in the $B_s^0 \rightarrow J/\psi\phi$ decay occurs due to interference between direct decays and decays with $B_s^0 - \bar{B}_s^0$ mixing. The oscillation frequency of B_s^0 meson mixing is characterized by the mass difference Δm_s of the heavy (B_H) and light (B_L) mass eigenstates. The CP violating phase ϕ_s is defined as the weak phase difference between the $B_s^0 - \bar{B}_s^0$ mixing amplitude and the $b \rightarrow c\bar{c}s$ decay amplitude. In the absence of CP violation, the B_H state would correspond to the CP odd state and the B_L to the CP even state. In the SM the phase ϕ_s is small and can be related to Cabibbo-Kobayashi-Maskawa quark mixing matrix elements via the relation $\phi_s \simeq -2\beta_s$, with $\beta_s = \arg[-(V_{ts}V_{tb}^*)/(V_{cs}V_{cb}^*)]$; a value of $\phi_s \simeq -2\beta_s = -0.037 \pm 0.002 \text{ rad}$ [1] is predicted in the SM. Many new physics models predict large ϕ_s values while satisfying all existing constraints, including the precisely measured value of Δm_s [2,3].

Another physical quantity involved in $B_s^0 - \bar{B}_s^0$ mixing is the width difference $\Delta\Gamma_s = \Gamma_L - \Gamma_H$, which is predicted to

be $\Delta\Gamma_s = 0.087 \pm 0.021 \text{ ps}^{-1}$ [4]. Physics beyond the SM is not expected to affect $\Delta\Gamma_s$ as significantly as ϕ_s [5]. Extracting $\Delta\Gamma_s$ from data is nevertheless useful as it allows theoretical predictions to be tested [5].

The decay of the pseudoscalar B_s^0 to the vector-vector final-state $J/\psi\phi$ results in an admixture of CP odd and CP even states, with orbital angular momentum $L = 0, 1$ or 2 . The final states with orbital angular momentum $L = 0$ or 2 are CP even while the state with $L = 1$ is CP odd. Flavor tagging is used to distinguish between the initial B_s^0 and \bar{B}_s^0 states. The CP states are separated statistically using an angular analysis of the final-state particles.

In this paper, an update to the previous measurement [6] with the addition of flavor tagging is presented. Flavor tagging significantly reduces the uncertainty of the measured value of ϕ_s while also allowing a measurement of one of the strong phases. Previous measurements of these quantities have been reported by the D0, CDF and LHCb collaborations [7–9]. The analysis presented here uses 4.9 fb^{-1} of LHC pp data at $\sqrt{s} = 7 \text{ TeV}$ collected by the ATLAS detector in 2011.

II. ATLAS DETECTOR AND MONTE CARLO SIMULATION

The ATLAS experiment [10] is a multipurpose particle physics detector with a forward-backward symmetric cylindrical geometry and near 4π solid angle coverage. The inner tracking detector (ID) consists of a silicon pixel

* Full author list given at the end of the article.

detector, a silicon microstrip detector and a transition radiation tracker. The ID is surrounded by a thin superconducting solenoid providing a 2T axial magnetic field and by a high granularity liquid-argon sampling electromagnetic calorimeter. A steel/scintillator tile calorimeter provides hadronic coverage in the central rapidity range. The end cap and forward regions are instrumented with liquid-argon calorimeters for both electromagnetic and hadronic measurements. The muon spectrometer (MS) surrounds the calorimeters and consists of three large superconducting toroids with eight coils each, a system of tracking chambers, and detectors for triggering.

The muon and tracking systems are of particular importance in the reconstruction of B meson candidates. Only data for which both systems were operating correctly and for which the LHC beams were declared to be stable are used. A muon identified using a combination of MS and ID track parameters is referred to as *combined*. A muon formed by track segments which are not associated with an MS track, but which are matched to ID tracks extrapolated to the MS is referred to as *segment tagged*.

The data were collected during a period of rising instantaneous luminosity, and the trigger conditions varied over this time. The triggers used to select events for this analysis are based on identification of a $J/\psi \rightarrow \mu^+\mu^-$ decay, with either a 4 GeV transverse momentum [11] (p_T) threshold for each muon or an asymmetric configuration that applies a p_T threshold of 4 GeV to one of the muons while accepting a second muon with p_T as low as 2 GeV.

Monte Carlo (MC) simulation is used to study the detector response, estimate backgrounds and model systematic effects. For this study, 12 million MC-simulated $B_s^0 \rightarrow J/\psi\phi$ events were generated using PYTHIA 6 [12] tuned with recent ATLAS data [13]. No p_T cuts were applied at the generator level. Detector responses for these events were simulated using the ATLAS simulation package based on GEANT4 [14,15]. Pileup corresponding to the conditions during data taking was included. To take into account the varying trigger configurations during data taking, the MC events were weighted to have the same trigger composition as the collected collision data. Additional samples of the background decay $B^0 \rightarrow J/\psi K^{0*}$ as well as the more general $bb \rightarrow J/\psi X$ and $pp \rightarrow J/\psi X$ backgrounds were also simulated using PYTHIA.

III. RECONSTRUCTION AND CANDIDATE SELECTION

Events passing the trigger and the data quality selections described in Sec. II are required to pass the following additional criteria: the event must contain at least one reconstructed primary vertex, built from at least four ID tracks, and at least one pair of oppositely charged muon candidates that are reconstructed using information from the MS and the ID [16]. Both combined and segment

tagged muons are used. In this analysis the muon track parameters are taken from the ID measurement alone, since the precision of the measured track parameters for muons in the p_T range of interest for this analysis is dominated by the ID track reconstruction. The pairs of muon tracks are refitted to a common vertex and accepted for further consideration if the fit results in $\chi^2/\text{d.o.f.} < 10$. The invariant mass of the muon pair is calculated from the refitted track parameters. To account for varying mass resolution, the J/ψ candidates are divided into three subsets according to the pseudorapidity η of the muons. A maximum likelihood fit is used to extract the J/ψ mass and the corresponding resolution for these three subsets. When both muons have $|\eta| < 1.05$, the dimuon invariant mass must fall in the range (2.959–3.229) GeV to be accepted as a J/ψ candidate. When one muon has $1.05 < |\eta| < 2.5$ and the other muon $|\eta| < 1.05$, the corresponding signal region is (2.913–3.273) GeV. For the third subset, where both muons have $1.05 < |\eta| < 2.5$, the signal region is (2.852–3.332) GeV. In each case the signal region is defined so as to retain 99.8% of the J/ψ candidates identified in the fits.

The candidates for $\phi \rightarrow K^+K^-$ are reconstructed from all pairs of oppositely charged particles with $p_T > 0.5$ GeV and $|\eta| < 2.5$ that are not identified as muons. Candidates for $B_s^0 \rightarrow J/\psi(\mu^+\mu^-)\phi(K^+K^-)$ are sought by fitting the tracks for each combination of $J/\psi \rightarrow \mu^+\mu^-$ and $\phi \rightarrow K^+K^-$ to a common vertex. Each of the four tracks is required to have at least one hit in the pixel detector and at least four hits in the silicon microstrip detector. The fit is further constrained by fixing the invariant mass calculated from the two muon tracks to the J/ψ mass [17]. These quadruplets of tracks are accepted for further analysis if the vertex fit has a $\chi^2/\text{d.o.f.} < 3$, the fitted p_T of each track from $\phi \rightarrow K^+K^-$ is greater than 1 GeV and the invariant mass of the track pairs (under the assumption that they are kaons) falls within the interval $1.0085 \text{ GeV} < m(K^+K^-) < 1.0305 \text{ GeV}$. If there is more than one accepted candidate in the event, the candidate with the lowest $\chi^2/\text{d.o.f.}$ is selected. In total 131513 B_s^0 candidates are collected within a mass range of $5.15 < m(B_s^0) < 5.65 \text{ GeV}$.

For each B_s^0 meson candidate the proper decay time t is estimated by the expression

$$t = \frac{L_{xy} M_B}{p_{T_B}},$$

where p_{T_B} is the reconstructed transverse momentum of the B_s^0 meson candidate and M_B denotes the world average mass value [17] of the B_s^0 meson. The transverse decay length, L_{xy} , is the displacement in the transverse plane of the B_s^0 meson decay vertex with respect to the primary vertex, projected onto the direction of the B_s^0 transverse momentum. The position of the primary vertex used to

calculate this quantity is refitted following the removal of the tracks used to reconstruct the B_s^0 meson candidate.

For the selected events the average number of pileup interactions is 5.6, necessitating a choice of the best candidate for the primary vertex at which the B_s^0 meson is produced. The variable used is the three-dimensional impact parameter d_0 , which is calculated as the distance between the line extrapolated from the reconstructed B_s^0 meson vertex in the direction of the B_s^0 momentum and each primary vertex candidate. The chosen primary vertex is the one with the smallest d_0 . Using MC simulation it is shown that the fraction of B_s^0 candidates which are assigned the wrong primary vertex is less than 1% and that the corresponding effect on the final results is negligible. No B_s^0 meson decay time cut is applied in the analysis.

IV. FLAVOR TAGGING

The determination of the initial flavor of neutral B -mesons can be inferred using information from the B -meson that is typically produced from the other b -quark in the event [18]. This is referred to as the opposite-side tagging (OST).

To study and calibrate the OST methods, events containing the decays of $B^\pm \rightarrow J/\psi K^\pm$ can be used, where flavor of the B -meson at production is provided by the kaon charge. Events from the entire 2011 run period satisfying the same data quality selections as described in Sec. II are used.

A. $B^\pm \rightarrow J/\psi K^\pm$ event selection

To be selected for use in the calibration analysis, events must satisfy a trigger condition requiring two oppositely charged muons within an invariant mass range around the nominal J/ψ mass. Candidate $B^\pm \rightarrow J/\psi K^\pm$ decays are identified using two oppositely charged combined muons forming a good vertex using information supplied by the inner detector. Each muon is required to have a transverse momentum of at least 4 GeV and pseudorapidity within $|\eta| < 2.5$. The invariant mass of the dimuon candidate is required to satisfy $2.8 < m(\mu^+\mu^-) < 3.4$ GeV. To form the B candidate an additional track with the charged kaon mass hypothesis, $p_T > 1$ GeV and $|\eta| < 2.5$ is combined with the dimuon candidate, and a vertex fit is performed with the mass of the dimuon pair constrained to the known value of the J/ψ mass. To reduce the prompt component of the combinatorial background, the requirement $L_{xy} > 0.1$ mm is applied to the B candidate. The choice of primary vertex is determined using the same procedure as done for the B_s^0 candidates.

To study the distributions corresponding to the signal processes with the background component removed, a sideband subtraction method is defined. Events are separated into five equal regions of B candidate rapidity from 0–2.5 and three mass regions. The mass regions are defined

as a signal region around the fitted peak signal mass position $\mu \pm 2\sigma$, and the sidebands are $[\mu - 5\sigma, \mu - 3\sigma]$ and $[\mu + 3\sigma, \mu + 5\sigma]$, where μ and σ are the mean and width of the Gaussian function describing the B signal mass, for each rapidity region. Individual binned extended maximum likelihood fits to the invariant mass distribution are performed in each region of rapidity.

The background is modelled by an exponential to describe combinatorial background and a hyperbolic tangent function to parametrize the low-mass contribution from incorrectly or partially reconstructed B decays. A Gaussian function is used to model the $B^\pm \rightarrow J/\psi \pi^\pm$ contribution. The contributions of noncombinatorial backgrounds are found to have a negligible effect in the tagging procedure. Figure 1 shows the invariant mass distribution of B candidates for all rapidity regions overlaid with the fit result for the combined data.

B. Tagging methods

Several methods are available to infer the flavor of the opposite-side b -quark, with varying efficiencies and discriminating powers. The measured charge of a muon from the semileptonic decay of the B meson provides strong separation power; however, the $b \rightarrow \mu$ transitions are diluted through neutral B meson oscillations, as well as by cascade decays $b \rightarrow c \rightarrow \mu$ which can alter the sign of the muon relative to the one from direct semileptonic decays $b \rightarrow \mu$. The separation power of tagging muons can be enhanced by considering a weighted sum of the charge of the tracks in a cone around the muon. If no muon is present, a weighted sum of the charge of tracks associated with the opposite-side

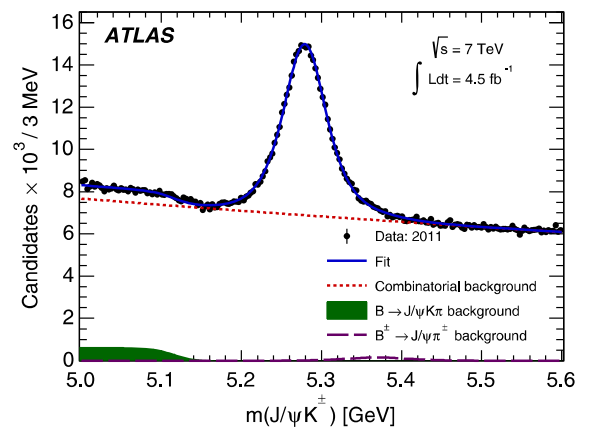


FIG. 1 (color online). The invariant mass distribution for $B^\pm \rightarrow J/\psi K^\pm$ candidates. Included in this plot are all events passing the selection criteria. The data are shown by points, and the overall result of the fit is given by the blue curve. The combinatorial background component is given by the red dotted line, partially reconstructed B decays by the green shaded area, and decays of $B^\pm \rightarrow J/\psi \pi^\pm$, where the pion is misassigned a kaon mass by a purple dashed line.

B meson decay will provide some separation. The tagging methods are described in detail below.

For muon-based tagging, an additional muon is required in the event, with $p_T > 2.5$ GeV, $|\eta| < 2.5$ and with $|\Delta z| < 5$ mm from the primary vertex. Muons are classified according to their reconstruction class, combined or segment tagged and subsequently treated as distinct tagging methods. In the case of multiple muons, the muon with highest transverse momentum is selected.

A *muon cone charge* is defined as

$$Q_\mu = \frac{\sum_i^{N_{\text{tracks}}} q^i \cdot (p_T^i)^\kappa}{\sum_i^{N_{\text{tracks}}} (p_T^i)^\kappa},$$

where q is the charge of the track, $\kappa = 1.1$ and the sum is performed over the reconstructed ID tracks within a cone size of $\Delta R = 0.5$ [19] around the muon direction and the muon track is included as well. The reconstructed ID tracks must have a $p_T > 0.5$ GeV and $|\eta| < 2.5$. The value of the parameter κ was determined while optimizing the tagging performance. Tracks associated with the signal decay are explicitly excluded from the sum. In Fig. 2 the

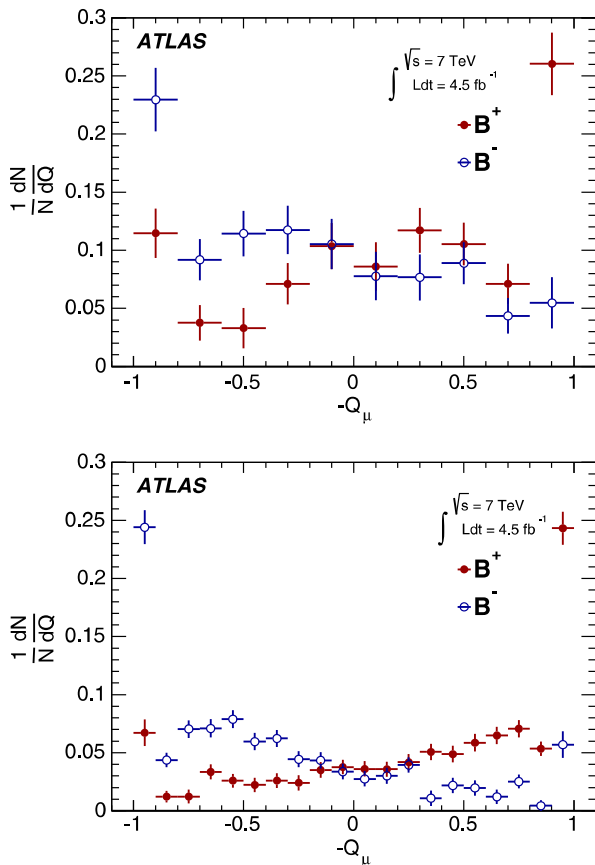


FIG. 2 (color online). The opposite-side muon cone charge distribution for B^\pm signal candidates for segment tagged (top) and combined (bottom) muons.

opposite-side muon cone charge distributions are shown for candidates from B^\pm signal decays. In the absence of a muon, a b -tagged jet [20] is required in the event, which is seeded from calorimeter clusters, with minimum energy threshold of 10 GeV, and where a minimum b -tag weight requirement of at least -0.5 is applied. The jet tracks are required to be associated with the same primary vertex as the signal decay, excluding those from the signal candidate. Jets within a cone of $\Delta R < 0.5$ of the signal momentum axis are excluded. The jet is reconstructed using the anti- k_r algorithm with a cone size of 0.6. In the case of multiple jets, the jet with the highest value of the b -tag weight is used.

A *jet charge* is defined as

$$Q_{\text{jet}} = \frac{\sum_i^{N_{\text{tracks}}} q^i \cdot (p_T^i)^\kappa}{\sum_i^{N_{\text{tracks}}} (p_T^i)^\kappa},$$

where $\kappa = 1.1$, and the sum is over the tracks associated with the jet, using the method described in Ref. [21]. Figure 3 shows the distribution of charges for opposite-side jet charge from B^\pm signal candidate events.

The efficiency ϵ of an individual tagger is defined as the ratio of the number of tagged events to the total number of candidates. A probability that a specific event has a signal decay containing a \bar{b} -quark given the value of the discriminating variable $P(B|Q)$ is constructed from the calibration samples for each of the B^+ and B^- samples, defining $P(Q|B^+)$ and $P(Q|B^-)$ respectively. The probability to tag a signal event as containing a \bar{b} -quark is therefore $P(B|Q) = P(Q|B^+) / (P(Q|B^+) + P(Q|B^-))$ and $P(\bar{B}|Q) = 1 - P(B|Q)$. The tagging power is defined as $\epsilon \mathcal{D}^2 = \sum_i \epsilon_i \cdot (2P_i(B|Q_i) - 1)^2$, where the sum is over the bins of the probability distribution as a function of the charge variable and ϵ_i is the number of tagged events in each bin divided by the total number of candidates. An

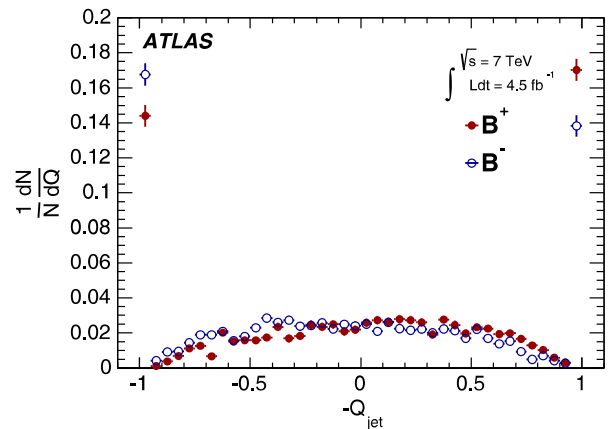


FIG. 3 (color online). Jet-charge distribution for B^\pm signal candidates.

TABLE I. Summary of tagging performance for the different tagging methods described in the text. Uncertainties shown are statistical only. The efficiency and tagging power are each determined by summing over the individual bins of the charge distribution. The effective dilution is obtained from the measured efficiency and tagging power. The uncertainties are determined by combining the appropriate uncertainties on the individual bins of each charge distribution.

| Tagger | Efficiency (%) | Dilution (%) | Tagging power (%) |
|----------------------|-----------------|------------------|-------------------|
| Combined μ | 3.37 ± 0.04 | 50.6 ± 0.5 | 0.86 ± 0.04 |
| Segment tagged μ | 1.08 ± 0.02 | 36.7 ± 0.7 | 0.15 ± 0.02 |
| Jet charge | 27.7 ± 0.1 | 12.68 ± 0.06 | 0.45 ± 0.03 |
| Total | 32.1 ± 0.1 | 21.3 ± 0.08 | 1.45 ± 0.05 |

effective dilution \mathcal{D} is calculated from the tagging power and the efficiency.

The combination of the tagging methods is applied according to the hierarchy of performance, based on the dilution of the tagging method. The single best performing tagging measurement is taken, according to the order: combined muon cone charge, segment tagged muon cone charge, and jet charge. If it is not possible to provide a tagging response for the event, then a probability of 0.5 is assigned. A summary of the tagging performance is given in Table 1.

V. MAXIMUM LIKELIHOOD FIT

An unbinned maximum likelihood fit is performed on the selected events to extract the parameters of the $B_s^0 \rightarrow J/\psi(\mu^+\mu^-)\phi(K^+K^-)$ decay. The fit uses information about the reconstructed mass m and its uncertainty σ_m , the measured proper decay time t and its uncertainty σ_t , the tag probability, and the transversity angles Ω of each $B_s^0 \rightarrow J/\psi\phi$ decay candidate. There are three transversity angles; $\Omega = (\theta_T, \psi_T, \phi_T)$, and these are defined in Sec. VA.

The likelihood function is defined as a combination of the signal and background probability density functions as follows:

$$\begin{aligned} \ln \mathcal{L} = & \sum_{i=1}^N \{w_i \cdot \ln(f_s \cdot \mathcal{F}_s(m_i, t_i, \Omega_i, P(B|Q))) \\ & + f_s \cdot f_{B^0} \cdot \mathcal{F}_{B^0}(m_i, t_i, \Omega_i, P(B|Q)) \\ & + (1 - f_s \cdot (1 + f_{B^0})) \cdot \mathcal{F}_{\text{bkg}}(m_i, t_i, \Omega_i, P(B|Q))\}, \end{aligned} \quad (1)$$

where N is the number of selected candidates, w_i is a weighting factor to account for the trigger efficiency, f_s is the fraction of signal candidates and f_{B^0} is the fraction of B^0 ($B^0 \rightarrow J/\psi K^{0*}$ and $B^0 \rightarrow J/\psi K^\pm \pi^\mp$) mesons misidentified as B_s^0 candidates calculated relative to the number of

signal events; this parameter is fixed in the likelihood fit. The mass m_i , the proper decay time t_i and the decay angles Ω_i are the values measured from the data for each event i . \mathcal{F}_s , \mathcal{F}_{B^0} and \mathcal{F}_{bkg} are the probability density functions (PDF) modelling the signal, the specific B^0 background and the other background distributions, respectively. A detailed description of the signal PDF terms in Eq. (1) is given in Sec. VA. The two background functions are, with the exception of new terms dependent on $P(B|Q)$ which are explained in Sec. VB, unchanged from the previous analysis [6]. They are each described by the product of eight terms which describe the distribution of each measured parameter. With the exception of the lifetime and its uncertainty the background parameters are assumed uncorrelated.

A. Signal PDF

The PDF describing the signal events, \mathcal{F}_s , has the form of a product of PDFs for each quantity measured from the data:

$$\begin{aligned} \mathcal{F}_s(m_i, t_i, \Omega_i, P(B|Q)) = & P_s(m_i, \sigma_{m_i}) \cdot P_s(\sigma_{m_i}) \\ & \cdot P_s(\Omega_i, t_i, P(B|Q), \sigma_{t_i}) \cdot P_s(\sigma_{t_i}) \\ & \cdot P_s(P(B|Q)) \cdot A(\Omega_i, p_{Ti}) \cdot P_s(p_{Ti}). \end{aligned}$$

The terms $P_s(m_i, \sigma_{m_i})$, $P_s(\Omega_i, t_i, P(B|Q), \sigma_{t_i})$ and $A(\Omega_i, p_{Ti})$ are explained in the current section. The tagging probability term $P_s(P(B|Q))$ is described in Sec. VB. The remaining probability terms $P_s(\sigma_{m_i})$, $P_s(\sigma_{t_i})$ and $P_s(p_{Ti})$ are described by Gamma functions. They are unchanged from the previous analysis and explained in detail in Ref. [6]. Ignoring detector effects, the joint distribution for the decay time t and the transversity angles Ω for the $B_s^0 \rightarrow J/\psi(\mu^+\mu^-)\phi(K^+K^-)$ decay is given by the differential decay rate [22]:

$$\frac{d^4\Gamma}{dt d\Omega} = \sum_{k=1}^{10} \mathcal{O}^{(k)}(t) g^{(k)}(\theta_T, \psi_T, \phi_T),$$

where $\mathcal{O}^{(k)}(t)$ are the time-dependent amplitudes and $g^{(k)}(\theta_T, \psi_T, \phi_T)$ are the angular functions, given in Table II. The formulas for the time-dependent amplitudes have the same structure for B_s^0 and \bar{B}_s^0 but with a sign reversal in the terms containing Δm_s . The addition of flavor tagging to the analysis means that these terms no longer cancel, so there are more terms in the fit that contain ϕ_s . In addition to this, the strong phase variable δ_\perp becomes accessible, and one of the symmetries in the untagged fit is removed. $A_\perp(t)$ describes a CP odd final-state configuration while both $A_0(t)$ and $A_\parallel(t)$ correspond to CP even final-state configurations. $A_S(t)$ describes the contribution of the CP odd nonresonant $B_s^0 \rightarrow J/\psi K^+ K^-$ S -wave state

TABLE II. Table showing the ten time-dependent amplitudes, $\mathcal{O}^{(k)}(t)$ and the functions of the transversity angles $g^{(k)}(\theta_T, \psi_T, \phi_T)$. The amplitudes $|A_0(0)|^2$ and $|A_{\parallel}(0)|^2$ are for the CP even components of the $B_s^0 \rightarrow J/\psi\phi$ decay, and $|A_{\perp}(0)|^2$ is the CP odd amplitude; they have corresponding strong phases δ_0 , δ_{\parallel} and δ_{\perp} , and by convention δ_0 is set to be zero. The S -wave amplitude $|A_S(0)|^2$ gives the fraction of $B_s^0 \rightarrow J/\psi K^+ K^- (f_0)$ and has a related strong phase δ_S . The \pm and \mp terms denote two cases: the upper sign describes the decay of a meson that was initially a B_s^0 , while the lower sign describes the decays of a meson that was initially \bar{B}_s^0 .

| k | $\mathcal{O}^{(k)}(t)$ | $g^{(k)}(\theta_T, \psi_T, \phi_T)$ |
|-----|--|--|
| 1 | $\frac{1}{2} A_0(0) ^2[(1 + \cos\phi_s)e^{-\Gamma_L^{(s)}t} + (1 - \cos\phi_s)e^{-\Gamma_H^{(s)}t} \pm 2e^{-\Gamma_s t} \sin(\Delta m_s t) \sin\phi_s]$ | $2\cos^2\psi_T(1 - \sin^2\theta_T \cos^2\phi_T)$ |
| 2 | $\frac{1}{2} A_{\parallel}(0) ^2[(1 + \cos\phi_s)e^{-\Gamma_L^{(s)}t} + (1 - \cos\phi_s)e^{-\Gamma_H^{(s)}t} \pm 2e^{-\Gamma_s t} \sin(\Delta m_s t) \sin\phi_s]$ | $\sin^2\psi_T(1 - \sin^2\theta_T \sin^2\phi_T)$ |
| 3 | $\frac{1}{2} A_{\perp}(0) ^2[(1 - \cos\phi_s)e^{-\Gamma_L^{(s)}t} + (1 + \cos\phi_s)e^{-\Gamma_H^{(s)}t} \mp 2e^{-\Gamma_s t} \sin(\Delta m_s t) \sin\phi_s]$ | $\sin^2\psi_T \sin^2\theta_T$ |
| 4 | $\frac{1}{2} A_0(0) A_{\parallel}(0) \cos\delta_{\parallel}$ $[(1 + \cos\phi_s)e^{-\Gamma_L^{(s)}t} + (1 - \cos\phi_s)e^{-\Gamma_H^{(s)}t} \pm 2e^{-\Gamma_s t} \sin(\Delta m_s t) \sin\phi_s]$ | $-\frac{1}{\sqrt{2}}\sin 2\psi_T \sin^2\theta_T \sin 2\phi_T$ |
| 5 | $ A_{\parallel}(0) A_{\perp}(0) [\frac{1}{2}(e^{-\Gamma_L^{(s)}t} - e^{-\Gamma_H^{(s)}t})\cos(\delta_{\perp} - \delta_{\parallel})\sin\phi_s$ $\pm e^{-\Gamma_s t}(\sin(\delta_{\perp} - \delta_{\parallel})\cos(\Delta m_s t) - \cos(\delta_{\perp} - \delta_{\parallel})\cos\phi_s \sin(\Delta m_s t))]$ | $\sin^2\psi_T \sin 2\theta_T \sin\phi_T$ |
| 6 | $ A_0(0) A_{\perp}(0) [\frac{1}{2}(e^{-\Gamma_L^{(s)}t} - e^{-\Gamma_H^{(s)}t})\cos\delta_{\perp}\sin\phi_s$ $\pm e^{-\Gamma_s t}(\sin\delta_{\perp}\cos(\Delta m_s t) - \cos\delta_{\perp}\cos\phi_s \sin(\Delta m_s t))]$ | $\frac{1}{\sqrt{2}}\sin 2\psi_T \sin 2\theta_T \cos\phi_T$ |
| 7 | $\frac{1}{2} A_S(0) ^2[(1 - \cos\phi_s)e^{-\Gamma_L^{(s)}t} + (1 + \cos\phi_s)e^{-\Gamma_H^{(s)}t} \mp 2e^{-\Gamma_s t} \sin(\Delta m_s t) \sin\phi_s]$ | $\frac{2}{3}(1 - \sin^2\theta_T \cos^2\phi_T)$ |
| 8 | $ A_S(0) A_{\parallel}(0) [\frac{1}{2}(e^{-\Gamma_L^{(s)}t} - e^{-\Gamma_H^{(s)}t})\sin(\delta_{\parallel} - \delta_S)\sin\phi_s$ $\pm e^{-\Gamma_s t}(\cos(\delta_{\parallel} - \delta_S)\cos(\Delta m_s t) - \sin(\delta_{\parallel} - \delta_S)\cos\phi_s \sin(\Delta m_s t))]$ | $\frac{1}{3}\sqrt{6}\sin\psi_T \sin^2\theta_T \sin 2\phi_T$ |
| 9 | $\frac{1}{2} A_S(0) A_{\perp}(0) \sin(\delta_{\perp} - \delta_S)$ $[(1 - \cos\phi_s)e^{-\Gamma_L^{(s)}t} + (1 + \cos\phi_s)e^{-\Gamma_H^{(s)}t} \mp 2e^{-\Gamma_s t} \sin(\Delta m_s t) \sin\phi_s]$ | $\frac{1}{3}\sqrt{6}\sin\psi_T \sin 2\theta_T \cos\phi_T$ |
| 10 | $ A_0(0) A_S(0) [\frac{1}{2}(e^{-\Gamma_H^{(s)}t} - e^{-\Gamma_L^{(s)}t})\sin\delta_S \sin\phi_s$ $\pm e^{-\Gamma_s t}(\cos\delta_S \cos(\Delta m_s t) + \sin\delta_S \cos\phi_s \sin(\Delta m_s t))]$ | $\frac{4}{3}\sqrt{3}\cos\psi_T(1 - \sin^2\theta_T \cos^2\phi_T)$ |

as well as the $B_s^0 \rightarrow J/\psi f_0$ decays. The corresponding amplitudes are given in the last four lines of Table II ($k = 7-10$) and follow the convention used in the previous analysis [23]. The likelihood is independent of the K^+K^- mass distribution.

The equations are normalized, such that the squares of the amplitudes sum to unity; three of the four amplitudes are fit parameters, and $|A_{\perp}(0)|^2$ is determined according to this constraint.

The angles $(\theta_T, \psi_T, \phi_T)$ are defined in the rest frames of the final-state particles. The x axis is determined by the direction of the ϕ meson in the J/ψ rest frame, and the K^+K^- system defines the x - y plane, where $p_y(K^+) > 0$. The three angles are defined as follows:

- (i) θ_T , the angle between $\vec{p}(\mu^+)$ and the normal to the x - y plane, in the J/ψ meson rest frame.
- (ii) ϕ_T , the angle between the x axis and $\vec{p}_{xy}(\mu^+)$, the projection of the μ^+ momentum in the x - y plane, in the J/ψ meson rest frame.
- (iii) ψ_T , the angle between $\vec{p}(K^+)$ and $-\vec{p}(J/\psi)$ in the ϕ meson rest frame.

The signal PDF, $P_s(\Omega, t, P(B|Q), \sigma_t)$, needs to take into account lifetime resolution, so each time element in Table II is smeared with a Gaussian function. This smearing is done

numerically on an event-by-event basis where the width of the Gaussian function is the proper decay time uncertainty, measured for each event, multiplied by a scale factor to account for any mismeasurements.

The angular sculpting of the detector and kinematic cuts on the angular distributions are included in the likelihood function through $A(\Omega_i, p_{Ti})$. This is calculated using a four-dimensional binned acceptance method, applying an event-by-event efficiency according to the transversity angles $(\theta_T, \psi_T, \phi_T)$ and the p_T of the candidate. The p_T binning is necessary, because the angular sculpting is influenced by the p_T of the B_s^0 . The acceptance was calculated from the $B_s^0 \rightarrow J/\psi\phi$ MC events. In the likelihood function, the acceptance is treated as an angular sculpting PDF, which is multiplied with the time- and angular-dependent PDF describing the $B_s^0 \rightarrow J/\psi(\mu^+\mu^-)\phi(K^+K^-)$ decays. As both the acceptance and time-angular decay PDFs depend on the transversity angles they must be normalized together. This normalization is done numerically during the likelihood fit.

The signal mass function, $P_s(m)$, is modelled using a single Gaussian function smeared with an event-by-event mass resolution. The PDF is normalized over the range $5.15 < m(B_s^0) < 5.65$ GeV.

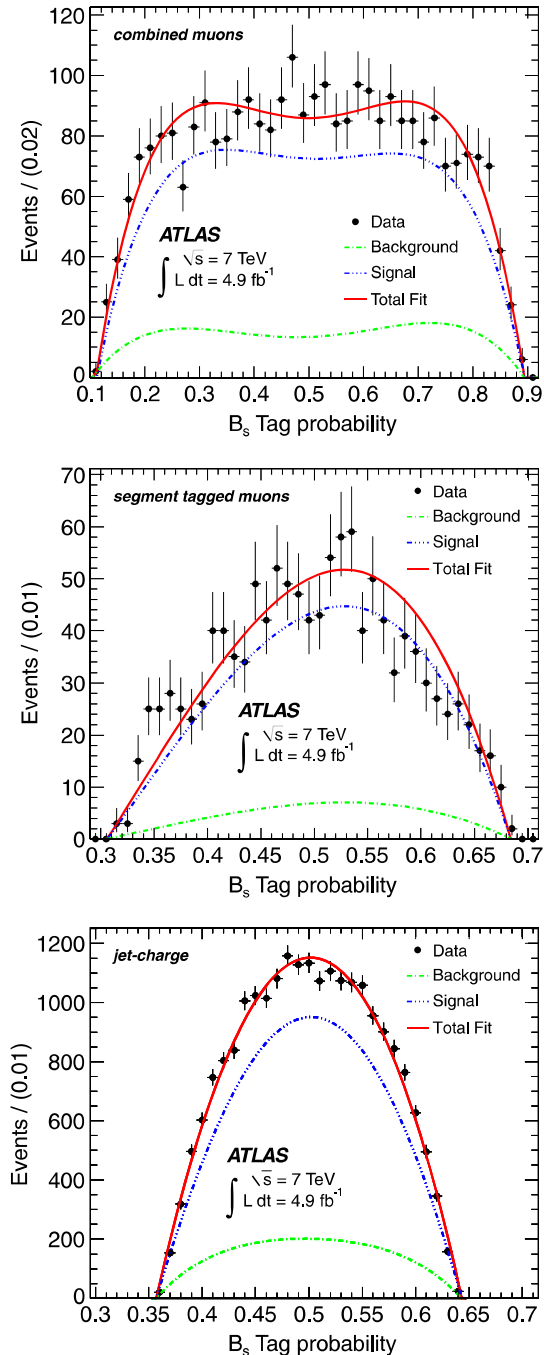


FIG. 4 (color online). The B_s^0 -tag probability distribution for the events tagged with combined muons (top), segment tagged muons (middle) and jet charge (bottom). Black dots are data after removing spikes, blue is the fit to the sidebands, green is to the signal, and red is a sum of both fits.

B. Using tag information in the fit

The tag probability for each B_s^0 candidate is determined from a weighted sum of charged-particle tracks in a cone, as described in Sec. IV. The tag probability is obtained

from this tag charge using the calibrations measured in the $B^\pm \rightarrow J/\psi K^\pm$ data. For the case where there is only one track, the cone charge can only be ± 1 . This leads to a tag probability distribution with continuous and discrete parts (spikes), which are estimated separately. The distributions of tag probabilities for the signal and background are also different, and since the background cannot be factorized out, extra PDF terms are included to account for this difference. For each event with a given B_s^0 tag probability $P(B|Q)$, a relative PDF factor, $P_{S/B}(P(B|Q))$, that this is a signal or a background event is calculated using the parametrizations of the continuous parts, shown in Fig. 4. In the case of the spikes the relative PDF factor is calculated as given in Table III.

To describe the continuous parts, the sidebands are parametrized first. Sidebands are selected according to B_s^0 mass, i.e. $m(B_s^0) < 5.317 \text{ GeV}$ or $m(B_s^0) > 5.417 \text{ GeV}$. In the fit the same function as for the sidebands is used to describe events in the signal region: background parameters are fixed to the values obtained in sidebands while signal parameters are free in this step. The ratio of background to signal (obtained from simultaneous mass–lifetime fit) is fixed as well. The function describing tagging using combined muons has the form of a fourth-order Chebychev polynomial. A third-order polynomial is used for the segment tagged muons’ tagging algorithm. A fourth-order Chebychev polynomial is also applied for the jet charge tagging algorithm. In all three cases unbinned maximum likelihood fits are used. Results of fits projected on histograms are shown in Fig. 4.

The spikes have their origin in tagging objects formed from a single track, providing a tag charge of exactly $+1$ or -1 . When a background candidate is formed from a random combination of a J/ψ and a pair of tracks, the positive and negative charges are equally probable. However, some of the background events are formed of partially reconstructed B hadrons, and in these cases tag charges of $+1$ or -1 are not equally probable. For signal events the tag charges are obviously not symmetric. The fractions f_{+1} and f_{-1} of events tagged with charges of $+1$ and -1 are derived separately for signal and background. The remaining $(1 - f_{+1} - f_{-1})$ is the fraction of events in the continuous region. The fractions f_{+1} and f_{-1} are determined using the same B_s^0 mass sidebands and signal regions as in case of continuous parts. Table III summarizes the obtained relative probabilities between tag charges $+1$ and -1 for signal and background events and for all tag methods.

Similarly, the sideband subtraction method is also used to determine, for signal and background events, the relative fraction of each tagging method. The results are summarized in Table IV.

If the tag-probability PDFs were ignored in the likelihood fit, equivalent to assuming identical signal and background behavior, the impact on the fit result would

TABLE III. Table summarizing the obtained relative probabilities between tag charges +1 and -1 for signal and background events for the different tagging methods. Only statistical errors are quoted. The asymmetry in the signal combined-muon tagging method has no impact on the results as it affects only 1% of the signal events (in addition to the negligible effect of the tag-probability distributions themselves).

| Tag method | Signal | | Background | |
|-------------------|-------------------|-------------------|-------------------|-------------------|
| | f_{+1} | f_{-1} | f_{+1} | f_{-1} |
| Combined μ | 0.106 ± 0.019 | 0.187 ± 0.022 | 0.098 ± 0.006 | 0.108 ± 0.006 |
| Segment tag μ | 0.152 ± 0.043 | 0.153 ± 0.043 | 0.098 ± 0.009 | 0.095 ± 0.008 |
| Jet charge | 0.167 ± 0.010 | 0.164 ± 0.010 | 0.176 ± 0.003 | 0.180 ± 0.003 |

TABLE IV. Table summarizing the relative population of the tagging methods in the background and signal events. Only statistical errors are quoted.

| Tag method | Signal | Background |
|-------------------|---------------------|---------------------|
| Combined μ | 0.0372 ± 0.0023 | 0.0272 ± 0.0005 |
| Segment tag μ | 0.0111 ± 0.0014 | 0.0121 ± 0.0003 |
| Jet charge | 0.277 ± 0.007 | 0.254 ± 0.002 |
| Untagged | 0.675 ± 0.011 | 0.707 ± 0.003 |

TABLE V. Fitted values for the physical parameters with their statistical and systematic uncertainties. For the parameters δ_{\parallel} and $\delta_{\perp} - \delta_S$ a 68% confidence level interval is given. The reason for this is described in Sec. VIII.

| Parameter | Value | Statistical uncertainty | Systematic uncertainty |
|--------------------------------|--------------|-------------------------|------------------------|
| ϕ_s [rad] | 0.12 | 0.25 | 0.05 |
| $\Delta\Gamma_s$ [ps $^{-1}$] | 0.053 | 0.021 | 0.010 |
| Γ_s [ps $^{-1}$] | 0.677 | 0.007 | 0.004 |
| $ A_{\parallel}(0) ^2$ | 0.220 | 0.008 | 0.009 |
| $ A_0(0) ^2$ | 0.529 | 0.006 | 0.012 |
| $ A_S(0) ^2$ | 0.024 | 0.014 | 0.028 |
| δ_{\perp} | 3.89 | 0.47 | 0.11 |
| δ_{\parallel} | [3.04, 3.23] | | 0.09 |
| $\delta_{\perp} - \delta_S$ | [3.02, 3.25] | | 0.04 |

TABLE VI. Correlations between the physics parameters. The physics parameters are, in general, uncorrelated to the remaining nuisance parameters in the fit. There are a few exceptions, but no correlation is greater than 0.12.

| | ϕ_s | $\Delta\Gamma$ | Γ_s | $ A_{\parallel}(0) ^2$ | $ A_0(0) ^2$ | $ A_S(0) ^2$ | δ_{\parallel} | δ_{\perp} | $\delta_{\perp} - \delta_S$ |
|-----------------------------|----------|----------------|------------|------------------------|--------------|--------------|----------------------|------------------|-----------------------------|
| ϕ_s | 1.000 | 0.107 | 0.026 | 0.010 | 0.002 | 0.029 | 0.021 | -0.043 | -0.003 |
| $\Delta\Gamma$ | | 1.000 | -0.617 | 0.105 | 0.103 | 0.069 | 0.006 | -0.017 | 0.001 |
| Γ_s | | | 1.000 | -0.093 | -0.063 | 0.034 | -0.003 | 0.001 | -0.009 |
| $ A_{\parallel}(0) ^2$ | | | | 1.000 | -0.316 | 0.077 | 0.008 | 0.005 | -0.010 |
| $ A_0(0) ^2$ | | | | | 1.000 | 0.283 | -0.003 | -0.016 | -0.025 |
| $ A_S(0) ^2$ | | | | | | 1.000 | -0.011 | -0.054 | -0.098 |
| δ_{\parallel} | | | | | | | 1.000 | 0.038 | 0.007 |
| δ_{\perp} | | | | | | | | 1.000 | 0.081 |
| $\delta_{\perp} - \delta_S$ | | | | | | | | | 1.000 |

be small, affecting the results by less than 10% of the statistical uncertainty.

VI. RESULTS

The full simultaneous maximum likelihood fit contains 25 free parameters. These include the nine physics parameters: $\Delta\Gamma_s$, ϕ_s , Γ_s , $|A_0(0)|^2$, $|A_{\parallel}(0)|^2$, δ_{\parallel} , δ_{\perp} , $|A_S|^2$ and δ_S . The other parameters in the likelihood function are the B_s^0 signal fraction f_s , the parameters describing the $J/\psi\phi$ mass distribution, the parameters describing the B_s^0 meson decay time plus angular distributions of background events, the parameters used to describe the estimated decay time uncertainty distributions for signal and background events, and scale factors between the estimated decay time and mass uncertainties and their true uncertainties.

The number of signal B_s^0 meson candidates extracted from the fits is 22670 ± 150 . The results and correlations for the measured physics parameters of the simultaneous unbinned maximum likelihood fit are given in Tables V and VI. Fit projections of the mass, proper decay time and angles are given in Figs. 5 and 6 respectively.

VII. SYSTEMATIC UNCERTAINTIES

Systematic uncertainties are assigned by considering several effects that are not accounted for in the likelihood fit. These are described below:

- (i) *Inner detector alignment*: Residual misalignments of the inner detector affect the impact parameter

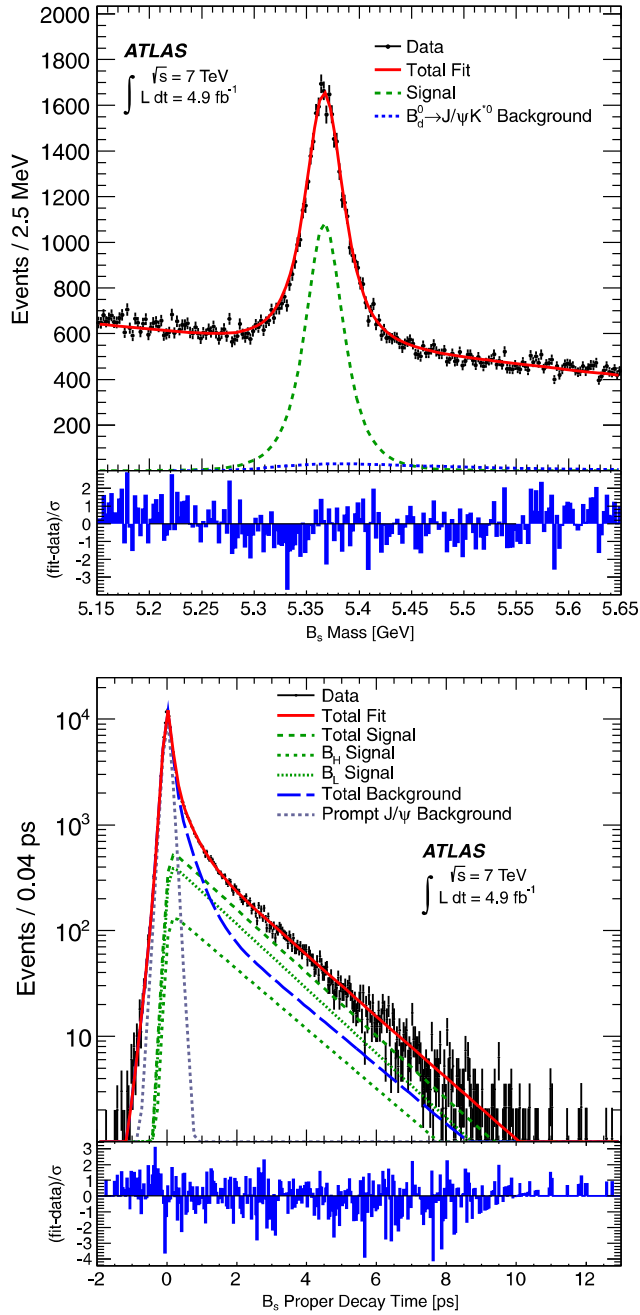


FIG. 5 (color online). (Top) Mass fit projection for the $B_s^0 \rightarrow J/\psi\phi$. The red line shows the total fit, the dashed green line shows the signal component while the dotted blue line shows the contribution from $B^0 \rightarrow J/\psi K^{0*}$ events. (Bottom) Proper decay time fit projection for the $B_s^0 \rightarrow J/\psi\phi$. The red line shows the total fit while the green dashed line shows the total signal. The light and heavy components of the signal are shown in green as a dotted and a dash-dotted line, respectively. The total background is shown as a blue dashed line with a grey dotted line showing the prompt J/ψ background. The pull distributions at the bottom show the difference between data and fit value normalized to the data statistical uncertainty.

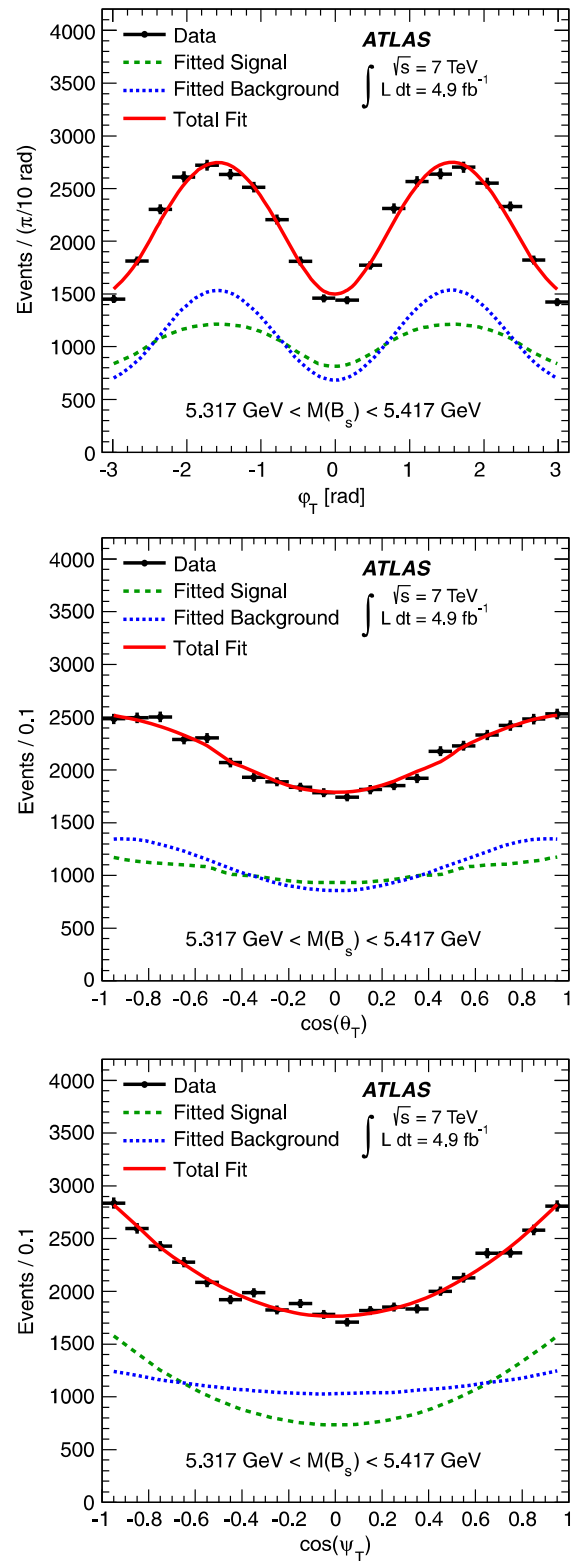


FIG. 6 (color online). Fit projections for transversity angles. (Top) ϕ_T , (middle) $\cos\theta_T$, (bottom) $\cos\psi_T$. In all three plots, the red line shows the total fit, the dashed green line shows the signal component, and the dotted blue line shows the background contribution.

distribution with respect to the primary vertex. The effect of the residual misalignment is estimated using simulated events with and without distorted geometry. For this, the impact parameter distribution with respect to the primary vertex is measured with data as a function of η and ϕ with the maximum deviation from zero being less than $10 \mu\text{m}$. The measurement is used to distort the geometry for simulated events in order to reproduce the impact parameter distribution measured as a function of η and ϕ . The difference between the measurement using simulated events with and without the distorted geometry is used as the systematic uncertainty.

- (ii) *Trigger efficiency*: It is observed that the muon trigger biases the transverse impact parameter of muons toward smaller values. To correct for this bias the events are reweighted according to

$$w = e^{-|t|/(\tau_{\text{sing}}+\epsilon)} / e^{-|t|/\tau_{\text{sing}}},$$

where τ_{sing} is a single B_s^0 lifetime measured before the correction, using an unbinned mass–lifetime maximum likelihood fit. The value of the parameter ϵ and its uncertainty are described in Ref. [6]. The systematic uncertainty is calculated by varying the value of ϵ by its uncertainty and rerunning the fit.

- (iii) *B^0 contribution*: Contaminations from $B^0 \rightarrow J/\psi K^{0*}$ and $B^0 \rightarrow J/\psi K\pi$ events misreconstructed as $B_s^0 \rightarrow J/\psi\phi$ are accounted for in the default fit. The fractions of $B^0 \rightarrow J/\psi K^{0*}$ and $B^0 \rightarrow J/\psi K\pi$ events in the default fit are $(6.5 + / - 2.4)\%$ and $(4.5 + / - 2.8)\%$ respectively. They were determined in MC simulation and using branching fractions from Ref. [17]. To estimate the systematic uncertainty arising from the precision of the fraction estimates, the data are fitted with these fractions increased and decreased by 1σ . The largest shifts in the fitted values from the default case are taken as the systematic uncertainty for each parameter of interest.

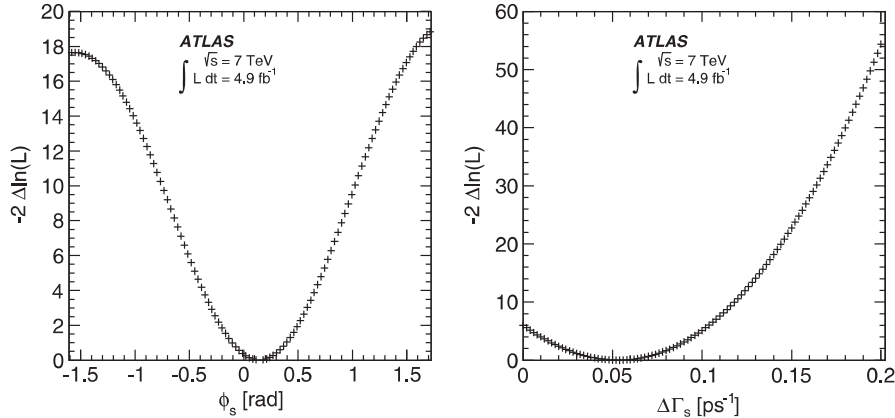
- (iv) *Tagging*: For the uncertainties in the fit parameters due to uncertainty in the tagging, the statistical and systematic components are separated. The statistical uncertainty is due to the sample size of $B^\pm \rightarrow J/\psi K^\pm$ decays available and is included in the overall statistical error. The systematic uncertainty arises from the precision of the tagging calibration and is estimated by varying the model parametrizing the probability distribution, $P(B|Q)$, as a function of tag charge. The default model is a linear function. For the combined-muon cone-charge tag and the segment tagged muons the alternative fit function is a third-order polynomial. For the jet-charge tag with no muons, a third- and a fifth-order polynomial are used. The B_s^0 fit was repeated using the alternative models, and the largest difference was assigned as the systematic uncertainty.

- (v) *Angular acceptance method*: The angular acceptance is calculated from a binned fit to Monte Carlo data. A separate set of Monte Carlo signal events were generated and fully simulated. Background was generated using pseudoexperiments as described below. There is sufficient data to perform 166 fits. The systematic uncertainty is calculated using the bias of the pull distribution multiplied by the statistical uncertainty of each parameter. To estimate the size of the systematic uncertainty introduced from the choice of binning, different acceptance functions are calculated using different bin widths and central values. These effects are found to be negligible.

- (vi) *Signal and background mass model, resolution model, background lifetime and background angles model*: To estimate the size of systematic uncertainties caused by the assumptions made in the fit model, variations of the model are tested in pseudoexperiments. A set of 2400 pseudoexperiments is generated for each variation considered and fitted with the default model. The systematic error quoted for each effect is the difference between the mean shift of

TABLE VII. Summary of systematic uncertainties assigned to the physics parameters.

| | ϕ_s [rad] | $\Delta\Gamma_s$ [ps^{-1}] | Γ_s [ps^{-1}] | $ A_{\parallel}(0) ^2$ | $ A_0(0) ^2$ | $ A_S(0) ^2$ | δ_{\perp} [rad] | δ_{\parallel} [rad] | $\delta_{\perp} - \delta_S$ [rad] |
|--------------------|----------------|---------------------------------------|---------------------------------|------------------------|--------------|--------------|------------------------|----------------------------|-----------------------------------|
| ID alignment | $<10^{-2}$ | $<10^{-3}$ | $<10^{-3}$ | $<10^{-3}$ | $<10^{-3}$ | ... | $<10^{-2}$ | $<10^{-2}$ | ... |
| Trigger efficiency | $<10^{-2}$ | $<10^{-3}$ | 0.002 | $<10^{-3}$ | $<10^{-3}$ | $<10^{-3}$ | $<10^{-2}$ | $<10^{-2}$ | $<10^{-2}$ |
| B^0 contribution | 0.03 | 0.001 | $<10^{-3}$ | $<10^{-3}$ | 0.005 | 0.001 | 0.02 | $<10^{-2}$ | $<10^{-2}$ |
| Tagging | 0.03 | $<10^{-3}$ | $<10^{-3}$ | $<10^{-3}$ | $<10^{-3}$ | $<10^{-3}$ | 0.04 | $<10^{-2}$ | $<10^{-2}$ |
| Acceptance | 0.02 | 0.004 | 0.002 | 0.002 | 0.004 | ... | ... | $<10^{-2}$ | ... |
| Models: | | | | | | | | | |
| Default fit | $<10^{-2}$ | 0.003 | $<10^{-3}$ | 0.001 | 0.001 | 0.006 | 0.07 | 0.01 | 0.01 |
| Signal mass | $<10^{-2}$ | 0.001 | $<10^{-3}$ | $<10^{-3}$ | 0.001 | $<10^{-3}$ | 0.03 | 0.04 | 0.01 |
| Background mass | $<10^{-2}$ | 0.001 | 0.001 | $<10^{-3}$ | $<10^{-3}$ | 0.002 | 0.06 | 0.02 | 0.02 |
| Resolution | 0.02 | $<10^{-3}$ | 0.001 | 0.001 | $<10^{-3}$ | 0.002 | 0.04 | 0.02 | 0.01 |
| Background time | 0.01 | 0.001 | $<10^{-3}$ | 0.001 | $<10^{-3}$ | 0.002 | 0.01 | 0.02 | 0.02 |
| Background angles | 0.02 | 0.008 | 0.002 | 0.008 | 0.009 | 0.027 | 0.06 | 0.07 | 0.03 |
| Total | 0.05 | 0.010 | 0.004 | 0.009 | 0.012 | 0.028 | 0.11 | 0.09 | 0.04 |


 FIG. 7. One-dimensional likelihood scans for ϕ_s (left) and $\Delta \Gamma_s$ (right).

the fitted value of each parameter from its input value for the pseudoexperiments with the systematic alteration included. The variations are as follows. Two different scale factors are used to generate the signal mass. The background mass is generated from an exponential function. Two different scale factors are used to generate the lifetime uncertainty. The background lifetimes are generated by sampling data from the mass sidebands. Pseudoexperiments are generated with background angles taken from histograms from sideband data and are fitted with the default fit model to assess the systematic uncertainty to the parameterization of the background angles in the fit.

- (vii) *Default fit model*: The systematic uncertainty of the default fit model is calculated using the bias of the pull distribution of 2400 pseudoexperiments, multiplied by the statistical uncertainty of each parameter.

The systematic uncertainties are provided in Table VII. For each variable, the total systematic error is obtained by adding in quadrature the different contributions.

VIII. DISCUSSION

The PDF describing the $B_s^0 \rightarrow J/\psi \phi$ decay is invariant under the following simultaneous transformations:

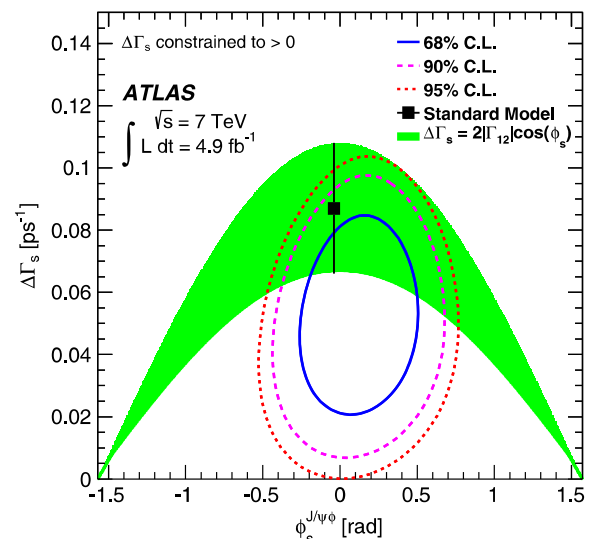
$$\{\phi_s, \Delta \Gamma_s, \delta_\perp, \delta_\parallel\} \rightarrow \{\pi - \phi_s, -\Delta \Gamma_s, \pi - \delta_\perp, 2\pi - \delta_\parallel\}.$$

$\Delta \Gamma_s$ has been determined to be positive [24]. Therefore, there is a unique solution, and only the case $\Delta \Gamma_s > 0$ is considered. Uncertainties on individual parameters were studied in detail in likelihood scans. Figure 7 shows the one-dimensional likelihood scans for ϕ_s and $\Delta \Gamma_s$. Figure 8 shows the likelihood contours in the $\phi_s - \Delta \Gamma_s$ plane.

The behavior of the amplitudes around their fitted values is Gaussian; however, the strong phases are more

complicated. Figure 9 shows the one-dimensional likelihood scans for the three measured strong phases.

The likelihood behavior of δ_\perp appears Gaussian, and therefore it is reasonable to quote $\delta_\perp = 3.89 \pm 0.47$ (stat) rad. For $\delta_\perp - \delta_s$ the scan shows a minimum close to π ; however, it is insensitive over the rest of the scan at the level of 2.1σ . Therefore, the measured value of the difference $\delta_\perp - \delta_s$ is only given as 1σ confidence interval [3.02, 3.25] rad. It should be noted that both $|A_S(0)|^2$ and the strong phase δ_s are determined for the K^+K^- invariant mass range $1.0085 \text{ GeV} < m(K^+K^-) < 1.0305 \text{ GeV}$ used in this analysis. For the strong phase δ_\parallel the central fit value is


 FIG. 8 (color online). Likelihood contours in the $\phi_s - \Delta \Gamma_s$ plane. The blue line shows the 68% likelihood contour, the dashed pink line shows the 90% likelihood contour, and the red dotted line shows the 95% likelihood contour (statistical errors only). The green band is the theoretical prediction of mixing-induced CP violation.

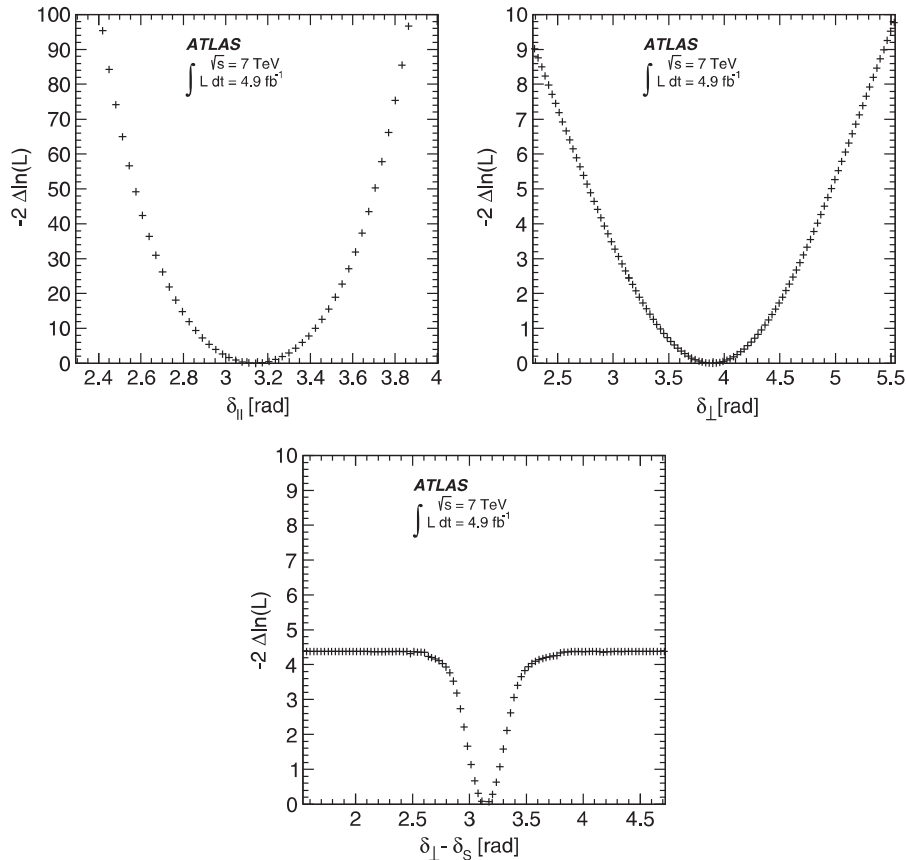


FIG. 9. One-dimensional likelihood scans for δ_{\parallel} (top left), δ_{\perp} (top right) and $\delta_{\perp} - \delta_S$ (bottom).

close to π (3.14 ± 0.10), and the one-dimensional likelihood scan shows normal Gaussian behavior around this minimum. However, the systematic pull plot based on 2400 pseudoexperiments fits reveals a double-Gaussian shape with 68% of the results included in the interval [2.92, 3.35] rad, and so we quote the result in the form of a 68% C.L. interval $\delta_{\parallel} \in [2.92, 3.35]$ rad (statistical only).

IX. CONCLUSION

A measurement of time-dependent CP asymmetry parameters in $B_s^0 \rightarrow J/\psi(\mu^+\mu^-)\phi(K^+K^-)$ decays from a 4.9 fb^{-1} data sample of pp collisions collected with the ATLAS detector during the 2011 $\sqrt{s} = 7 \text{ TeV}$ LHC run is presented. Several parameters describing the B_s^0 meson system are measured. These include the mean B_s^0 lifetime $1/\Gamma_s$, the decay width difference $\Delta\Gamma_s$ between the heavy and light mass eigenstates, and the transversity amplitudes $|A_0(0)|$ and $|A_{\parallel}(0)|$. Each of these is consistent with its respective world average. Likelihood contours in the $\phi_s - \Delta\Gamma_s$ plane are also provided. The fraction $|A_S(0)|^2$, the signal contribution from $B_s^0 \rightarrow J/\psi K^+K^-$ and $B_s^0 \rightarrow J/\psi f_0$ decays, is measured to be consistent with zero, at $0.024 \pm 0.014(\text{stat}) \pm 0.028(\text{syst})$.

The results are

$$\begin{aligned} \phi_s &= 0.12 \pm 0.25(\text{stat}) \pm 0.05(\text{syst}) \text{ rad} \\ \Delta\Gamma_s &= 0.053 \pm 0.021(\text{stat}) \pm 0.010(\text{syst}) \text{ ps}^{-1} \\ \Gamma_s &= 0.677 \pm 0.007(\text{stat}) \pm 0.004(\text{syst}) \text{ ps}^{-1} \\ |A_{\parallel}(0)|^2 &= 0.220 \pm 0.008(\text{stat}) \pm 0.009(\text{syst}) \\ |A_0(0)|^2 &= 0.529 \pm 0.006(\text{stat}) \pm 0.012(\text{syst}) \\ \delta_{\perp} &= 3.89 \pm 0.47(\text{stat}) \pm 0.11(\text{syst}) \text{ rad.} \end{aligned}$$

The values are consistent with those obtained in our untagged analysis [6] and significantly reduce the overall uncertainty on ϕ_s . These results are consistent with the values predicted in the Standard Model.

ACKNOWLEDGMENTS

We thank CERN for the very successful operation of the LHC, as well as the support staff from our institutions without whom ATLAS could not be operated efficiently. We acknowledge the support of ANPCyT, Argentina; YerPhI, Armenia; ARC, Australia; BMWF and FWF, Austria; ANAS, Azerbaijan; SSTC, Belarus; CNPq and

FAPESP, Brazil; NSERC, NRC and CFI, Canada; CERN; CONICYT, Chile; CAS, MOST and NSFC, China; COLCIENCIAS, Colombia; MSMT CR, MPO CR and VSC CR, Czech Republic; DNRF, DNSRC and Lundbeck Foundation, Denmark; EPLANET, ERC and NSRF, European Union; IN2P3-CNRS, CEA-DSM/IRFU, France; GNSF, Georgia; BMBF, DFG, HGF, MPG and AvH Foundation, Germany; GSRT and NSRF, Greece; ISF, MINERVA, GIF, I-CORE and Benozio Center, Israel; INFN, Italy; MEXT and JSPS, Japan; CNRST, Morocco; FOM and NWO, Netherlands; BRF and RCN, Norway; MNiSW and NCN, Poland; GRICES and FCT, Portugal; MNE/IFA, Romania; MES of Russia and ROSATOM, Russian Federation; JINR; MSTD, Serbia; MSSR,

Slovakia; ARRS and MIZŠ, Slovenia; DST/NRF, South Africa; MINECO, Spain; SRC and Wallenberg Foundation, Sweden; SER, SNSF and Cantons of Bern and Geneva, Switzerland; NSC, Taiwan; TAEK, Turkey; STFC, the Royal Society and Leverhulme Trust, United Kingdom; DOE and NSF, United States of America. The crucial computing support from all WLCG partners is acknowledged gratefully, in particular from CERN and the ATLAS Tier-1 facilities at TRIUMF (Canada), NDGF (Denmark, Norway, Sweden), CC-IN2P3 (France), KIT/GridKA (Germany), INFN-CNAF (Italy), NL-T1 (Netherlands), PIC (Spain), ASGC (Taiwan), RAL (UK) and BNL (USA) and in the Tier-2 facilities worldwide.

-
- [1] M. Bona *et al.* (UTfit Collaboration), *Phys. Rev. Lett.* **97**, 151803 (2006).
- [2] A. Abulencia *et al.* (CDF Collaboration), *Phys. Rev. Lett.* **97**, 242003 (2006).
- [3] R. Aaij *et al.* (LHCb Collaboration), *Phys. Lett. B* **709**, 177 (2012).
- [4] A. Lenz and U. Nierste, [arXiv:1102.4274](https://arxiv.org/abs/1102.4274).
- [5] A. Lenz and U. Nierste, *J. High Energy Phys.* **06** (2007) 072.
- [6] ATLAS Collaboration, *J. High Energy Phys.* **12** (2012) 072.
- [7] V. M. Abazov *et al.* (D0 Collaboration), *Phys. Rev. D* **85** (2012) 032006.
- [8] T. Aaltonen *et al.* (CDF Collaboration), *Phys. Rev. Lett.* **109**, 171802 (2012).
- [9] R. Aaij *et al.* (LHCb Collaboration), *Phys. Rev. D* **87**, 112010 (2013).
- [10] ATLAS Collaboration, *JINST* **3**, S08003 (2008).
- [11] ATLAS uses a right-handed coordinate system with its origin at the nominal interaction point in the center of the detector and the z axis along the beam pipe. The x axis points from the IP to the center of the LHC ring, and the y axis points upward. Cylindrical coordinates (r, ϕ) are used in the transverse plane, ϕ being the azimuthal angle around the beam pipe. The pseudorapidity is defined in terms of the polar angle θ as $\eta = -\ln \tan(\theta/2)$.
- [12] T. Sjostrand, S. Mrenna, and P. Z. Skands, *J. High Energy Phys.* **05** (2006) 026.
- [13] ATLAS Collaboration, Report No. ATL-PHYS-PUB-2011-009, <http://cds.cern.ch/record/1363300>.
- [14] ATLAS Collaboration, *Eur. Phys. J. C* **70**, 823 (2010).
- [15] S. Agostinelli *et al.* (GEANT4 Collaboration), *Nucl. Instrum. Methods Phys. Res., Sect. A* **506**, 250 (2003).
- [16] ATLAS Collaboration, *Nucl. Phys.* **B850**, 387 (2011).
- [17] J. Beringer *et al.* (Particle Data Group Collaboration), *Phys. Rev. D* **86**, 010001 (2012) (and 2013 partial update for the 2014 edition).
- [18] R. Field and R. Feynman, *Nucl. Phys.* **B136**, 1 (1978).
- [19] $\Delta R^2 = \Delta\phi^2 + \Delta\eta^2$, where $\Delta\phi$ and $\Delta\eta$ are the differences between the measured ϕ and η of the tracks respectively.
- [20] ATLAS Collaboration, Report No. ATLAS-CONF-2011-102, <http://cds.cern.ch/record/1369219>.
- [21] ATLAS Collaboration, [arXiv:0901.0512](https://arxiv.org/abs/0901.0512).
- [22] A. S. Dighe, I. Dunietz, and R. Fleischer, *Eur. Phys. J. C* **6**, 647 (1999).
- [23] R. Aaij *et al.* (LHCb Collaboration), *Phys. Rev. Lett.* **108**, 101803 (2012).
- [24] R. Aaij *et al.*, *Phys. Rev. Lett.* **108**, 241801 (2012).

G. Aad,⁸⁴ T. Abajyan,²¹ B. Abbott,¹¹² J. Abdallah,¹⁵² S. Abdel Khalek,¹¹⁶ O. Abidinov,¹¹ R. Aben,¹⁰⁶ B. Abi,¹¹³ M. Abolins,⁸⁹ O. S. AbouZeid,¹⁵⁹ H. Abramowicz,¹⁵⁴ H. Abreu,¹³⁷ Y. Abulaiti,^{147a,147b} B. S. Acharya,^{165a,165b,b} L. Adamczyk,^{38a} D. L. Adams,²⁵ T. N. Addy,⁵⁶ J. Adelman,¹⁷⁷ S. Adomeit,⁹⁹ T. Adye,¹³⁰ T. Agatonovic-Jovin,^{13b} J. A. Aguilar-Saavedra,^{125f,125a} M. Agustoni,¹⁷ S. P. Ahlen,²² A. Ahmad,¹⁴⁹ F. Ahmadov,^{64,c} G. Aielli,^{134a,134b} T. P. A. Åkesson,⁸⁰ G. Akimoto,¹⁵⁶ A. V. Akimov,⁹⁵ J. Albert,¹⁷⁰ S. Albrand,⁵⁵ M. J. Alconada Verzini,⁷⁰ M. Aleksa,³⁰ I. N. Aleksandrov,⁶⁴ C. Alexa,^{26a} G. Alexander,¹⁵⁴ G. Alexandre,⁴⁹ T. Alexopoulos,¹⁰ M. Althroob,^{165a,165c} G. Alimonti,^{90a} L. Alio,⁸⁴ J. Alison,³¹ B. M. M. Allbrooke,¹⁸ L. J. Allison,⁷¹ P. P. Allport,⁷³ S. E. Allwood-Spiers,⁵³ J. Almond,⁸³ A. Aloisio,^{103a,103b} R. Alon,¹⁷³ A. Alonso,³⁶ F. Alonso,⁷⁰ C. Alpigiani,⁷⁵ A. Altheimer,³⁵ B. Alvarez Gonzalez,⁸⁹

M. G. Alviggi,^{103a,103b} K. Amako,⁶⁵ Y. Amaral Coutinho,^{24a} C. Amelung,²³ D. Amidei,⁸⁸ V. V. Ammosov,^{129,a}
 S. P. Amor Dos Santos,^{125a,125c} A. Amorim,^{125a,125b} S. Amoroso,⁴⁸ N. Amram,¹⁵⁴ G. Amundsen,²³ C. Anastopoulos,¹⁴⁰
 L. S. Ancu,¹⁷ N. Andari,³⁰ T. Andeen,³⁵ C. F. Anders,^{58b} G. Anders,³⁰ K. J. Anderson,³¹ A. Andreazza,^{90a,90b} V. Andrei,^{58a}
 X. S. Anduaga,⁷⁰ S. Angelidakis,⁹ P. Anger,⁴⁴ A. Angerami,³⁵ F. Anghinolfi,³⁰ A. V. Anisenkov,¹⁰⁸ N. Anjos,^{125a}
 A. Annovi,⁴⁷ A. Antonaki,⁹ M. Antonelli,⁴⁷ A. Antonov,⁹⁷ J. Antos,^{145b} F. Anulli,^{133a} M. Aoki,⁶⁵ L. Aperio Bella,¹⁸
 R. Apolle,^{119,d} G. Arabidze,⁸⁹ I. Aracena,¹⁴⁴ Y. Arai,⁶⁵ J. P. Araque,^{125a} A. T. H. Arce,⁴⁵ J-F. Arguin,⁹⁴ S. Argyropoulos,⁴²
 M. Arik,^{19a} A. J. Armbruster,³⁰ O. Arnaez,⁸² V. Arnal,⁸¹ O. Arslan,²¹ A. Artamonov,⁹⁶ G. Artoni,²³ S. Asai,¹⁵⁶ N. Asbah,⁹⁴
 A. Ashkenazi,¹⁵⁴ S. Ask,²⁸ B. Åsman,^{147a,147b} L. Asquith,⁶ K. Assamagan,²⁵ R. Astalos,^{145a} M. Atkinson,¹⁶⁶ N. B. Atlay,¹⁴²
 B. Auerbach,⁶ E. Auge,¹¹⁶ K. Augsten,¹²⁷ M. Aourousseau,^{146b} G. Avolio,³⁰ G. Azuelos,^{94,e} Y. Azuma,¹⁵⁶ M. A. Baak,³⁰
 C. Bacci,^{135a,135b} A. M. Bach,¹⁵ H. Bachacou,¹³⁷ K. Bachas,¹⁵⁵ M. Backes,³⁰ M. Backhaus,³⁰ J. Backus Mayes,¹⁴⁴
 E. Badescu,^{26a} P. Bagiacchi,^{133a,133b} P. Bagnaia,^{133a,133b} Y. Bai,^{33a} D. C. Bailey,¹⁵⁹ T. Bain,³⁵ J. T. Baines,¹³⁰ O. K. Baker,¹⁷⁷
 S. Baker,⁷⁷ P. Balek,¹²⁸ F. Balli,¹³⁷ E. Banas,³⁹ Sw. Banerjee,¹⁷⁴ D. Banfi,³⁰ A. Bangert,¹⁵¹ A. A. E. Bannoura,¹⁷⁶
 V. Bansal,¹⁷⁰ H. S. Bansil,¹⁸ L. Barak,¹⁷³ S. P. Baranov,⁹⁵ T. Barber,⁴⁸ E. L. Barberio,⁸⁷ D. Barberis,^{50a,50b} M. Barbero,⁸⁴
 T. Barillari,¹⁰⁰ M. Barisonzi,¹⁷⁶ T. Barklow,¹⁴⁴ N. Barlow,²⁸ B. M. Barnett,¹³⁰ R. M. Barnett,¹⁵ Z. Barnovska,⁵
 A. Baroncelli,^{135a} G. Barone,⁴⁹ A. J. Barr,¹¹⁹ F. Barreiro,⁸¹ J. Barreiro Guimarães da Costa,⁵⁷ R. Bartoldus,¹⁴⁴ A. E. Barton,⁷¹
 P. Bartos,^{145a} V. Bartsch,¹⁵⁰ A. Bassalat,¹¹⁶ A. Basye,¹⁶⁶ R. L. Bates,⁵³ L. Batkova,^{145a} J. R. Batley,²⁸ M. Battistin,³⁰
 F. Bauer,¹³⁷ H. S. Bawa,^{144,f} T. Beau,⁷⁹ P. H. Beauchemin,¹⁶² R. Beccherle,^{123a,123b} P. Bechtel,²¹ H. P. Beck,¹⁷ K. Becker,¹⁷⁶
 S. Becker,⁹⁹ M. Beckingham,¹³⁹ C. Becot,¹¹⁶ A. J. Beddall,^{19c} A. Beddall,^{19c} S. Bedikian,¹⁷⁷ V. A. Bednyakov,⁶⁴ C. P. Bee,¹⁴⁹
 L. J. Beemster,¹⁰⁶ T. A. Beermann,¹⁷⁶ M. Begel,²⁵ K. Behr,¹¹⁹ C. Belanger-Champagne,⁸⁶ P. J. Bell,⁴⁹ W. H. Bell,⁴⁹
 G. Bella,¹⁵⁴ L. Bellagamba,^{20a} A. Bellerive,²⁹ M. Bellomo,⁸⁵ A. Belloni,⁵⁷ O. L. Beloborodova,^{108,g} K. Belotskiy,⁹⁷
 O. Beltramello,³⁰ O. Benary,¹⁵⁴ D. Bencheekroun,^{136a} K. Bendtz,^{147a,147b} N. Benekos,¹⁶⁶ Y. Benhammou,¹⁵⁴
 E. Benhar Noccioli,⁴⁹ J. A. Benitez Garcia,^{160b} D. P. Benjamin,⁴⁵ J. R. Bensinger,²³ K. Benslama,¹³¹ S. Bentvelsen,¹⁰⁶
 D. Berge,¹⁰⁶ E. Bergeas Kuutmann,¹⁶ N. Berger,⁵ F. Berghaus,¹⁷⁰ E. Berglund,¹⁰⁶ J. Beringer,¹⁵ C. Bernard,²² P. Bernat,⁷⁷
 C. Bernius,⁷⁸ F. U. Bernlochner,¹⁷⁰ T. Berry,⁷⁶ P. Berta,¹²⁸ C. Bertella,⁸⁴ F. Bertolucci,^{123a,123b} M. I. Besana,^{90a}
 G. J. Besjes,¹⁰⁵ O. Bessidskaia,^{147a,147b} N. Besson,¹³⁷ C. Betancourt,⁴⁸ S. Bethke,¹⁰⁰ W. Bhimji,⁴⁶ R. M. Bianchi,¹²⁴
 L. Bianchini,²³ M. Bianco,³⁰ O. Biebel,⁹⁹ S. P. Bieniek,⁷⁷ K. Bierwagen,⁵⁴ J. Biesiada,¹⁵ M. Biglietti,^{135a}
 J. Bilbao De Mendizabal,⁴⁹ H. Bilokon,⁴⁷ M. Bindi,⁵⁴ S. Binet,¹¹⁶ A. Bingul,^{19c} C. Bini,^{133a,133b} C. W. Black,¹⁵¹
 J. E. Black,¹⁴⁴ K. M. Black,²² D. Blackburn,¹³⁹ R. E. Blair,⁶ J.-B. Blanchard,¹³⁷ T. Blazek,^{145a} I. Bloch,⁴² C. Blocker,²³
 W. Blum,^{82,a} U. Blumenschein,⁵⁴ G. J. Bobbink,¹⁰⁶ V. S. Bobrovnikov,¹⁰⁸ S. S. Bocchetta,⁸⁰ A. Bocchi,⁴⁵ C. R. Boddy,¹¹⁹
 M. Boehler,⁴⁸ J. Boek,¹⁷⁶ T. T. Boek,¹⁷⁶ J. A. Bogaerts,³⁰ A. G. Bogdanchikov,¹⁰⁸ A. Bogouch,^{91,a} C. Bohm,^{147a} J. Bohm,¹²⁶
 V. Boisvert,⁷⁶ T. Bold,^{38a} V. Boldea,^{26a} A. S. Boldyrev,⁹⁸ N. M. Bolnet,¹³⁷ M. Bomben,⁷⁹ M. Bona,⁷⁵ M. Boonekamp,¹³⁷
 A. Borisov,¹²⁹ G. Borissov,⁷¹ M. Borri,⁸³ S. Borroni,⁴² J. Bortfeldt,⁹⁹ V. Bortolotto,^{135a,135b} K. Bos,¹⁰⁶ D. Boscherini,^{20a}
 M. Bosman,¹² H. Boterenbrood,¹⁰⁶ J. Boudreau,¹²⁴ J. Bouffard,² E. V. Bouhova-Thacker,⁷¹ D. Boumediene,³⁴
 C. Bourdarios,¹¹⁶ N. Bousson,¹¹³ S. Boutouil,^{136d} A. Boveia,³¹ J. Boyd,³⁰ I. R. Boyko,⁶⁴ I. Bozovic-Jelisavcic,^{13b}
 J. Bracinik,¹⁸ P. Branchini,^{135a} A. Brandt,⁸ G. Brandt,¹⁵ O. Brandt,^{58a} U. Bratzler,¹⁵⁷ B. Brau,⁸⁵ J. E. Brau,¹¹⁵
 H. M. Braun,^{176,a} S. F. Brazzale,^{165a,165c} B. Brelier,¹⁵⁹ K. Brendlinger,¹²¹ A. J. Brennan,⁸⁷ R. Brenner,¹⁶⁷ S. Bressler,¹⁷³
 K. Bristow,^{146c} T. M. Bristow,⁴⁶ D. Britton,⁵³ F. M. Brochu,²⁸ I. Brock,²¹ R. Brock,⁸⁹ C. Bromberg,⁸⁹ J. Bronner,¹⁰⁰
 G. Brooijmans,³⁵ T. Brooks,⁷⁶ W. K. Brooks,^{32b} J. Brosamer,¹⁵ E. Brost,¹¹⁵ G. Brown,⁸³ J. Brown,⁵⁵
 P. A. Bruckman de Renstrom,³⁹ D. Bruncko,^{145b} R. Bruneliere,⁴⁸ S. Brunet,⁶⁰ A. Bruni,^{20a} G. Bruni,^{20a} M. Bruschi,^{20a}
 L. Bryngemark,⁸⁰ T. Buanes,¹⁴ Q. Buat,¹⁴³ F. Bucci,⁴⁹ P. Buchholz,¹⁴² R. M. Buckingham,¹¹⁹ A. G. Buckley,⁵³ S. I. Buda,^{26a}
 I. A. Budagov,⁶⁴ F. Buehrer,⁴⁸ L. Bugge,¹¹⁸ M. K. Bugge,¹¹⁸ O. Bulekov,⁹⁷ A. C. Bundock,⁷³ H. Burckhart,³⁰ S. Burdin,⁷³
 B. Burghgrave,¹⁰⁷ S. Burke,¹³⁰ I. Burmeister,⁴³ E. Busato,³⁴ V. Büscher,⁸² P. Bussey,⁵³ C. P. Buszello,¹⁶⁷ B. Butler,⁵⁷
 J. M. Butler,²² A. I. Butt,³ C. M. Buttar,⁵³ J. M. Butterworth,⁷⁷ P. Butti,¹⁰⁶ W. Buttinger,²⁸ A. Buzatu,⁵³ M. Byszewski,¹⁰
 S. Cabrera Urbán,¹⁶⁸ D. Caforio,^{20a,20b} O. Cakir,^{4a} P. Calafiura,¹⁵ G. Calderini,⁷⁹ P. Calfayan,⁹⁹ R. Calkins,¹⁰⁷ L. P. Caloba,^{24a}
 D. Calvet,³⁴ S. Calvet,³⁴ R. Camacho Toro,⁴⁹ S. Camarda,⁴² D. Cameron,¹¹⁸ L. M. Caminada,¹⁵ R. Caminal Armadans,¹²
 S. Campana,³⁰ M. Campanelli,⁷⁷ A. Campoverde,¹⁴⁹ V. Canale,^{103a,103b} A. Canepa,^{160a} J. Cantero,⁸¹ R. Cantrill,⁷⁶ T. Cao,⁴⁰
 M. D. M. Capeans Garrido,³⁰ I. Caprini,^{26a} M. Caprini,^{26a} M. Capua,^{37a,37b} R. Caputo,⁸² R. Cardarelli,^{134a} T. Carli,³⁰
 G. Carlino,^{103a} L. Carminati,^{90a,90b} S. Caron,¹⁰⁵ E. Carquin,^{32a} G. D. Carrillo-Montoya,^{146c} A. A. Carter,⁷⁵ J. R. Carter,²⁸
 J. Carvalho,^{125a,125c} D. Casadei,⁷⁷ M. P. Casado,¹² E. Castaneda-Miranda,^{146b} A. Castelli,¹⁰⁶ V. Castillo Gimenez,¹⁶⁸

- N. F. Castro,^{125a} P. Catastini,⁵⁷ A. Catinaccio,³⁰ J. R. Catmore,⁷¹ A. Cattai,³⁰ G. Cattani,^{134a,134b} S. Caughron,⁸⁹
V. Cavaliere,¹⁶⁶ D. Cavalli,^{90a} M. Cavalli-Sforza,¹² V. Cavadini,^{123a,123b} F. Ceradini,^{135a,135b} B. Cerio,⁴⁵ K. Cerny,¹²⁸
A. S. Cerqueira,^{24b} A. Cerri,¹⁵⁰ L. Cerrito,⁷⁵ F. Cerutti,¹⁵ M. Cerv,³⁰ A. Cervelli,¹⁷ S. A. Cetin,^{19b} A. Chafaq,^{136a}
D. Chakraborty,¹⁰⁷ I. Chalupkova,¹²⁸ K. Chan,³ P. Chang,¹⁶⁶ B. Chapleau,⁸⁶ J. D. Chapman,²⁸ D. Charfeddine,¹¹⁶
D. G. Charlton,¹⁸ C. C. Chau,¹⁵⁹ C. A. Chavez Barajas,¹⁵⁰ S. Cheatham,⁸⁶ A. Chegwidan,⁸⁹ S. Chekanov,⁶
S. V. Chekulaev,^{160a} G. A. Chelkov,⁶⁴ M. A. Chelstowska,⁸⁸ C. Chen,⁶³ H. Chen,²⁵ K. Chen,¹⁴⁹ L. Chen,^{33d,h} S. Chen,^{33c}
X. Chen,^{146c} Y. Chen,³⁵ H. C. Cheng,⁸⁸ Y. Cheng,³¹ A. Cheplakov,⁶⁴ R. Cherkaoui El Moursli,^{136e} V. Chernyatin,^{25,a}
E. Cheu,⁷ L. Chevalier,¹³⁷ V. Chiarella,⁴⁷ G. Chiefari,^{103a,103b} J. T. Childers,⁶ A. Chilingarov,⁷¹ G. Chiodini,^{72a}
A. S. Chisholm,¹⁸ R. T. Chislett,⁷⁷ A. Chitan,^{26a} M. V. Chizhov,⁶⁴ S. Chouridou,⁹ B. K. B. Chow,⁹⁹ I. A. Christidi,⁷⁷
D. Chromek-Burckhart,³⁰ M. L. Chu,¹⁵² J. Chudoba,¹²⁶ L. Chytka,¹¹⁴ G. Ciapetti,^{133a,133b} A. K. Ciftci,^{4a} R. Ciftci,^{4a}
D. Cinca,⁶² V. Cindro,⁷⁴ A. Ciocio,¹⁵ P. Cirkovic,^{13b} Z. H. Citron,¹⁷³ M. Citterio,^{90a} M. Ciubancan,^{26a} A. Clark,⁴⁹
P. J. Clark,⁴⁶ R. N. Clarke,¹⁵ W. Cleland,¹²⁴ J. C. Clemens,⁸⁴ B. Clement,⁵⁵ C. Clement,^{147a,147b} Y. Coadou,⁸⁴
M. Cobal,^{165a,165c} A. Coccaro,¹³⁹ J. Cochran,⁶³ L. Coffey,²³ J. G. Cogan,¹⁴⁴ J. Coggeshall,¹⁶⁶ B. Cole,³⁵ S. Cole,¹⁰⁷
A. P. Colijn,¹⁰⁶ C. Collins-Tooth,⁵³ J. Collot,⁵⁵ T. Colombo,^{58c} G. Colon,⁸⁵ G. Compostella,¹⁰⁰ P. Conde Muiño,^{125a,125b}
E. Coniavitis,¹⁶⁷ M. C. Conidi,¹² S. H. Connell,^{146b} I. A. Connelly,⁷⁶ S. M. Consonni,^{90a,90b} V. Consorti,⁴⁸
S. Constantinescu,^{26a} C. Conta,^{120a,120b} G. Conti,⁵⁷ F. Conventi,^{103a,i} M. Cooke,¹⁵ B. D. Cooper,⁷⁷ A. M. Cooper-Sarkar,¹¹⁹
N. J. Cooper-Smith,⁷⁶ K. Copic,¹⁵ T. Cornelissen,¹⁷⁶ M. Corradi,^{20a} F. Corriveau,^{86j} A. Corso-Radu,¹⁶⁴
A. Cortes-Gonzalez,¹² G. Cortiana,¹⁰⁰ G. Costa,^{90a} M. J. Costa,¹⁶⁸ D. Costanzo,¹⁴⁰ D. Côté,⁸ G. Cottin,²⁸ G. Cowan,⁷⁶
B. E. Cox,⁸³ K. Cranmer,¹⁰⁹ G. Cree,²⁹ S. Crépe-Renaudin,⁵⁵ F. Crescioli,⁷⁹ M. Crispin Ortuzar,¹¹⁹ M. Cristinziani,²¹
G. Crosetti,^{37a,37b} C.-M. Cuciuc,^{26a} C. Cuenca Almenar,¹⁷⁷ T. Cuhadar Donszelmann,¹⁴⁰ J. Cummings,¹⁷⁷ M. Curatolo,⁴⁷
C. Cuthbert,¹⁵¹ H. Czirr,¹⁴² P. Czodrowski,³ Z. Czyczula,¹⁷⁷ S. D'Auria,⁵³ M. D'Onofrio,⁷³
M. J. Da Cunha Sargedas De Sousa,^{125a,125b} C. Da Via,⁸³ W. Dabrowski,^{38a} A. Dafinca,¹¹⁹ T. Dai,⁸⁸ O. Dale,¹⁴ F. Dallaire,⁹⁴
C. Dallapiccola,⁸⁵ M. Dam,³⁶ A. C. Daniells,¹⁸ M. Dano Hoffmann,¹³⁷ V. Dao,¹⁰⁵ G. Darbo,^{50a} G. L. Darlea,^{26c} S. Darmora,⁸
J. A. Dassoulas,⁴² W. Davey,²¹ C. David,¹⁷⁰ T. Davidek,¹²⁸ E. Davies,^{119,d} M. Davies,⁹⁴ O. Davignon,⁷⁹ A. R. Davison,⁷⁷
P. Davison,⁷⁷ Y. Davygora,^{58a} E. Dawe,¹⁴³ I. Dawson,¹⁴⁰ R. K. Daya-Ishmukhametova,²³ K. De,⁸ R. de Asmundis,^{103a}
S. De Castro,^{20a,20b} S. De Cecco,⁷⁹ J. de Graat,⁹⁹ N. De Groot,¹⁰⁵ P. de Jong,¹⁰⁶ C. De La Taille,¹¹⁶ H. De la Torre,⁸¹
F. De Lorenzi,⁶³ L. De Nooij,¹⁰⁶ D. De Pedis,^{133a} A. De Salvo,^{133a} U. De Sanctis,^{165a,165c} A. De Santo,¹⁵⁰
J. B. De Vivie De Regie,¹¹⁶ G. De Zorzi,^{133a,133b} W. J. Dearnaley,⁷¹ R. Debbe,²⁵ C. Debenedetti,⁴⁶ B. Dechenaux,⁵⁵
D. V. Dedovich,⁶⁴ J. Degenhardt,¹²¹ I. Deigaard,¹⁰⁶ J. Del Peso,⁸¹ T. Del Prete,^{123a,123b} F. Deliot,¹³⁷ M. Deliyergiyev,⁷⁴
A. Dell'Acqua,³⁰ L. Dell'Asta,²² M. Dell'Orso,^{123a,123b} M. Della Pietra,^{103a,i} D. della Volpe,⁴⁹ M. Delmastro,⁵ P. A. Delsart,⁵⁵
C. Deluca,¹⁰⁶ S. Demers,¹⁷⁷ M. Demichev,⁶⁴ A. Demilly,⁷⁹ S. P. Denisov,¹²⁹ D. Derendarz,³⁹ J. E. Derkaoui,^{136d} F. Derue,⁷⁹
P. Dervan,⁷³ K. Desch,²¹ C. Deterre,⁴² P. O. Deviveiros,¹⁰⁶ A. Dewhurst,¹³⁰ S. Dhaliwal,¹⁰⁶ A. Di Ciaccio,^{134a,134b}
L. Di Ciaccio,⁵ A. Di Domenico,^{133a,133b} C. Di Donato,^{103a,103b} A. Di Girolamo,³⁰ B. Di Girolamo,³⁰ A. Di Mattia,¹⁵³
B. Di Micco,^{135a,135b} R. Di Nardo,⁴⁷ A. Di Simone,⁴⁸ R. Di Sipio,^{20a,20b} D. Di Valentino,²⁹ M. A. Diaz,^{32a} E. B. Diehl,⁸⁸
J. Dietrich,⁴² T. A. Dietzsch,^{58a} S. Diglio,⁸⁷ A. Dimitrievska,^{13a} J. Dingfelder,²¹ C. Dionisi,^{133a,133b} P. Dita,^{26a} S. Dita,^{26a}
F. Dittus,³⁰ F. Djama,⁸⁴ T. Djobava,^{51b} M. A. B. do Vale,^{24c} A. Do Valle Wemans,^{125a,125g} T. K. O. Doan,⁵ D. Dobos,³⁰
E. Dobson,⁷⁷ C. Doglioni,⁴⁹ T. Doherty,⁵³ T. Dohmae,¹⁵⁶ J. Dolejsi,¹²⁸ Z. Dolezal,¹²⁸ B. A. Dolgoshein,^{97,a} M. Donadelli,^{24d}
S. Donati,^{123a,123b} P. Dondero,^{120a,120b} J. Donini,³⁴ J. Dopke,³⁰ A. Doria,^{103a} A. Dos Anjos,¹⁷⁴ M. T. Dova,⁷⁰ A. T. Doyle,⁵³
M. Dris,¹⁰ J. Dubbert,⁸⁸ S. Dube,¹⁵ E. Dubreuil,³⁴ E. Duchovni,¹⁷³ G. Duckeck,⁹⁹ O. A. Ducu,^{26a} D. Duda,¹⁷⁶ A. Dudarev,³⁰
F. Dudziak,⁶³ L. Duflot,¹¹⁶ L. Duguid,⁷⁶ M. Dührssen,³⁰ M. Dunford,^{58a} H. Duran Yildiz,^{4a} M. Düren,⁵² A. Durglishvili,^{51b}
M. Dwuznik,^{38a} M. Dyndal,^{38a} J. Ebke,⁹⁹ W. Edson,² N. C. Edwards,⁴⁶ W. Ehrenfeld,²¹ T. Eifert,¹⁴⁴ G. Eigen,¹⁴
K. Einsweiler,¹⁵ T. Ekelof,¹⁶⁷ M. El Kacimi,^{136c} M. Ellert,¹⁶⁷ S. Elles,⁵ F. Ellinghaus,⁸² N. Ellis,³⁰ J. Elmsheuser,⁹⁹
M. Elsing,³⁰ D. Emelianov,¹³⁰ Y. Enari,¹⁵⁶ O. C. Endner,⁸² M. Endo,¹¹⁷ R. Engelmann,¹⁴⁹ J. Erdmann,¹⁷⁷ A. Ereditato,¹⁷
D. Eriksson,^{147a} G. Ernis,¹⁷⁶ J. Ernst,²⁵ M. Ernst,¹³⁷ J. Ernwein,¹³⁷ D. Errede,¹⁶⁶ S. Errede,¹⁶⁶ E. Ertel,⁸² M. Escalier,¹¹⁶
H. Esch,⁴³ C. Escobar,¹²⁴ B. Esposito,⁴⁷ A. I. Etiennevire,¹³⁷ E. Etzion,¹⁵⁴ H. Evans,⁶⁰ L. Fabbri,^{20a,20b} G. Facini,³⁰
R. M. Fakhruddinov,¹²⁹ S. Falciano,^{133a} Y. Fang,^{33a} M. Fanti,^{90a,90b} A. Farbin,⁸ A. Farilla,^{135a} T. Farooque,¹² S. Farrell,¹⁶⁴
S. M. Farrington,¹⁷¹ P. Farthouat,³⁰ F. Fassi,¹⁶⁸ P. Fassnacht,³⁰ D. Fassouliotis,⁹ A. Favareto,^{50a,50b} L. Fayard,¹¹⁶
P. Federic,^{145a} O. L. Fedin,^{122,k} W. Fedorko,¹⁶⁹ M. Fehling-Kaschek,⁴⁸ S. Feigl,³⁰ L. Feligioni,⁸⁴ C. Feng,^{33d} E. J. Feng,⁶
H. Feng,⁸⁸ A. B. Fenyuk,¹²⁹ S. Fernandez Perez,³⁰ W. Fernando,⁶ S. Ferrag,⁵³ J. Ferrando,⁵³ V. Ferrara,⁴² A. Ferrari,¹⁶⁷

- P. Ferrari,¹⁰⁶ R. Ferrari,^{120a} D. E. Ferreira de Lima,⁵³ A. Ferrer,¹⁶⁸ D. Ferrere,⁴⁹ C. Ferretti,⁸⁸ A. Ferretto Parodi,^{50a,50b}
M. Fiascaris,³¹ F. Fiedler,⁸² A. Filipčič,⁷⁴ M. Filipuzzi,⁴² F. Filthaut,¹⁰⁵ M. Fincke-Keeler,¹⁷⁰ K. D. Finelli,¹⁵¹
M. C. N. Fiolhais,^{125a,125c} L. Fiorini,¹⁶⁸ A. Firan,⁴⁰ J. Fischer,¹⁷⁶ M. J. Fisher,¹¹⁰ W. C. Fisher,⁸⁹ E. A. Fitzgerald,²³
M. Flechl,⁴⁸ I. Fleck,¹⁴² P. Fleischmann,¹⁷⁵ S. Fleischmann,¹⁷⁶ G. T. Fletcher,¹⁴⁰ G. Fletcher,⁷⁵ T. Flick,¹⁷⁶ A. Floderus,⁸⁰
L. R. Flores Castillo,¹⁷⁴ A. C. Florez Bustos,^{160b} M. J. Flowerdew,¹⁰⁰ A. Formica,¹³⁷ A. Forti,⁸³ D. Fortin,^{160a} D. Fournier,¹¹⁶
H. Fox,⁷¹ S. Fracchia,¹² P. Francavilla,¹² M. Franchini,^{20a,20b} S. Franchino,³⁰ D. Francis,³⁰ M. Franklin,⁵⁷ S. Franz,⁶¹
M. Fraternali,^{120a,120b} S. T. French,²⁸ C. Friedrich,⁴² F. Friedrich,⁴⁴ D. Froidevaux,³⁰ J. A. Frost,²⁸ C. Fukunaga,¹⁵⁷
E. Fullana Torregrosa,⁸² B. G. Fulsom,¹⁴⁴ J. Fuster,¹⁶⁸ C. Gabaldon,⁵⁵ O. Gabizon,¹⁷³ A. Gabrielli,^{20a,20b} A. Gabrielli,^{133a,133b}
S. Gadatsch,¹⁰⁶ S. Gadomski,⁴⁹ G. Gagliardi,^{50a,50b} P. Gagnon,⁶⁰ C. Galea,¹⁰⁵ B. Galhardo,^{125a,125c} E. J. Gallas,¹¹⁹ V. Gallo,¹⁷
B. J. Gallop,¹³⁰ P. Gallus,¹²⁷ G. Galster,³⁶ K. K. Gan,¹¹⁰ R. P. Gandrajula,⁶² J. Gao,^{33b,h} Y. S. Gao,^{144,f} F. M. Garay Walls,⁴⁶
F. Garberon,¹⁷⁷ C. García,¹⁶⁸ J. E. García Navarro,¹⁶⁸ M. Garcia-Sciveres,¹⁵ R. W. Gardner,³¹ N. Garelli,¹⁴⁴ V. Garonne,³⁰
C. Gatti,⁴⁷ G. Gaudio,^{120a} B. Gaur,¹⁴² L. Gauthier,⁹⁴ P. Gauzzi,^{133a,133b} I. L. Gavrilenko,⁹⁵ C. Gay,¹⁶⁹ G. Gaycken,²¹
E. N. Gazis,¹⁰ P. Ge,^{33d} Z. Gece,¹⁶⁹ C. N. P. Gee,¹³⁰ D. A. A. Geerts,¹⁰⁶ Ch. Geich-Gimbel,²¹ K. Gellerstedt,^{147a,147b}
C. Gemme,^{50a} A. Gemmell,⁵³ M. H. Genest,⁵⁵ S. Gentile,^{133a,133b} M. George,⁵⁴ S. George,⁷⁶ D. Gerbaudo,¹⁶⁴ A. Gershon,¹⁵⁴
H. Ghazlane,^{136b} N. Ghodbane,³⁴ B. Giacobbe,^{20a} S. Giagu,^{133a,133b} V. Giangiobbe,¹² P. Giannetti,^{123a,123b} F. Gianotti,³⁰
B. Gibbard,²⁵ S. M. Gibson,⁷⁶ M. Gilchriese,¹⁵ T. P. S. Gillam,²⁸ D. Gillberg,³⁰ D. M. Gingrich,^{3,e} N. Giokaris,⁹
M. P. Giordani,^{165a,165c} R. Giordano,^{103a,103b} F. M. Giorgi,¹⁶ P. F. Giraud,¹³⁷ D. Giugni,^{90a} C. Giuliani,⁴⁸ M. Giulini,^{58b}
B. K. Gjelsten,¹¹⁸ I. Gkialas,^{155,l} L. K. Gladilin,⁹⁸ C. Glasman,⁸¹ J. Glatzer,³⁰ P. C. F. Glaysheer,⁴⁶ A. Glazov,⁴² G. L. Glonti,⁶⁴
M. Goblirsch-Kolb,¹⁰⁰ J. R. Goddard,⁷⁵ J. Godfrey,¹⁴³ J. Godlewski,³⁰ C. Goeringer,⁸² S. Goldfarb,⁸⁸ T. Golling,¹⁷⁷
D. Golubkov,¹²⁹ A. Gomes,^{125a,125b,125d} L. S. Gomez Fajardo,⁴² R. Gonçalves,^{125a} J. Goncalves Pinto Firmino Da Costa,⁴²
L. Gonella,²¹ S. González de la Hoz,¹⁶⁸ G. Gonzalez Parra,¹² M. L. Gonzalez Silva,²⁷ S. Gonzalez-Sevilla,⁴⁹ L. Goossens,³⁰
P. A. Gorbounov,⁹⁶ H. A. Gordon,²⁵ I. Gorelov,¹⁰⁴ G. Gorfine,¹⁷⁶ B. Gorini,³⁰ E. Gorini,^{72a,72b} A. Gorišek,⁷⁴ E. Gornicki,³⁹
A. T. Goshaw,⁶ C. Gössling,⁴³ M. I. Gostkin,⁶⁴ M. Gouighri,^{136a} D. Goujdami,^{136c} M. P. Goulette,⁴⁹ A. G. Goussiou,¹³⁹
C. Goy,⁵ S. Gozpinar,²³ H. M. X. Grabas,¹³⁷ L. Graber,⁵⁴ I. Grabowska-Bold,^{38a} P. Grafström,^{20a,20b} K.-J. Grahn,⁴²
J. Gramling,⁴⁹ E. Gramstad,¹¹⁸ F. Grancagnolo,^{72a} S. Grancagnolo,¹⁶ V. Grassi,¹⁴⁹ V. Gratchev,¹²² H. M. Gray,³⁰
E. Graziani,^{135a} O. G. Grebenyuk,¹²² Z. D. Greenwood,^{78,m} K. Gregersen,³⁶ I. M. Gregor,⁴² P. Grenier,¹⁴⁴ J. Griffiths,⁸
N. Grigalashvili,⁶⁴ A. A. Grillo,¹³⁸ K. Grimm,⁷¹ S. Grinstein,^{12,n} Ph. Gris,³⁴ Y. V. Grishkevich,⁹⁸ J.-F. Grivaz,¹¹⁶
J. P. Grohs,⁴⁴ A. Grohsjean,⁴² E. Gross,¹⁷³ J. Grosse-Knetter,⁵⁴ G. C. Grossi,^{134a,134b} J. Groth-Jensen,¹⁷³ Z. J. Grout,¹⁵⁰
K. Grybel,¹⁴² L. Guan,^{33b} F. Guescini,⁴⁹ D. Guest,¹⁷⁷ O. Gueta,¹⁵⁴ C. Guicheney,³⁴ E. Guido,^{50a,50b} T. Guillemin,¹¹⁶
S. Guindon,² U. Gul,⁵³ C. Gumpert,⁴⁴ J. Gunther,¹²⁷ J. Guo,³⁵ S. Gupta,¹¹⁹ P. Gutierrez,¹¹² N. G. Gutierrez Ortiz,⁵³
C. Gutsche,⁷⁷ N. Guttman,¹⁵⁴ C. Guyot,¹³⁷ C. Gwenlan,¹¹⁹ C. B. Gwilliam,⁷³ A. Haas,¹⁰⁹ C. Haber,¹⁵ H. K. Hadavand,⁸
N. Haddad,^{136e} P. Haefner,²¹ S. Hageboeck,²¹ Z. Hajduk,³⁹ H. Hakobyan,¹⁷⁸ M. Haleem,⁴² D. Hall,¹¹⁹ G. Halladjian,⁸⁹
K. Hamacher,¹⁷⁶ P. Hamal,¹¹⁴ K. Hamano,⁸⁷ M. Hamer,⁵⁴ A. Hamilton,^{146a} S. Hamilton,¹⁶² P. G. Hamnett,⁴² L. Han,^{33b}
K. Hanagaki,¹¹⁷ K. Hanawa,¹⁵⁶ M. Hance,¹⁵ P. Hanke,^{58a} J. R. Hansen,³⁶ J. B. Hansen,³⁶ J. D. Hansen,³⁶ P. H. Hansen,³⁶
K. Hara,¹⁶¹ A. S. Hard,¹⁷⁴ T. Harenberg,¹⁷⁶ S. Harkusha,⁹¹ D. Harper,⁸⁸ R. D. Harrington,⁴⁶ O. M. Harris,¹³⁹ P. F. Harrison,¹⁷¹
F. Hartjes,¹⁰⁶ A. Harvey,⁵⁶ S. Hasegawa,¹⁰² Y. Hasegawa,¹⁴¹ A. Hasib,¹¹² S. Hassani,¹³⁷ S. Haug,¹⁷ M. Hauschild,³⁰
R. Hauser,⁸⁹ M. Havranek,¹²⁶ C. M. Hawkes,¹⁸ R. J. Hawkings,³⁰ A. D. Hawkins,⁸⁰ T. Hayashi,¹⁶¹ D. Hayden,⁸⁹
C. P. Hays,¹¹⁹ H. S. Hayward,⁷³ S. J. Haywood,¹³⁰ S. J. Head,¹⁸ T. Heck,⁸² V. Hedberg,⁸⁰ L. Heelan,⁸ S. Heim,¹²¹ T. Heim,¹⁷⁶
B. Heinemann,¹⁵ L. Heinrich,¹⁰⁹ S. Heisterkamp,³⁶ J. Hejbal,¹²⁶ L. Helary,²² C. Heller,⁹⁹ M. Heller,³⁰ S. Hellman,^{147a,147b}
D. Hellmich,²¹ C. Helsens,³⁰ J. Henderson,¹¹⁹ R. C. W. Henderson,⁷¹ C. Hengler,⁴² A. Henrichs,¹⁷⁷
A. M. Henriques Correia,³⁰ S. Henrot-Versille,¹¹⁶ C. Hensel,⁵⁴ G. H. Herbert,¹⁶ Y. Hernández Jiménez,¹⁶⁸
R. Herrberg-Schubert,¹⁶ G. Herten,⁴⁸ R. Hertenberger,⁹⁹ L. Hervas,³⁰ G. G. Hesketh,⁷⁷ N. P. Hessey,¹⁰⁶ R. Hickling,⁷⁵
E. Higón-Rodríguez,¹⁶⁸ J. C. Hill,²⁸ K. H. Hiller,⁴² S. Hillert,²¹ S. J. Hillier,¹⁸ I. Hinchliffe,¹⁵ E. Hines,¹²¹ M. Hirose,¹¹⁷
D. Hirschebuehl,¹⁷⁶ J. Hobbs,¹⁴⁹ N. Hod,¹⁰⁶ M. C. Hodgkinson,¹⁴⁰ P. Hodgson,¹⁴⁰ A. Hoecker,³⁰ M. R. Hoferkamp,¹⁰⁴
J. Hoffman,⁴⁰ D. Hoffmann,⁸⁴ J. I. Hofmann,^{58a} M. Hohlfeld,⁸² T. R. Holmes,¹⁵ T. M. Hong,¹²¹ L. Hooft van Huysduynen,¹⁰⁹
J.-Y. Hostachy,⁵⁵ S. Hou,¹⁵² A. Hoummada,^{136a} J. Howard,¹¹⁹ J. Howarth,⁴² M. Hrabovsky,¹¹⁴ I. Hristova,¹⁶ J. Hrivnac,¹¹⁶
T. Hryn'ova,⁵ P. J. Hsu,⁸² S.-C. Hsu,¹³⁹ D. Hu,³⁵ X. Hu,²⁵ Y. Huang,⁴² Z. Hubacek,³⁰ F. Hubaut,⁸⁴ F. Huegging,²¹
T. B. Huffman,¹¹⁹ E. W. Hughes,³⁵ G. Hughes,⁷¹ M. Huhtinen,³⁰ T. A. Hülsing,⁸² M. Hurwitz,¹⁵ N. Huseynov,^{64,c}
J. Huston,⁸⁹ J. Huth,⁵⁷ G. Iacobucci,⁴⁹ G. Iakovidis,¹⁰ I. Ibragimov,¹⁴² L. Iconomidou-Fayard,¹¹⁶ J. Idarraga,¹¹⁶ E. Ideal,¹⁷⁷

- P. Iengo,^{103a} O. Igonkina,¹⁰⁶ T. Iizawa,¹⁷² Y. Ikegami,⁶⁵ K. Ikematsu,¹⁴² M. Ikeno,⁶⁵ D. Iliadis,¹⁵⁵ N. Ilic,¹⁵⁹ Y. Inamaru,⁶⁶ T. Ince,¹⁰⁰ P. Ioannou,⁹ M. Iodice,^{135a} K. Iordanidou,⁹ V. Ippolito,⁵⁷ A. Irlles Quiles,¹⁶⁸ C. Isaksson,¹⁶⁷ M. Ishino,⁶⁷ M. Ishitsuka,¹⁵⁸ R. Ishmukhametov,¹¹⁰ C. Issever,¹¹⁹ S. Istin,^{19a} J. M. Iturbe Ponce,⁸³ A. V. Ivashin,¹²⁹ W. Iwanski,³⁹ H. Iwasaki,⁶⁵ J. M. Izen,⁴¹ V. Izzo,^{103a} B. Jackson,¹²¹ J. N. Jackson,⁷³ M. Jackson,⁷³ P. Jackson,¹ M. R. Jaekel,³⁰ V. Jain,² K. Jakobs,⁴⁸ S. Jakobsen,³⁶ T. Jakoubek,¹²⁶ J. Jakubek,¹²⁷ D. O. Jamin,¹⁵² D. K. Jana,⁷⁸ E. Jansen,⁷⁷ H. Jansen,³⁰ J. Janssen,²¹ M. Janus,¹⁷¹ G. Jarlskog,⁸⁰ T. Javůrek,⁴⁸ L. Jeanty,¹⁵ G.-Y. Jeng,¹⁵¹ D. Jennens,⁸⁷ P. Jenni,^{48,o} J. Jentzsch,⁴³ C. Jeske,¹⁷¹ S. Jézéquel,⁵ H. Ji,¹⁷⁴ W. Ji,⁸² J. Jia,¹⁴⁹ Y. Jiang,^{33b} M. Jimenez Belenguer,⁴² S. Jin,^{33a} A. Jinaru,^{26a} O. Jinnouchi,¹⁵⁸ M. D. Joergensen,³⁶ K. E. Johansson,^{147a} P. Johansson,¹⁴⁰ K. A. Johns,⁷ K. Jon-And,^{147a,147b} G. Jones,¹⁷¹ R. W. L. Jones,⁷¹ T. J. Jones,⁷³ J. Jongmanns,^{58a} P. M. Jorge,^{125a,125b} K. D. Joshi,⁸³ J. Jovicevic,¹⁴⁸ X. Ju,¹⁷⁴ C. A. Jung,⁴³ R. M. Jungst,³⁰ P. Jussel,⁶¹ A. Juste Rozas,^{12,n} M. Kaci,¹⁶⁸ A. Kaczmarek,³⁹ M. Kado,¹¹⁶ H. Kagan,¹¹⁰ M. Kagan,¹⁴⁴ E. Kajomovitz,⁴⁵ S. Kama,⁴⁰ N. Kanaya,¹⁵⁶ M. Kaneda,³⁰ S. Kaneti,²⁸ T. Kanno,¹⁵⁸ V. A. Kantserov,⁹⁷ J. Kanzaki,⁶⁵ B. Kaplan,¹⁰⁹ A. Kapliy,³¹ D. Kar,⁵³ K. Karakostas,¹⁰ N. Karastathis,¹⁰ M. Karnevskiy,⁸² S. N. Karpov,⁶⁴ K. Karthik,¹⁰⁹ V. Kartvelishvili,⁷¹ A. N. Karyukhin,¹²⁹ L. Kashif,¹⁷⁴ G. Kasieczka,^{58b} R. D. Kass,¹¹⁰ A. Kastanas,¹⁴ Y. Kataoka,¹⁵⁶ A. Katre,⁴⁹ J. Katzy,⁴² V. Kaushik,⁷ K. Kawagoe,⁶⁹ T. Kawamoto,¹⁵⁶ G. Kawamura,⁵⁴ S. Kazama,¹⁵⁶ V. F. Kazanin,¹⁰⁸ M. Y. Kazarinov,⁶⁴ R. Keeler,¹⁷⁰ P. T. Keener,¹²¹ R. Kehoe,⁴⁰ M. Keil,⁵⁴ J. S. Keller,⁴² H. Keoshkerian,⁵ O. Kepka,¹²⁶ B. P. Kerševan,⁷⁴ S. Kersten,¹⁷⁶ K. Kessoku,¹⁵⁶ J. Keung,¹⁵⁹ F. Khalil-zada,¹¹ H. Khandanyan,^{147a,147b} A. Khanov,¹¹³ A. Khodinov,⁹⁷ A. Khomich,^{58a} T. J. Khoo,²⁸ G. Khoriali,²¹ A. Khoroshilov,¹⁷⁶ V. Khovanskii,⁹⁶ E. Khramov,⁶⁴ J. Khubua,^{51b} H. Y. Kim,⁸ H. Kim,^{147a,147b} S. H. Kim,¹⁶¹ N. Kimura,¹⁷² O. Kind,¹⁶ B. T. King,⁷³ M. King,¹⁶⁸ R. S. B. King,¹¹⁹ S. B. King,¹⁶⁹ J. Kirk,¹³⁰ A. E. Kiryunin,¹⁰⁰ T. Kishimoto,⁶⁶ D. Kisielewska,^{38a} F. Kiss,⁴⁸ T. Kitamura,⁶⁶ T. Kittelmann,¹²⁴ K. Kiuchi,¹⁶¹ E. Kladiva,^{145b} M. Klein,⁷³ U. Klein,⁷³ K. Kleinknecht,⁸² P. Klimek,^{147a,147b} A. Klimentov,²⁵ R. Klingenberg,⁴³ J. A. Klinger,⁸³ E. B. Klinkby,³⁶ T. Klioutchnikova,³⁰ P. F. Klok,¹⁰⁵ E.-E. Kluge,^{58a} P. Kluit,¹⁰⁶ S. Kluth,¹⁰⁰ E. Kneringer,⁶¹ E. B. F. G. Knoop,⁸⁴ A. Knue,⁵³ T. Kobayashi,¹⁵⁶ M. Kobel,⁴⁴ M. Kocian,¹⁴⁴ P. Kodys,¹²⁸ P. Koevesarki,²¹ T. Koffas,²⁹ E. Koffeman,¹⁰⁶ L. A. Kogan,¹¹⁹ S. Kohlmann,¹⁷⁶ Z. Kohout,¹²⁷ T. Kohriki,⁶⁵ T. Koi,¹⁴⁴ H. Kolanoski,¹⁶ I. Koletsou,⁵ J. Koll,⁸⁹ A. A. Komar,^{95a} Y. Komori,¹⁵⁶ T. Kondo,⁶⁵ K. Köneke,⁴⁸ A. C. König,¹⁰⁵ S. König,⁸² T. Kono,^{65,p} R. Konoplich,^{109,q} N. Konstantinidis,⁷⁷ R. Kopeliansky,¹⁵³ S. Koperny,^{38a} L. Köpke,⁸² A. K. Kopp,⁴⁸ K. Korcyl,³⁹ K. Kordas,¹⁵⁵ A. Korn,⁷⁷ A. A. Korol,¹⁰⁸ I. Korolkov,¹² E. V. Korolkova,¹⁴⁰ V. A. Korotkov,¹²⁹ O. Kortner,¹⁰⁰ S. Kortner,¹⁰⁰ V. V. Kostyukhin,²¹ S. Kotov,¹⁰⁰ V. M. Kotov,⁶⁴ A. Kotwal,⁴⁵ C. Kourkoumelis,⁹ V. Kouskoura,¹⁵⁵ A. Koutsman,^{160a} R. Kowalewski,¹⁷⁰ T. Z. Kowalski,^{38a} W. Kozanecki,¹³⁷ A. S. Kozhin,¹²⁹ V. Kral,¹²⁷ V. A. Kramarenko,⁹⁸ G. Kramberger,⁷⁴ D. Krasnoperov,⁹⁷ M. W. Krasny,⁷⁹ A. Krasznahorkay,³⁰ J. K. Kraus,²¹ A. Kravchenko,²⁵ S. Kreiss,¹⁰⁹ M. Kretz,^{58c} J. Kretzschmar,⁷³ K. Kreutzfeldt,⁵² P. Krieger,¹⁵⁹ K. Kroeninger,⁵⁴ H. Kroha,¹⁰⁰ J. Kroll,¹²¹ J. Kroseberg,²¹ J. Krstic,^{13a} U. Kruchonak,⁶⁴ H. Krüger,²¹ T. Kruker,¹⁷ N. Krumnack,⁶³ Z. V. Krumshcheyn,⁶⁴ A. Kruse,¹⁷⁴ M. C. Kruse,⁴⁵ M. Kruskal,²² T. Kubota,⁸⁷ S. Kuday,^{4a} S. Kuehn,⁴⁸ A. Kugel,^{58c} A. Kuhl,¹³⁸ T. Kuhl,⁴² V. Kukhtin,⁶⁴ Y. Kulchitsky,⁹¹ S. Kuleshov,^{32b} M. Kuna,^{133a,133b} J. Kunkle,¹²¹ A. Kupco,¹²⁶ H. Kurashige,⁶⁶ Y. A. Kurochkin,⁹¹ R. Kurumida,⁶⁶ V. Kus,¹²⁶ E. S. Kuwertz,¹⁴⁸ M. Kuze,¹⁵⁸ J. Kvita,¹⁴³ A. La Rosa,⁴⁹ L. La Rotonda,^{37a,37b} L. Labarga,⁸¹ C. Lacasta,¹⁶⁸ F. Lacava,^{133a,133b} J. Lacey,²⁹ H. Lacker,¹⁶ D. Lacour,⁷⁹ V. R. Lacuesta,¹⁶⁸ E. Ladygin,⁶⁴ R. Lafaye,⁵ B. Laforge,⁷⁹ T. Lagouri,¹⁷⁷ S. Lai,⁴⁸ H. Laier,^{58a} L. Lambourne,⁷⁷ S. Lammers,⁶⁰ C. L. Lampen,⁷ W. Lampl,⁷ E. Lançon,¹³⁷ U. Landgraf,⁴⁸ M. P. J. Landon,⁷⁵ V. S. Lang,^{58a} C. Lange,⁴² A. J. Lankford,¹⁶⁴ F. Lanni,²⁵ K. Lantzsch,³⁰ S. Laplace,⁷⁹ C. Lapoire,²¹ J. F. Laporte,¹³⁷ T. Lari,^{90a} M. Lassnig,³⁰ P. Laurelli,⁴⁷ V. Lavorini,^{37a,37b} W. Lavrijsen,¹⁵ A. T. Law,¹³⁸ P. Laycock,⁷³ B. T. Le,⁵⁵ O. Le Dortz,⁷⁹ E. Le Guirriec,⁸⁴ E. Le Menedeu,¹² T. LeCompte,⁶ F. Ledroit-Guillon,⁵⁵ C. A. Lee,¹⁵² H. Lee,¹⁰⁶ J. S. H. Lee,¹¹⁷ S. C. Lee,¹⁵² L. Lee,¹⁷⁷ G. Lefebvre,⁷⁹ M. Lefebvre,¹⁷⁰ F. Legger,⁹⁹ C. Leggett,¹⁵ A. Lehan,⁷³ M. Lehmann,²¹ G. Lehmann Miotto,³⁰ X. Lei,⁷ A. G. Leister,¹⁷⁷ M. A. L. Leite,^{24d} R. Leitner,¹²⁸ D. Lellouch,¹⁷³ B. Lemmer,⁵⁴ K. J. C. Leney,⁷⁷ T. Lenz,¹⁰⁶ G. Lenzen,¹⁷⁶ B. Lenzi,³⁰ R. Leone,⁷ K. Leonhardt,⁴⁴ S. Leontsinis,¹⁰ C. Leroy,⁹⁴ C. G. Lester,²⁸ C. M. Lester,¹²¹ J. Levêque,⁵ D. Levin,⁸⁸ L. J. Levinson,¹⁷³ M. Levy,¹⁸ A. Lewis,¹¹⁹ G. H. Lewis,¹⁰⁹ A. M. Leyko,²¹ M. Leyton,⁴¹ B. Li,^{33b,r} B. Li,⁸⁴ H. Li,¹⁴⁹ H. L. Li,³¹ S. Li,⁴⁵ X. Li,⁸⁸ Y. Li,^{33c,s} Z. Liang,^{119,t} H. Liao,³⁴ B. Liberti,^{134a} P. Lichard,³⁰ K. Lie,¹⁶⁶ J. Liebal,²¹ W. Liebig,¹⁴ C. Limbach,²¹ A. Limosani,⁸⁷ M. Limper,⁶² S. C. Lin,^{152,u} F. Linde,¹⁰⁶ B. E. Lindquist,¹⁴⁹ J. T. Linnemann,⁸⁹ E. Lipeles,¹²¹ A. Lipniacka,¹⁴ M. Lisovyi,⁴² T. M. Liss,¹⁶⁶ D. Lissauer,²⁵ A. Lister,¹⁶⁹ A. M. Litke,¹³⁸ B. Liu,¹⁵² D. Liu,¹⁵² J. B. Liu,^{33b} K. Liu,^{33b,v} L. Liu,⁸⁸ M. Liu,⁴⁵ M. Liu,^{33b} Y. Liu,^{33b} M. Livan,^{120a,120b} S. S. A. Livermore,¹¹⁹ A. Lleres,⁵⁵ J. Llorente Merino,⁸¹ S. L. Lloyd,⁷⁵ F. Lo Sterzo,¹⁵² E. Lobodzinska,⁴² P. Loch,⁷ W. S. Lockman,¹³⁸ T. Loddenkoetter,²¹ F. K. Loebinger,⁸³ A. E. Loevschall-Jensen,³⁶ A. Loginov,¹⁷⁷ C. W. Loh,¹⁶⁹ T. Lohse,¹⁶ K. Lohwasser,⁴⁸ M. Lokajicek,¹²⁶

V. P. Lombardo,⁵ J. D. Long,⁸⁸ R. E. Long,⁷¹ L. Lopes,^{125a} D. Lopez Mateos,⁵⁷ B. Lopez Paredes,¹⁴⁰ J. Lorenz,⁹⁹ N. Lorenzo Martinez,⁶⁰ M. Losada,¹⁶³ P. Loscutoff,¹⁵ M. J. Losty,^{160a,a} X. Lou,⁴¹ A. Lounis,¹¹⁶ J. Love,⁶ P. A. Love,⁷¹ A. J. Lowe,^{144,f} F. Lu,^{33a} H. J. Lubatti,¹³⁹ C. Luci,^{133a,133b} A. Lucotte,⁵⁵ F. Luehring,⁶⁰ W. Lukas,⁶¹ L. Luminari,^{133a} O. Lundberg,^{147a,147b} B. Lund-Jensen,¹⁴⁸ M. Lungwitz,⁸² D. Lynn,²⁵ R. Lysak,¹²⁶ E. Lytken,⁸⁰ H. Ma,²⁵ L. L. Ma,^{33d} G. Maccarrone,⁴⁷ A. Macchiolo,¹⁰⁰ B. Maček,⁷⁴ J. Machado Miguens,^{125a,125b} D. Macina,³⁰ D. Madaffari,⁸⁴ R. Madar,⁴⁸ H. J. Maddocks,⁷¹ W. F. Mader,⁴⁴ A. Madsen,¹⁶⁷ M. Maeno,⁸ T. Maeno,²⁵ E. Magradze,⁵⁴ K. Mahboubi,⁴⁸ J. Mahlstedt,¹⁰⁶ S. Mahmoud,⁷³ C. Maiani,¹³⁷ C. Maidantchik,^{24a} A. Maio,^{125a,125b,125d} S. Majewski,¹¹⁵ Y. Makida,⁶⁵ N. Makovec,¹¹⁶ P. Mal,^{137,w} B. Malaescu,⁷⁹ Pa. Malecki,³⁹ V. P. Maleev,¹²² F. Malek,⁵⁵ U. Mallik,⁶² D. Malon,⁶ C. Malone,¹⁴⁴ S. Maltezos,¹⁰ V. M. Malyshev,¹⁰⁸ S. Malyukov,³⁰ J. Mamuzic,^{13b} B. Mandelli,³⁰ L. Mandelli,^{90a} I. Mandić,⁷⁴ R. Mandrysch,⁶² J. Maneira,^{125a,125b} A. Manfredini,¹⁰⁰ L. Manhaes de Andrade Filho,^{24b} J. A. Manjarres Ramos,^{160b} A. Mann,⁹⁹ P. M. Manning,¹³⁸ A. Manousakis-Katsikakis,⁹ B. Mansoulie,¹³⁷ R. Mantifel,⁸⁶ L. Mapelli,³⁰ L. March,¹⁶⁸ J. F. Marchand,²⁹ F. Marchese,^{134a,134b} G. Marchiori,⁷⁹ M. Marcisovsky,¹²⁶ C. P. Marino,¹⁷⁰ C. N. Marques,^{125a} F. Marroquim,^{24a} S. P. Marsden,⁸³ Z. Marshall,¹⁵ L. F. Marti,¹⁷ S. Marti-Garcia,¹⁶⁸ B. Martin,³⁰ B. Martin,⁸⁹ J. P. Martin,⁹⁴ T. A. Martin,¹⁷¹ V. J. Martin,⁴⁶ B. Martin dit Latour,⁴⁹ H. Martinez,¹³⁷ M. Martinez,^{12,n} S. Martin-Haugh,¹³⁰ A. C. Martyniuk,⁷⁷ M. Marx,¹³⁹ F. Marzano,^{133a} A. Marzin,³⁰ L. Masetti,⁸² T. Mashimo,¹⁵⁶ R. Mashinistov,⁹⁵ J. Masik,⁸³ A. L. Maslennikov,¹⁰⁸ I. Massa,^{20a,20b} N. Massol,⁵ P. Mastrandrea,¹⁴⁹ A. Mastroberardino,^{37a,37b} T. Masubuchi,¹⁵⁶ P. Matricon,¹¹⁶ H. Matsunaga,¹⁵⁶ T. Matsushita,⁶⁶ P. Mättig,¹⁷⁶ S. Mättig,⁴² J. Mattmann,⁸² J. Maurer,^{26a} S. J. Maxfield,⁷³ D. A. Maximov,^{108,g} R. Mazini,¹⁵² L. Mazzaferro,^{134a,134b} G. Mc Goldrick,¹⁵⁹ S. P. Mc Kee,⁸⁸ A. McCarn,⁸⁸ R. L. McCarthy,¹⁴⁹ T. G. McCarthy,²⁹ N. A. McCubbin,¹³⁰ K. W. McFarlane,^{56,a} J. A. McFayden,⁷⁷ G. Mchedlidze,⁵⁴ T. McLaughlan,¹⁸ S. J. McMahon,¹³⁰ R. A. McPherson,^{170,j} A. Meade,⁸⁵ J. Mechnich,¹⁰⁶ M. Medinnis,⁴² S. Meehan,³¹ R. Meera-Lebbai,¹¹² S. Mehlhase,³⁶ A. Mehta,⁷³ K. Meier,^{58a} C. Meineck,⁹⁹ B. Meirose,⁸⁰ C. Melachrinou,³¹ B. R. Mellado Garcia,^{146c} F. Meloni,^{90a,90b} L. Mendoza Navas,¹⁶³ A. Mengarelli,^{20a,20b} S. Menke,¹⁰⁰ E. Meoni,¹⁶² K. M. Mercurio,⁵⁷ S. Mergelmeyer,²¹ N. Meric,¹³⁷ P. Mermod,⁴⁹ L. Merola,^{103a,103b} C. Meroni,^{90a} F. S. Merritt,³¹ H. Merritt,¹¹⁰ A. Messina,^{30,x} J. Metcalfe,²⁵ A. S. Mete,¹⁶⁴ C. Meyer,⁸² C. Meyer,³¹ J-P. Meyer,¹³⁷ J. Meyer,³⁰ R. P. Middleton,¹³⁰ S. Migas,⁷³ L. Mijović,¹³⁷ G. Mikenberg,¹⁷³ M. Mikestikova,¹²⁶ M. Mikuž,⁷⁴ D. W. Miller,³¹ C. Mills,⁴⁶ A. Milov,¹⁷³ D. A. Milstead,^{147a,147b} D. Milstein,¹⁷³ A. A. Minaenko,¹²⁹ M. Miñano Moya,¹⁶⁸ I. A. Minashvili,⁶⁴ A. I. Mincer,¹⁰⁹ B. Mindur,^{38a} M. Mineev,⁶⁴ Y. Ming,¹⁷⁴ L. M. Mir,¹² G. Mirabelli,^{133a} T. Mitani,¹⁷² J. Mitrevski,⁹⁹ V. A. Mitsou,¹⁶⁸ S. Mitsui,⁶⁵ A. Miucci,⁴⁹ P. S. Miyagawa,¹⁴⁰ J. U. Mjörnmark,⁸⁰ T. Moa,^{147a,147b} K. Mochizuki,⁸⁴ V. Moeller,²⁸ S. Mohapatra,³⁵ W. Mohr,⁴⁸ S. Molander,^{147a,147b} R. Moles-Valls,¹⁶⁸ K. Mönig,⁴² C. Monini,⁵⁵ J. Monk,³⁶ E. Monnier,⁸⁴ J. Montejo Berlingen,¹² F. Monticelli,⁷⁰ S. Monzani,^{133a,133b} R. W. Moore,³ C. Mora Herrera,⁴⁹ A. Moraes,⁵³ N. Morange,⁶² J. Morel,⁵⁴ D. Moreno,⁸² M. Moreno Llácer,⁵⁴ P. Morettini,^{50a} M. Morgenstern,⁴⁴ M. Morii,⁵⁷ S. Moritz,⁸² A. K. Morley,¹⁴⁸ G. Mornacchi,³⁰ J. D. Morris,⁷⁵ L. Morvaj,¹⁰² H. G. Moser,¹⁰⁰ M. Mosidze,^{51b} J. Moss,¹¹⁰ R. Mount,¹⁴⁴ E. Mountricha,²⁵ S. V. Mouraviev,^{95,a} E. J. W. Moyse,⁸⁵ S. Muanza,⁸⁴ R. D. Mudd,¹⁸ F. Mueller,^{58a} J. Mueller,¹²⁴ K. Mueller,²¹ T. Mueller,²⁸ T. Mueller,⁸² D. Muenstermann,⁴⁹ Y. Munwes,¹⁵⁴ J. A. Murillo Quijada,¹⁸ W. J. Murray,^{171,130} E. Musto,¹⁵³ A. G. Myagkov,^{129,y} M. Myska,¹²⁶ O. Nackenhorst,⁵⁴ J. Nadal,⁵⁴ K. Nagai,⁶¹ R. Nagai,¹⁵⁸ Y. Nagai,⁸⁴ K. Nagano,⁶⁵ A. Nagarkar,¹¹⁰ Y. Nagasaka,⁵⁹ M. Nagel,¹⁰⁰ A. M. Nairz,³⁰ Y. Nakahama,³⁰ K. Nakamura,⁶⁵ T. Nakamura,¹⁵⁶ I. Nakano,¹¹¹ H. Namasivayam,⁴¹ G. Nanava,²¹ R. Narayan,^{58b} T. Nattermann,²¹ T. Naumann,⁴² G. Navarro,¹⁶³ R. Nayyar,⁷ H. A. Neal,⁸⁸ P. Yu. Nechaeva,⁹⁵ T. J. Neep,⁸³ A. Negri,^{120a,120b} G. Negri,³⁰ M. Negrini,^{20a} S. Nektarijevic,⁴⁹ A. Nelson,¹⁶⁴ T. K. Nelson,¹⁴⁴ S. Nemecek,¹²⁶ P. Nemethy,¹⁰⁹ A. A. Nepomuceno,^{24a} M. Nessi,^{30,z} M. S. Neubauer,¹⁶⁶ M. Neumann,¹⁷⁶ R. M. Neves,¹⁰⁹ P. Nevski,²⁵ F. M. Newcomer,¹²¹ P. R. Newman,¹⁸ D. H. Nguyen,⁶ R. B. Nickerson,¹¹⁹ R. Nicolaidou,¹³⁷ B. Niquevert,³⁰ J. Nielsen,¹³⁸ N. Nikiforou,³⁵ A. Nikiforov,¹⁶ V. Nikolaenko,^{129,y} I. Nikolic-Audit,⁷⁹ K. Nikolics,⁴⁹ K. Nikolopoulos,¹⁸ P. Nilsson,⁸ Y. Ninomiya,¹⁵⁶ A. Nisati,^{133a} R. Nisius,¹⁰⁰ T. Nobe,¹⁵⁸ L. Nodulman,⁶ M. Nomachi,¹¹⁷ I. Nomidis,¹⁵⁵ S. Norberg,¹¹² M. Nordberg,³⁰ J. Novakova,¹²⁸ S. Nowak,¹⁰⁰ M. Nozaki,⁶⁵ L. Nozka,¹¹⁴ K. Ntekas,¹⁰ G. Nunes Hanninger,⁸⁷ T. Nunnemann,⁹⁹ E. Nurse,⁷⁷ F. Nuti,⁸⁷ B. J. O'Brien,⁴⁶ F. O'grady,⁷ D. C. O'Neil,¹⁴³ V. O'Shea,⁵³ F. G. Oakham,^{29,e} H. Oberlack,¹⁰⁰ T. Obermann,²¹ J. Ocariz,⁷⁹ A. Ochi,⁶⁶ M. I. Ochoa,⁷⁷ S. Oda,⁶⁹ S. Odaka,⁶⁵ H. Ogren,⁶⁰ A. Oh,⁸³ S. H. Oh,⁴⁵ C. C. Ohm,³⁰ H. Ohman,¹⁶⁷ T. Ohshima,¹⁰² W. Okamura,¹¹⁷ H. Okawa,²⁵ Y. Okumura,³¹ T. Okuyama,¹⁵⁶ A. Olariu,^{26a} A. G. Olchevski,⁶⁴ S. A. Olivares Pino,⁴⁶ D. Oliveira Damazio,²⁵ E. Oliver Garcia,¹⁶⁸ D. Olivito,¹²¹ A. Olszewski,³⁹ J. Olszowska,³⁹ A. Onofre,^{125a,125e} P. U. E. Onyisi,^{31,aa} C. J. Oram,^{160a} M. J. Oreglia,³¹ Y. Oren,¹⁵⁴ D. Orestano,^{135a,135b} N. Orlando,^{72a,72b} C. Oropeza Barrera,⁵³ R. S. Orr,¹⁵⁹ B. Osculati,^{50a,50b} R. Ospanov,¹²¹ G. Otero y Garzon,²⁷ H. Otono,⁶⁹

- M. Ouchrif,^{136d} E. A. Ouellette,¹⁷⁰ F. Ould-Saada,¹¹⁸ A. Ouraou,¹³⁷ K. P. Oussoren,¹⁰⁶ Q. Ouyang,^{33a} A. Ovcharova,¹⁵
M. Owen,⁸³ V. E. Ozcan,^{19a} N. Ozturk,⁸ K. Pachal,¹¹⁹ A. Pacheco Pages,¹² C. Padilla Aranda,¹² M. Pagáčová,⁴⁸
S. Pagan Griso,¹⁵ E. Paganis,¹⁴⁰ C. Pahl,¹⁰⁰ F. Paige,²⁵ P. Pais,⁸⁵ K. Pajchel,¹¹⁸ G. Palacino,^{160b} S. Palestini,³⁰ D. Pallin,³⁴
A. Palma,^{125a,125b} J. D. Palmer,¹⁸ Y. B. Pan,¹⁷⁴ E. Panagiotopoulou,¹⁰ J. G. Panduro Vazquez,⁷⁶ P. Pani,¹⁰⁶ N. Panikashvili,⁸⁸
S. Panitkin,²⁵ D. Pantea,^{26a} L. Paolozzi,^{134a,134b} Th. D. Papadopoulou,¹⁰ K. Papageorgiou,^{155,1} A. Paramonov,⁶
D. Paredes Hernandez,³⁴ M. A. Parker,²⁸ F. Parodi,^{50a,50b} J. A. Parsons,³⁵ U. Parzefall,⁴⁸ E. Pasqualucci,^{133a} S. Passaggio,^{50a}
A. Passeri,^{135a} F. Pastore,^{135a,135b,a} Fr. Pastore,⁷⁶ G. Pásztor,^{49,bb} S. Patariaia,¹⁷⁶ N. D. Patel,¹⁵¹ J. R. Pater,⁸³
S. Patricelli,^{103a,103b} T. Pauly,³⁰ J. Pearce,¹⁷⁰ M. Pedersen,¹¹⁸ S. Pedraza Lopez,¹⁶⁸ R. Pedro,^{125a,125b} S. V. Peleganchuk,¹⁰⁸
D. Pelikan,¹⁶⁷ H. Peng,^{33b} B. Penning,³¹ J. Penwell,⁶⁰ D. V. Perepelitsa,²⁵ E. Perez Codina,^{160a} M. T. Pérez García-Estañ,¹⁶⁸
V. Perez Reale,³⁵ L. Perini,^{90a,90b} H. Pernegger,³⁰ R. Perrino,^{72a} R. Peschke,⁴² V. D. Peshekhonov,⁶⁴ K. Peters,³⁰
R. F. Y. Peters,⁸³ B. A. Petersen,⁸⁷ J. Petersen,³⁰ T. C. Petersen,³⁶ E. Petit,⁴² A. Petridis,^{147a,147b} C. Petridou,¹⁵⁵ E. Petrolo,^{133a}
F. Petrucci,^{135a,135b} M. Petteni,¹⁴³ N. E. Pettersson,¹⁵⁸ R. Pezoa,^{32b} P. W. Phillips,¹³⁰ G. Piacquadio,¹⁴⁴ E. Pianori,¹⁷¹
A. Picazio,⁴⁹ E. Piccaro,⁷⁵ M. Piccinini,^{20a,20b} S. M. Piec,⁴² R. Piegaiia,²⁷ D. T. Pignotti,¹¹⁰ J. E. Pilcher,³¹ A. D. Pilkington,⁷⁷
J. Pina,^{125a,125b,125d} M. Pinamonti,^{165a,165c,cc} A. Pinder,¹¹⁹ J. L. Pinfold,³ A. Pingel,³⁶ B. Pinto,^{125a} S. Pires,⁷⁹ C. Pizio,^{90a,90b}
M.-A. Pleier,²⁵ V. Pleskot,¹²⁸ E. Plotnikova,⁶⁴ P. Plucinski,^{147a,147b} S. Poddar,^{58a} F. Podlyski,³⁴ R. Poettgen,⁸² L. Poggioli,¹¹⁶
D. Pohl,²¹ M. Pohl,⁴⁹ G. Polesello,^{120a} A. Policicchio,^{37a,37b} R. Polifka,¹⁵⁹ A. Polini,^{20a} C. S. Pollard,⁴⁵ V. Polychronakos,²⁵
K. Pommès,³⁰ L. Pontecorvo,^{133a} B. G. Pope,⁸⁹ G. A. Popeneciu,^{26b} D. S. Popovic,^{13a} A. Poppleton,³⁰ X. Portell Bueso,¹²
G. E. Pospelov,¹⁰⁰ S. Pospisil,¹²⁷ K. Potamianos,¹⁵ I. N. Potrap,⁶⁴ C. J. Potter,¹⁵⁰ C. T. Potter,¹¹⁵ G. Poulard,³⁰ J. Poveda,⁶⁰
V. Pozdnyakov,⁶⁴ R. Prabhu,⁷⁷ P. Pralavorio,⁸⁴ A. Pranko,¹⁵ S. Prasad,³⁰ R. Pravahan,⁸ S. Prell,⁶³ D. Price,⁸³ J. Price,⁷³
L. E. Price,⁶ D. Prieur,¹²⁴ M. Primavera,^{72a} M. Proissl,⁴⁶ K. Prokofiev,⁴⁷ F. Prokoshin,^{32b} E. Protopapadaki,¹³⁷
S. Protopopescu,²⁵ J. Proudfoot,⁶ M. Przybycien,^{38a} H. Przysiezniak,⁵ E. Ptacek,¹¹⁵ E. Pueschel,⁸⁵ D. Puldon,¹⁴⁹
M. Purohit,^{25,dd} P. Puzo,¹¹⁶ Y. Pylypchenko,⁶² J. Qian,⁸⁸ G. Qin,⁵³ A. Quadt,⁵⁴ D. R. Quarrie,¹⁵ W. B. Quayle,^{165a,165b}
D. Quilty,⁵³ A. Qureshi,^{160b} V. Radeka,²⁵ V. Radescu,⁴² S. K. Radhakrishnan,¹⁴⁹ P. Radloff,¹¹⁵ P. Rados,⁸⁷ F. Ragusa,^{90a,90b}
G. Rahal,¹⁷⁹ S. Rajagopalan,²⁵ M. Rammensee,³⁰ M. Rammes,¹⁴² A. S. Randle-Conde,⁴⁰ C. Rangel-Smith,⁷⁹ K. Rao,¹⁶⁴
F. Rauscher,⁹⁹ T. C. Rave,⁴⁸ T. Ravenscroft,⁵³ M. Raymond,³⁰ A. L. Read,¹¹⁸ D. M. Rebuffi,^{120a,120b} A. Redelbach,¹⁷⁵
G. Redlinger,²⁵ R. Reece,¹³⁸ K. Reeves,⁴¹ L. Rehnisch,¹⁶ A. Reinsch,¹¹⁵ H. Reisin,²⁷ M. Relich,¹⁶⁴ C. Rembser,³⁰
Z. L. Ren,¹⁵² A. Renaud,¹¹⁶ M. Rescigno,^{133a} S. Resconi,^{90a} B. Resende,¹³⁷ P. Reznicek,¹²⁸ R. Rezvani,⁹⁴ R. Richter,¹⁰⁰
M. Ridel,⁷⁹ P. Rieck,¹⁶ M. Rijssenbeek,¹⁴⁹ A. Rimoldi,^{120a,120b} L. Rinaldi,^{20a} E. Ritsch,⁶¹ I. Riu,¹² F. Rizatdinova,¹¹³
E. Rizvi,⁷⁵ S. H. Robertson,^{86,j} A. Robichaud-Veronneau,¹¹⁹ D. Robinson,²⁸ J. E. M. Robinson,⁸³ A. Robson,⁵³
C. Roda,^{123a,123b} L. Rodrigues,³⁰ S. Roe,³⁰ O. Røhne,¹¹⁸ S. Rolli,¹⁶² A. Romaniouk,⁹⁷ M. Romano,^{20a,20b} G. Romeo,²⁷
E. Romero Adam,¹⁶⁸ N. Rompotis,¹³⁹ L. Roos,⁷⁹ E. Ros,¹⁶⁸ S. Rosati,^{133a} K. Rosbach,⁴⁹ A. Rose,¹⁵⁰ M. Rose,⁷⁶
P. L. Rosendahl,¹⁴ O. Rosenthal,¹⁴² V. Rossetti,^{147a,147b} E. Rossi,^{103a,103b} L. P. Rossi,^{50a} R. Rosten,¹³⁹ M. Rotaru,^{26a} I. Roth,¹⁷³
J. Rothberg,¹³⁹ D. Rousseau,¹¹⁶ C. R. Royon,¹³⁷ A. Rozanov,⁸⁴ Y. Rozen,¹⁵³ X. Ruan,^{146c} F. Rubbo,¹² I. Rubinskiy,⁴²
V. I. Rud,⁹⁸ C. Rudolph,⁴⁴ M. S. Rudolph,¹⁵⁹ F. Rühr,⁴⁸ A. Ruiz-Martinez,⁶³ Z. Rurikova,⁴⁸ N. A. Rusakovich,⁶⁴
A. Ruschke,⁹⁹ J. P. Rutherford,⁷ N. Ruthmann,⁴⁸ Y. F. Ryabov,¹²² M. Rybar,¹²⁸ G. Rybkin,¹¹⁶ N. C. Ryder,¹¹⁹
A. F. Saavedra,¹⁵¹ S. Sacerdoti,²⁷ A. Saddique,³ I. Sadeh,¹⁵⁴ H. F.-W. Sadrozinski,¹³⁸ R. Sadykov,⁶⁴ F. Safai Tehrani,^{133a}
H. Sakamoto,¹⁵⁶ Y. Sakurai,¹⁷² G. Salamanna,⁷⁵ A. Salamon,^{134a} M. Saleem,¹¹² D. Salek,¹⁰⁶ P. H. Sales De Bruin,¹³⁹
D. Salihagic,¹⁰⁰ A. Salkov,¹⁴⁴ J. Salt,¹⁶⁸ B. M. Salvachua Ferrando,⁶ D. Salvatore,^{37a,37b} F. Salvatore,¹⁵⁰ A. Salvucci,¹⁰⁵
A. Salzburger,³⁰ D. Sampsonidis,¹⁵⁵ A. Sanchez,^{103a,103b} J. Sánchez,¹⁶⁸ V. Sanchez Martinez,¹⁶⁸ H. Sandaker,¹⁴
H. G. Sander,⁸² M. P. Sanders,⁹⁹ M. Sandhoff,¹⁷⁶ T. Sandoval,²⁸ C. Sandoval,¹⁶³ R. Sandstroem,¹⁰⁰ D. P. C. Sankey,¹³⁰
A. Sansoni,⁴⁷ C. Santoni,³⁴ R. Santonico,^{134a,134b} H. Santos,^{125a} I. Santoyo Castillo,¹⁵⁰ K. Sapp,¹²⁴ A. Saponov,⁶⁴
J. G. Saraiva,^{125a,125d} B. Sarrazin,²¹ G. Sartisohn,¹⁷⁶ O. Sasaki,⁶⁵ Y. Sasaki,¹⁵⁶ I. Satsounkevitch,⁹¹ G. Sauvage,^{5,a} E. Sauvan,⁵
P. Savard,^{159,e} D. O. Savu,³⁰ C. Sawyer,¹¹⁹ L. Sawyer,^{78,m} D. H. Saxon,⁵³ J. Saxon,¹²¹ C. Sbarra,^{20a} A. Sbrizzi,³ T. Scanlon,³⁰
D. A. Scannicchio,¹⁶⁴ M. Scarcella,¹⁵¹ J. Schaarschmidt,¹⁷³ P. Schacht,¹⁰⁰ D. Schaefer,¹²¹ R. Schaefer,⁴² A. Schaelicke,⁴⁶
S. Schaepe,²¹ S. Schaezel,^{58b} U. Schäfer,⁸² A. C. Schaffer,¹¹⁶ D. Schaile,⁹⁹ R. D. Schamberger,¹⁴⁹ V. Scharf,^{58a}
V. A. Schegelsky,¹²² D. Scheirich,¹²⁸ M. Schernau,¹⁶⁴ M. I. Scherzer,³⁵ C. Schiavi,^{50a,50b} J. Schieck,⁹⁹ C. Schillo,⁴⁸
M. Schioppa,^{37a,37b} S. Schlenker,³⁰ E. Schmidt,⁴⁸ K. Schmieden,³⁰ C. Schmitt,⁸² C. Schmitt,⁹⁹ S. Schmitt,^{58b} B. Schneider,¹⁷
Y. J. Schnellbach,⁷³ U. Schnoor,⁴⁴ L. Schoeffel,¹³⁷ A. Schoening,^{58b} B. D. Schoenrock,⁸⁹ A. L. S. Schorlemmer,⁵⁴
M. Schott,⁸² D. Schouten,^{160a} J. Schovancova,²⁵ M. Schram,⁸⁶ S. Schramm,¹⁵⁹ M. Schreyer,¹⁷⁵ C. Schroeder,⁸² N. Schuh,⁸²

M. J. Schultens,²¹ H.-C. Schultz-Coulon,^{58a} H. Schulz,¹⁶ M. Schumacher,⁴⁸ B. A. Schumm,¹³⁸ Ph. Schune,¹³⁷
 A. Schwartzman,¹⁴⁴ Ph. Schwegler,¹⁰⁰ Ph. Schwemling,¹³⁷ R. Schwienhorst,⁸⁹ J. Schwindling,¹³⁷ T. Schwindt,²¹
 M. Schwoerer,⁵ F. G. Sciacca,¹⁷ E. Scifo,¹¹⁶ G. Sciolla,²³ W. G. Scott,¹³⁰ F. Scuri,^{123a,123b} F. Scutti,²¹ J. Searcy,⁸⁸ G. Sedov,⁴²
 E. Sedykh,¹²² S. C. Seidel,¹⁰⁴ A. Seiden,¹³⁸ F. Seifert,¹²⁷ J. M. Seixas,^{24a} G. Sekhniaidze,^{103a} S. J. Sekula,⁴⁰ K. E. Selbach,⁴⁶
 D. M. Seliverstov,^{122,a} G. Sellers,⁷³ N. Semprini-Cesari,^{20a,20b} C. Serfon,³⁰ L. Serin,¹¹⁶ L. Serkin,⁵⁴ T. Serre,⁸⁴ R. Seuster,^{160a}
 H. Severini,¹¹² F. Sforza,¹⁰⁰ A. Sfyrta,³⁰ E. Shabalina,⁵⁴ M. Shamim,¹¹⁵ L. Y. Shan,^{33a} J. T. Shank,²² Q. T. Shao,⁸⁷
 M. Shapiro,¹⁵ P. B. Shatalov,⁹⁶ K. Shaw,^{165a,165b} P. Sherwood,⁷⁷ S. Shimizu,⁶⁶ C. O. Shimmin,¹⁶⁴ M. Shimojima,¹⁰¹ T. Shin,⁵⁶
 M. Shiyakova,⁶⁴ A. Shmeleva,⁹⁵ M. J. Shochet,³¹ D. Short,¹¹⁹ S. Shrestha,⁶³ E. Shulga,⁹⁷ M. A. Shupe,⁷ S. Shushkevich,⁴²
 P. Sicho,¹²⁶ D. Sidorov,¹¹³ A. Sidoti,^{133a} F. Siegert,⁴⁴ Dj. Sijacki,^{13a} O. Silbert,¹⁷³ J. Silva,^{125a,125d} Y. Silver,¹⁵⁴
 D. Silverstein,¹⁴⁴ S. B. Silverstein,^{147a} V. Simak,¹²⁷ O. Simard,⁵ Lj. Simic,^{13a} S. Simion,¹¹⁶ E. Simioni,⁸² B. Simmons,⁷⁷
 R. Simoniello,^{90a,90b} M. Simonyan,³⁶ P. Sinervo,¹⁵⁹ N. B. Sinev,¹¹⁵ V. Sipica,¹⁴² G. Siragusa,¹⁷⁵ A. Sircar,⁷⁸
 A. N. Sisakyan,^{64,a} S. Yu. Sivoklokov,⁹⁸ J. Sjölin,^{147a,147b} T. B. Sjursen,¹⁴ L. A. Skinnari,¹⁵ H. P. Skottowe,⁵⁷
 K. Yu. Skovpen,¹⁰⁸ P. Skubic,¹¹² M. Slater,¹⁸ T. Slavicek,¹²⁷ K. Sliwa,¹⁶² V. Smakhtin,¹⁷³ B. H. Smart,⁴⁶ L. Smestad,¹¹⁸
 S. Yu. Smirnov,⁹⁷ Y. Smirnov,⁹⁷ L. N. Smirnova,^{98,ee} O. Smirnova,⁸⁰ K. M. Smith,⁵³ M. Smizanska,⁷¹ K. Smolek,¹²⁷
 A. A. Snesarev,⁹⁵ G. Snidero,⁷⁵ J. Snow,¹¹² S. Snyder,²⁵ R. Sobie,^{170,j} F. Socher,⁴⁴ J. Sodomka,¹²⁷ A. Soffer,¹⁵⁴ D. A. Soh,^{152,t}
 C. A. Solans,³⁰ M. Solar,¹²⁷ J. Solc,¹²⁷ E. Yu. Soldatov,⁹⁷ U. Soldevila,¹⁶⁸ E. Solfaroli Camillocci,^{133a,133b} A. A. Solodkov,¹²⁹
 O. V. Solovyanov,¹²⁹ V. Solovyevev,¹²² P. Sommer,⁴⁸ H. Y. Song,^{33b} N. Soni,¹ A. Sood,¹⁵ V. Sopko,¹²⁷ B. Sopko,¹²⁷ V. Sorin,¹²
 M. Sosebee,⁸ R. Soualah,^{165a,165c} P. Soueid,⁹⁴ A. M. Soukharev,¹⁰⁸ D. South,⁴² S. Spagnolo,^{72a,72b} F. Spanò,⁷⁶
 W. R. Spearman,⁵⁷ R. Spighi,^{20a} G. Spigo,³⁰ M. Spousta,¹²⁸ T. Spreitzer,¹⁵⁹ B. Spurlock,⁸ R. D. St. Denis,⁵³ S. Staerz,⁴⁴
 J. Stahlman,¹²¹ R. Stamen,^{58a} E. Stanecka,³⁹ R. W. Stanek,⁶ C. Stanescu,^{135a} M. Stanescu-Bellu,⁴² M. M. Stanitzki,⁴²
 S. Stapnes,¹¹⁸ E. A. Starchenko,¹²⁹ J. Stark,⁵⁵ P. Staroba,¹²⁶ P. Starovoitov,⁴² R. Staszewski,³⁹ P. Stavina,^{145a,a} G. Steele,⁵³
 P. Steinberg,²⁵ I. Stekl,¹²⁷ B. Stelzer,¹⁴³ H. J. Stelzer,³⁰ O. Stelzer-Chilton,^{160a} H. Stenzel,⁵² S. Stern,¹⁰⁰ G. A. Stewart,⁵³
 J. A. Stillings,²¹ M. C. Stockton,⁸⁶ M. Stoebe,⁸⁶ K. Stoerig,⁴⁸ G. Stoicea,^{26a} P. Stolte,⁵⁴ S. Stonjek,¹⁰⁰ A. R. Stradling,⁸
 A. Straessner,⁴⁴ J. Strandberg,¹⁴⁸ S. Strandberg,^{147a,147b} A. Strandlie,¹¹⁸ E. Strauss,¹⁴⁴ M. Strauss,¹¹² P. Strizenec,^{145b}
 R. Ströhmer,¹⁷⁵ D. M. Strom,¹¹⁵ R. Stroynowski,⁴⁰ S. A. Stucci,¹⁷ B. Stugu,¹⁴ N. A. Styles,⁴² D. Su,¹⁴⁴ J. Su,¹²⁴
 HS. Subramania,³ R. Subramaniam,⁷⁸ A. Succurro,¹² Y. Sugaya,¹¹⁷ C. Suhr,¹⁰⁷ M. Suk,¹²⁷ V. V. Sulin,⁹⁵ S. Sultansoy,^{4c}
 T. Sumida,⁶⁷ X. Sun,^{33a} J. E. Sundermann,⁴⁸ K. Suruliz,¹⁴⁰ G. Susinno,^{37a,37b} M. R. Sutton,¹⁵⁰ Y. Suzuki,⁶⁵ M. Svatos,¹²⁶
 S. Swedish,¹⁶⁹ M. Swiatlowski,¹⁴⁴ I. Sykora,^{145a} T. Sykora,¹²⁸ D. Ta,⁸⁹ K. Tackmann,⁴² J. Taenzer,¹⁵⁹ A. Taffard,¹⁶⁴
 R. Tafirout,^{160a} N. Taiblum,¹⁵⁴ Y. Takahashi,¹⁰² H. Takai,²⁵ R. Takashima,⁶⁸ H. Takeda,⁶⁶ T. Takeshita,¹⁴¹ Y. Takubo,⁶⁵
 M. Talby,⁸⁴ A. A. Talyshev,^{108,g} J. Y. C. Tam,¹⁷⁵ M. C. Tamssett,^{78,ff} K. G. Tan,⁸⁷ J. Tanaka,¹⁵⁶ R. Tanaka,¹¹⁶ S. Tanaka,¹³²
 S. Tanaka,⁶⁵ A. J. Tanasijczuk,¹⁴³ K. Tani,⁶⁶ N. Tannoury,⁸⁴ S. Tapprogge,⁸² S. Tarem,¹⁵³ F. Tarrade,²⁹ G. F. Tartarelli,^{90a}
 P. Tas,¹²⁸ M. Tasevsky,¹²⁶ T. Tashiro,⁶⁷ E. Tassi,^{37a,37b} A. Tavares Delgado,^{125a,125b} Y. Tayalati,^{136d} C. Taylor,⁷⁷ F. E. Taylor,⁹³
 G. N. Taylor,⁸⁷ W. Taylor,^{160b} F. A. Teischinger,³⁰ M. Teixeira Dias Castanheira,⁷⁵ P. Teixeira-Dias,⁷⁶ K. K. Temming,⁴⁸
 H. Ten Kate,³⁰ P. K. Teng,¹⁵² S. Terada,⁶⁵ K. Terashi,¹⁵⁶ J. Terron,⁸¹ S. Terzo,¹⁰⁰ M. Testa,⁴⁷ R. J. Teuscher,^{159,j} J. Therhaag,²¹
 T. Theveneaux-Pelzer,³⁴ S. Thoma,⁴⁸ J. P. Thomas,¹⁸ J. Thomas-Wilsker,⁷⁶ E. N. Thompson,³⁵ P. D. Thompson,¹⁸
 P. D. Thompson,¹⁵⁹ A. S. Thompson,⁵³ L. A. Thomsen,³⁶ E. Thomson,¹²¹ M. Thomson,²⁸ W. M. Thong,⁸⁷ R. P. Thun,^{88,a}
 F. Tian,³⁵ M. J. Tibbetts,¹⁵ V. O. Tikhomirov,^{95,gg} Yu. A. Tikhonov,^{108,g} S. Timoshenko,⁹⁷ E. Tiouchichine,⁸⁴ P. Tipton,¹⁷⁷
 S. Tisserant,⁸⁴ T. Todorov,⁵ S. Todorova-Nova,¹²⁸ B. Toggerson,¹⁶⁴ J. Tojo,⁶⁹ S. Tokár,^{145a} K. Tokushuku,⁶⁵ K. Tollefson,⁸⁹
 L. Tomlinson,⁸³ M. Tomoto,¹⁰² L. Tompkins,³¹ K. Toms,¹⁰⁴ N. D. Topilin,⁶⁴ E. Torrence,¹¹⁵ H. Torres,¹⁴³ E. Torrón Pastor,¹⁶⁸
 J. Toth,^{84,bb} F. Touchard,⁸⁴ D. R. Tovey,¹⁴⁰ H. L. Tran,¹¹⁶ T. Trefzger,¹⁷⁵ L. Tremblet,³⁰ A. Tricoli,³⁰ I. M. Trigger,^{160a}
 S. Trincaz-Duvold,⁷⁹ M. F. Tripania,⁷⁰ N. Triplett,²⁵ W. Trischuk,¹⁵⁹ B. Trocme,⁵⁵ C. Troncon,^{90a} M. Trotter-McDonald,¹⁴³
 M. Trovatelli,^{135a,135b} P. True,⁸⁹ M. Trzebinski,³⁹ A. Trzupek,³⁹ C. Tsarouchas,³⁰ J. C.-L. Tseng,¹¹⁹ P. V. Tsiarshka,⁹¹
 D. Tsionou,¹³⁷ G. Tsipolitis,¹⁰ N. Tsirintanis,⁹ S. Tsiskaridze,¹² V. Tsiskaridze,⁴⁸ E. G. Tskhadadze,^{51a} I. I. Tsukerman,⁹⁶
 V. Tsulaia,¹⁵ S. Tsuno,⁶⁵ D. Tsybychev,¹⁴⁹ A. Tua,¹⁴⁰ A. Tudorache,^{26a} V. Tudorache,^{26a} A. N. Tuna,¹²¹ S. A. Tupputti,^{20a,20b}
 S. Turchikhin,^{98,ee} D. Turecek,¹²⁷ I. Turk Cakir,^{4d} R. Turra,^{90a,90b} P. M. Tuts,³⁵ A. Tykhonov,⁷⁴ M. Tylmad,^{147a,147b}
 M. Tyndel,¹³⁰ K. Uchida,²¹ I. Ueda,¹⁵⁶ R. Ueno,²⁹ M. Ughetto,⁸⁴ M. Ugland,¹⁴ M. Uhlenbrock,²¹ F. Ukegawa,¹⁶¹ G. Unal,³⁰
 A. Undrus,²⁵ G. Unel,¹⁶⁴ F. C. Ungaro,⁴⁸ Y. Unno,⁶⁵ D. Urbaniec,³⁵ P. Urquijo,²¹ G. Usai,⁸ A. Usanova,⁶¹ L. Vacavant,⁸⁴
 V. Vacek,¹²⁷ B. Vachon,⁸⁶ N. Valencic,¹⁰⁶ S. Valentinetti,^{20a,20b} A. Valero,¹⁶⁸ L. Valery,³⁴ S. Valkar,¹²⁸
 E. Valladolid Gallego,¹⁶⁸ S. Vallecorsa,⁴⁹ J. A. Valls Ferrer,¹⁶⁸ R. Van Berg,¹²¹ P. C. Van Der Deijl,¹⁰⁶ R. van der Geer,¹⁰⁶

H. van der Graaf,¹⁰⁶ R. Van Der Leeuw,¹⁰⁶ D. van der Ster,³⁰ N. van Eldik,³⁰ P. van Gemmeren,⁶ J. Van Nieuwkoop,¹⁴³ I. van Vulpen,¹⁰⁶ M. C. van Woerden,³⁰ M. Vanadia,^{133a,133b} W. Vandelli,³⁰ A. Vaniachine,⁶ P. Vankov,⁴² F. Vannucci,⁷⁹ G. Vardanyan,¹⁷⁸ R. Vari,^{133a} E. W. Varnes,⁷ T. Varol,⁸⁵ D. Varouchas,⁷⁹ A. Vartapetian,⁸ K. E. Varvell,¹⁵¹ V. I. Vassilakopoulos,⁵⁶ F. Vazeille,³⁴ T. Vazquez Schroeder,⁵⁴ J. Veatch,⁷ F. Veloso,^{125a,125c} S. Veneziano,^{133a} A. Ventura,^{72a,72b} D. Ventura,⁸⁵ M. Venturi,⁴⁸ N. Venturi,¹⁵⁹ A. Venturini,²³ V. Vercesi,^{120a} M. Verducci,¹³⁹ W. Verkerke,¹⁰⁶ J. C. Vermeulen,¹⁰⁶ A. Vest,⁴⁴ M. C. Vetterli,^{143,c} O. Viazlo,⁸⁰ I. Vichou,¹⁶⁶ T. Vickey,^{146c,hh} O. E. Vickey Boeriu,^{146c} G. H. A. Viehhauser,¹¹⁹ S. Viel,¹⁶⁹ R. Vigne,³⁰ M. Villa,^{20a,20b} M. Villaplana Perez,¹⁶⁸ E. Vilucchi,⁴⁷ M. G. Vincter,²⁹ V. B. Vinogradov,⁶⁴ J. Virzi,¹⁵ O. Vitells,¹⁷³ I. Vivarelli,¹⁵⁰ F. Vives Vaque,³ S. Vlachos,¹⁰ D. Vladoiu,⁹⁹ M. Vlasak,¹²⁷ A. Vogel,²¹ P. Vokac,¹²⁷ G. Volpi,^{123a,123b} M. Volpi,⁸⁷ H. von der Schmitt,¹⁰⁰ H. von Radziewski,⁴⁸ E. von Toerne,²¹ V. Vorobel,¹²⁸ M. Vos,¹⁶⁸ R. Voss,³⁰ J. H. Vosseveld,⁷³ N. Vranjes,¹³⁷ M. Vranjes Milosavljevic,¹⁰⁶ V. Vrba,¹²⁶ M. Vreeswijk,¹⁰⁶ T. Vu Anh,⁴⁸ R. Vuillermet,³⁰ I. Vukotic,³¹ Z. Vykydal,¹²⁷ W. Wagner,¹⁷⁶ P. Wagner,²¹ S. Wahrmund,⁴⁴ J. Wakabayashi,¹⁰² J. Walder,⁷¹ R. Walker,⁹⁹ W. Walkowiak,¹⁴² R. Wall,¹⁷⁷ P. Waller,⁷³ B. Walsh,¹⁷⁷ C. Wang,^{152,ii} C. Wang,⁴⁵ F. Wang,¹⁷⁴ H. Wang,¹⁵ H. Wang,⁴⁰ J. Wang,⁴² J. Wang,^{33a} K. Wang,⁸⁶ R. Wang,¹⁰⁴ S. M. Wang,¹⁵² T. Wang,²¹ X. Wang,¹⁷⁷ A. Warburton,⁸⁶ C. P. Ward,²⁸ D. R. Wardrope,⁷⁷ M. Warsinsky,⁴⁸ A. Washbrook,⁴⁶ C. Wasicki,⁴² I. Watanabe,⁶⁶ P. M. Watkins,¹⁸ A. T. Watson,¹⁸ I. J. Watson,¹⁵¹ M. F. Watson,¹⁸ G. Watts,¹³⁹ S. Watts,⁸³ B. M. Waugh,⁷⁷ S. Webb,⁸³ M. S. Weber,¹⁷ S. W. Weber,¹⁷⁵ J. S. Webster,³¹ A. R. Weidberg,¹¹⁹ P. Weigell,¹⁰⁰ B. Weinert,⁶⁰ J. Weingarten,⁵⁴ C. Weiser,⁴⁸ H. Weits,¹⁰⁶ P. S. Wells,³⁰ T. Wenaus,²⁵ D. Wendland,¹⁶ Z. Weng,^{152,i} T. Wengler,³⁰ S. Wenig,³⁰ N. Wermes,²¹ M. Werner,⁴⁸ P. Werner,³⁰ M. Wessels,^{58a} J. Wetter,¹⁶² K. Whalen,²⁹ A. White,⁸ M. J. White,¹ R. White,^{32b} S. White,^{123a,123b} D. Whiteson,¹⁶⁴ D. Wicke,¹⁷⁶ F. J. Wickens,¹³⁰ W. Wiedenmann,¹⁷⁴ M. Wielers,¹³⁰ P. Wienemann,²¹ C. Wiglesworth,³⁶ L. A. M. Wiik-Fuchs,²¹ P. A. Wijeratne,⁷⁷ A. Wildauer,¹⁰⁰ M. A. Wildt,^{42,ij} H. G. Wilkens,³⁰ J. Z. Will,⁹⁹ H. H. Williams,¹²¹ S. Williams,²⁸ C. Willis,⁸⁹ S. Willocq,⁸⁵ J. A. Wilson,¹⁸ A. Wilson,⁸⁸ I. Wingerter-Seez,⁵ S. Winkelmann,⁴⁸ F. Winklmeier,¹¹⁵ M. Wittgen,¹⁴⁴ T. Wittig,⁴³ J. Wittkowski,⁹⁹ S. J. Wollstadt,⁸² M. W. Wolter,³⁹ H. Wolters,^{125a,125c} B. K. Wosiek,³⁹ J. Wotschack,³⁰ M. J. Woudstra,⁸³ K. W. Wozniak,³⁹ M. Wright,⁵³ S. L. Wu,¹⁷⁴ X. Wu,⁴⁹ Y. Wu,⁸⁸ E. Wulf,³⁵ T. R. Wyatt,⁸³ B. M. Wynne,⁴⁶ S. Xella,³⁶ M. Xiao,¹³⁷ D. Xu,^{33a} L. Xu,^{33b,kk} B. Yabsley,¹⁵¹ S. Yacoub,^{146b,ll} M. Yamada,⁶⁵ H. Yamaguchi,¹⁵⁶ Y. Yamaguchi,¹⁵⁶ A. Yamamoto,⁶⁵ K. Yamamoto,⁶³ S. Yamamoto,¹⁵⁶ T. Yamamura,¹⁵⁶ T. Yamanaka,¹⁵⁶ K. Yamauchi,¹⁰² Y. Yamazaki,⁶⁶ Z. Yan,²² H. Yang,^{33e} H. Yang,¹⁷⁴ U. K. Yang,⁸³ Y. Yang,¹¹⁰ S. Yanush,⁹² L. Yao,^{33a} W-M. Yao,¹⁵ Y. Yasu,⁶⁵ E. Yatsenko,⁴² K. H. Yau Wong,²¹ J. Ye,⁴⁰ S. Ye,²⁵ A. L. Yen,⁵⁷ E. Yildirim,⁴² M. Yilmaz,^{4b} R. Yoosoofmiya,¹²⁴ K. Yorita,¹⁷² R. Yoshida,⁶ K. Yoshihara,¹⁵⁶ C. Young,¹⁴⁴ C. J. S. Young,³⁰ S. Youssef,²² D. R. Yu,¹⁵ J. Yu,⁸ J. M. Yu,⁸⁸ J. Yu,¹¹³ L. Yuan,⁶⁶ A. Yurkewicz,¹⁰⁷ B. Zabinski,³⁹ R. Zaidan,⁶² A. M. Zaitsev,^{129,y} A. Zaman,¹⁴⁹ S. Zambito,²³ L. Zanello,^{133a,133b} D. Zanzi,¹⁰⁰ A. Zaytsev,²⁵ C. Zeitnitz,¹⁷⁶ M. Zeman,¹²⁷ A. Zemla,^{38a} K. Zengel,²³ O. Zenin,¹²⁹ T. Ženiš,^{145a} D. Zerwas,¹¹⁶ G. Zevi della Porta,⁵⁷ D. Zhang,⁸⁸ F. Zhang,¹⁷⁴ H. Zhang,⁸⁹ J. Zhang,⁶ L. Zhang,¹⁵² X. Zhang,^{33d} Z. Zhang,¹¹⁶ Z. Zhao,^{33b} A. Zhemchugov,⁶⁴ J. Zhong,¹¹⁹ B. Zhou,⁸⁸ L. Zhou,³⁵ N. Zhou,¹⁶⁴ C. G. Zhu,^{33d} H. Zhu,^{33a} J. Zhu,⁸⁸ Y. Zhu,^{33b} X. Zhuang,^{33a} A. Zibell,⁹⁹ D. Zieminska,⁶⁰ N. I. Zimine,⁶⁴ C. Zimmermann,⁸² R. Zimmermann,²¹ S. Zimmermann,²¹ S. Zimmermann,⁴⁸ Z. Zinonos,⁵⁴ M. Ziolkowski,¹⁴² R. Zitoun,⁵ G. Zoernig,¹⁷⁴ A. Zoccoli,^{20a,20b} M. zur Nedden,¹⁶ G. Zurzolo,^{103a,103b} V. Zutshi,¹⁰⁷ and L. Zwalinski³⁰

(ATLAS Collaboration)

¹Department of Physics, University of Adelaide, Adelaide, Australia²Physics Department, SUNY Albany, Albany, New York, USA³Department of Physics, University of Alberta, Edmonton, AB, Canada^{4a}Department of Physics, Ankara University, Ankara, Turkey^{4b}Department of Physics, Gazi University, Ankara, Turkey^{4c}Division of Physics, TOBB University of Economics and Technology, Ankara, Turkey^{4d}Turkish Atomic Energy Authority, Ankara, Turkey⁵LAPP, CNRS/IN2P3 and Université de Savoie, Annecy-le-Vieux, France⁶High Energy Physics Division, Argonne National Laboratory, Argonne, Illinois, USA⁷Department of Physics, University of Arizona, Tucson, Arizona, USA⁸Department of Physics, The University of Texas at Arlington, Arlington, Texas, USA⁹Physics Department, University of Athens, Athens, Greece¹⁰Physics Department, National Technical University of Athens, Zografou, Greece¹¹Institute of Physics, Azerbaijan Academy of Sciences, Baku, Azerbaijan

- ¹²*Institut de Física d'Altes Energies and Departament de Física de la Universitat Autònoma de Barcelona, Barcelona, Spain*
- ^{13a}*Institute of Physics, University of Belgrade, Belgrade, Serbia*
- ^{13b}*Vinca Institute of Nuclear Sciences, University of Belgrade, Belgrade, Serbia*
- ¹⁴*Department for Physics and Technology, University of Bergen, Bergen, Norway*
- ¹⁵*Physics Division, Lawrence Berkeley National Laboratory and University of California, Berkeley, California, USA*
- ¹⁶*Department of Physics, Humboldt University, Berlin, Germany*
- ¹⁷*Albert Einstein Center for Fundamental Physics and Laboratory for High Energy Physics, University of Bern, Bern, Switzerland*
- ¹⁸*School of Physics and Astronomy, University of Birmingham, Birmingham, United Kingdom*
- ^{19a}*Department of Physics, Bogazici University, Istanbul, Turkey*
- ^{19b}*Department of Physics, Dogus University, Istanbul, Turkey*
- ^{19c}*Department of Physics Engineering, Gaziantep University, Gaziantep, Turkey*
- ^{20a}*INFN Sezione di Bologna, Bologna, Italy*
- ^{20b}*Dipartimento di Fisica e Astronomia, Università di Bologna, Bologna, Italy*
- ²¹*Physikalisches Institut, University of Bonn, Bonn, Germany*
- ²²*Department of Physics, Boston University, Boston, Massachusetts, USA*
- ²³*Department of Physics, Brandeis University, Waltham, Massachusetts, USA*
- ^{24a}*Universidade Federal do Rio De Janeiro COPPE/EE/IF, Rio de Janeiro, Brazil*
- ^{24b}*Federal University of Juiz de Fora (UFJF), Juiz de Fora, Brazil*
- ^{24c}*Federal University of Sao Joao del Rei (UFSJ), Sao Joao del Rei, Brazil*
- ^{24d}*Instituto de Física, Universidade de Sao Paulo, Sao Paulo, Brazil*
- ²⁵*Physics Department, Brookhaven National Laboratory, Upton, New York, USA*
- ^{26a}*National Institute of Physics and Nuclear Engineering, Bucharest, Romania*
- ^{26b}*National Institute for Research and Development of Isotopic and Molecular Technologies, Physics Department, Cluj Napoca, Romania*
- ^{26c}*University Politehnica Bucharest, Bucharest, Romania*
- ^{26d}*West University in Timisoara, Timisoara, Romania*
- ²⁷*Departamento de Física, Universidad de Buenos Aires, Buenos Aires, Argentina*
- ²⁸*Cavendish Laboratory, University of Cambridge, Cambridge, United Kingdom*
- ²⁹*Department of Physics, Carleton University, Ottawa, ON, Canada*
- ³⁰*CERN, Geneva, Switzerland*
- ³¹*Enrico Fermi Institute, University of Chicago, Chicago, Illinois, USA*
- ^{32a}*Departamento de Física, Pontificia Universidad Católica de Chile, Santiago, Chile*
- ^{32b}*Departamento de Física, Universidad Técnica Federico Santa María, Valparaíso, Chile*
- ^{33a}*Institute of High Energy Physics, Chinese Academy of Sciences, Beijing, China*
- ^{33b}*Department of Modern Physics, University of Science and Technology of China, Anhui, China*
- ^{33c}*Department of Physics, Nanjing University, Jiangsu, China*
- ^{33d}*School of Physics, Shandong University, Shandong, China*
- ^{33e}*Physics Department, Shanghai Jiao Tong University, Shanghai, China*
- ³⁴*Laboratoire de Physique Corpusculaire, Clermont Université and Université Blaise Pascal and CNRS/IN2P3, Clermont-Ferrand, France*
- ³⁵*Nevis Laboratory, Columbia University, Irvington, New York, USA*
- ³⁶*Niels Bohr Institute, University of Copenhagen, Kobenhavn, Denmark*
- ^{37a}*INFN Gruppo Collegato di Cosenza, Laboratori Nazionali di Frascati, Italy*
- ^{37b}*Dipartimento di Fisica, Università della Calabria, Rende, Italy*
- ^{38a}*AGH University of Science and Technology, Faculty of Physics and Applied Computer Science, Krakow, Poland*
- ^{38b}*Marian Smoluchowski Institute of Physics, Jagiellonian University, Krakow, Poland*
- ³⁹*The Henryk Niewodniczanski Institute of Nuclear Physics, Polish Academy of Sciences, Krakow, Poland*
- ⁴⁰*Physics Department, Southern Methodist University, Dallas, Texas, USA*
- ⁴¹*Physics Department, University of Texas at Dallas, Richardson Texas, USA*
- ⁴²*DESY, Hamburg and Zeuthen, Germany*
- ⁴³*Institut für Experimentelle Physik IV, Technische Universität Dortmund, Dortmund, Germany*
- ⁴⁴*Institut für Kern- und Teilchenphysik, Technische Universität Dresden, Dresden, Germany*
- ⁴⁵*Department of Physics, Duke University, Durham, North Carolina, USA*
- ⁴⁶*SUPA - School of Physics and Astronomy, University of Edinburgh, Edinburgh, United Kingdom*
- ⁴⁷*INFN Laboratori Nazionali di Frascati, Frascati, Italy*
- ⁴⁸*Fakultät für Mathematik und Physik, Albert-Ludwigs-Universität, Freiburg, Germany*

- ⁴⁹*Section de Physique, Université de Genève, Geneva, Switzerland*
- ^{50a}*INFN Sezione di Genova, Genova, Italy*
- ^{50b}*Dipartimento di Fisica, Università di Genova, Genova, Italy*
- ^{51a}*E. Andronikashvili Institute of Physics, Iv. Javakishvili Tbilisi State University, Tbilisi, Georgia*
- ^{51b}*High Energy Physics Institute, Tbilisi State University, Tbilisi, Georgia*
- ⁵²*II Physikalisches Institut, Justus-Liebig-Universität Giessen, Giessen, Germany*
- ⁵³*SUPA-School of Physics and Astronomy, University of Glasgow, Glasgow, United Kingdom*
- ⁵⁴*II Physikalisches Institut, Georg-August-Universität, Göttingen, Germany*
- ⁵⁵*Laboratoire de Physique Subatomique et de Cosmologie, Université Grenoble-Alpes, CNRS/IN2P3, Grenoble, France*
- ⁵⁶*Department of Physics, Hampton University, Hampton, Virginia, USA*
- ⁵⁷*Laboratory for Particle Physics and Cosmology, Harvard University, Cambridge, Massachusetts, USA*
- ^{58a}*Kirchhoff-Institut für Physik, Ruprecht-Karls-Universität Heidelberg, Heidelberg, Germany*
- ^{58b}*Physikalisches Institut, Ruprecht-Karls-Universität Heidelberg, Heidelberg, Germany*
- ^{58c}*ZITI Institut für technische Informatik, Ruprecht-Karls-Universität Heidelberg, Mannheim, Germany*
- ⁵⁹*Faculty of Applied Information Science, Hiroshima Institute of Technology, Hiroshima, Japan*
- ⁶⁰*Department of Physics, Indiana University, Bloomington, Indiana, USA*
- ⁶¹*Institut für Astro- und Teilchenphysik, Leopold-Franzens-Universität, Innsbruck, Austria*
- ⁶²*University of Iowa, Iowa City, Iowa, USA*
- ⁶³*Department of Physics and Astronomy, Iowa State University, Ames, Iowa, USA*
- ⁶⁴*Joint Institute for Nuclear Research, JINR Dubna, Dubna, Russia*
- ⁶⁵*KEK, High Energy Accelerator Research Organization, Tsukuba, Japan*
- ⁶⁶*Graduate School of Science, Kobe University, Kobe, Japan*
- ⁶⁷*Faculty of Science, Kyoto University, Kyoto, Japan*
- ⁶⁸*Kyoto University of Education, Kyoto, Japan*
- ⁶⁹*Department of Physics, Kyushu University, Fukuoka, Japan*
- ⁷⁰*Instituto de Física La Plata, Universidad Nacional de La Plata and CONICET, La Plata, Argentina*
- ⁷¹*Physics Department, Lancaster University, Lancaster, United Kingdom*
- ^{72a}*INFN Sezione di Lecce, Lecce, Italy*
- ^{72b}*Dipartimento di Matematica e Fisica, Università del Salento, Lecce, Italy*
- ⁷³*Oliver Lodge Laboratory, University of Liverpool, Liverpool, United Kingdom*
- ⁷⁴*Department of Physics, Jožef Stefan Institute and University of Ljubljana, Ljubljana, Slovenia*
- ⁷⁵*School of Physics and Astronomy, Queen Mary University of London, London, United Kingdom*
- ⁷⁶*Department of Physics, Royal Holloway University of London, Surrey, United Kingdom*
- ⁷⁷*Department of Physics and Astronomy, University College London, London, United Kingdom*
- ⁷⁸*Louisiana Tech University, Ruston, Louisiana, USA*
- ⁷⁹*Laboratoire de Physique Nucléaire et de Hautes Energies, UPMC and Université Paris-Diderot and CNRS/IN2P3, Paris, France*
- ⁸⁰*Fysiska institutionen, Lunds universitet, Lund, Sweden*
- ⁸¹*Departamento de Física Teórica C-15, Universidad Autónoma de Madrid, Madrid, Spain*
- ⁸²*Institut für Physik, Universität Mainz, Mainz, Germany*
- ⁸³*School of Physics and Astronomy, University of Manchester, Manchester, United Kingdom*
- ⁸⁴*CPPM, Aix-Marseille Université and CNRS/IN2P3, Marseille, France*
- ⁸⁵*Department of Physics, University of Massachusetts, Amherst, Massachusetts, USA*
- ⁸⁶*Department of Physics, McGill University, Montreal, QC, Canada*
- ⁸⁷*School of Physics, University of Melbourne, Victoria, Australia*
- ⁸⁸*Department of Physics, The University of Michigan, Ann Arbor Michigan, USA*
- ⁸⁹*Department of Physics and Astronomy, Michigan State University, East Lansing, Michigan, USA*
- ^{90a}*INFN Sezione di Milano, Milano, Italy*
- ^{90b}*Dipartimento di Fisica, Università di Milano, Milano, Italy*
- ⁹¹*B.I. Stepanov Institute of Physics, National Academy of Sciences of Belarus, Minsk, Republic of Belarus*
- ⁹²*National Scientific and Educational Centre for Particle and High Energy Physics, Minsk, Republic of Belarus*
- ⁹³*Department of Physics, Massachusetts Institute of Technology, Cambridge, Massachusetts, USA*
- ⁹⁴*Group of Particle Physics, University of Montreal, Montreal, QC, Canada*
- ⁹⁵*P.N. Lebedev Institute of Physics, Academy of Sciences, Moscow, Russia*
- ⁹⁶*Institute for Theoretical and Experimental Physics (ITEP), Moscow, Russia*
- ⁹⁷*Moscow Engineering and Physics Institute (MEPhI), Moscow, Russia*
- ⁹⁸*D.V. Skobel'syn Institute of Nuclear Physics, M.V. Lomonosov Moscow State University, Moscow, Russia*
- ⁹⁹*Fakultät für Physik, Ludwig-Maximilians-Universität München, München, Germany*

- ¹⁰⁰Max-Planck-Institut für Physik (Werner-Heisenberg-Institut), München, Germany
- ¹⁰¹Nagasaki Institute of Applied Science, Nagasaki, Japan
- ¹⁰²Graduate School of Science and Kobayashi-Maskawa Institute, Nagoya University, Nagoya, Japan
- ^{103a}INFN Sezione di Napoli, Napoli, Italy
- ^{103b}Dipartimento di Fisica, Università di Napoli, Napoli, Italy
- ¹⁰⁴Department of Physics and Astronomy, University of New Mexico, Albuquerque, New Mexico, USA
- ¹⁰⁵Institute for Mathematics, Astrophysics and Particle Physics, Radboud University Nijmegen/Nikhef, Nijmegen, Netherlands
- ¹⁰⁶Nikhef National Institute for Subatomic Physics and University of Amsterdam, Amsterdam, Netherlands
- ¹⁰⁷Department of Physics, Northern Illinois University, DeKalb, Illinois, USA
- ¹⁰⁸Budker Institute of Nuclear Physics, SB RAS, Novosibirsk, Russia
- ¹⁰⁹Department of Physics, New York University, New York, New York, USA
- ¹¹⁰Ohio State University, Columbus, Ohio, USA
- ¹¹¹Faculty of Science, Okayama University, Okayama, Japan
- ¹¹²Homer L. Dodge Department of Physics and Astronomy, University of Oklahoma, Norman, Oklahoma, USA
- ¹¹³Department of Physics, Oklahoma State University, Stillwater Oklahoma, USA
- ¹¹⁴Palacký University, RCPTM, Olomouc, Czech Republic
- ¹¹⁵Center for High Energy Physics, University of Oregon, Eugene, Oregon, USA
- ¹¹⁶LAL, Université Paris-Sud and CNRS/IN2P3, Orsay, France
- ¹¹⁷Graduate School of Science, Osaka University, Osaka, Japan
- ¹¹⁸Department of Physics, University of Oslo, Oslo, Norway
- ¹¹⁹Department of Physics, Oxford University, Oxford, United Kingdom
- ^{120a}INFN Sezione di Pavia, Pavia, Italy
- ^{120b}Dipartimento di Fisica, Università di Pavia, Pavia, Italy
- ¹²¹Department of Physics, University of Pennsylvania, Philadelphia, Pennsylvania, USA
- ¹²²Petersburg Nuclear Physics Institute, Gatchina, Russia
- ^{123a}INFN Sezione di Pisa, Pisa, Italy
- ^{123b}Dipartimento di Fisica E. Fermi, Università di Pisa, Pisa, Italy
- ¹²⁴Department of Physics and Astronomy, University of Pittsburgh, Pittsburgh, Pennsylvania, USA
- ^{125a}Laboratorio de Instrumentacao e Fisica Experimental de Particulas - LIP, Lisboa, Portugal
- ^{125b}Faculdade de Ciências, Universidade de Lisboa, Lisboa, Portugal
- ^{125c}Department of Physics, University of Coimbra, Coimbra, Portugal
- ^{125d}Centro de Física Nuclear da Universidade de Lisboa, Lisboa, Portugal
- ^{125e}Departamento de Física, Universidade do Minho, Braga, Portugal
- ^{125f}Departamento de Física Teórica y del Cosmos and CAFPE, Universidad de Granada, Granada (Spain), Portugal
- ^{125g}Dep Física and CEFITEC of Faculdade de Ciências e Tecnologia, Universidade Nova de Lisboa, Caparica, Portugal
- ¹²⁶Institute of Physics, Academy of Sciences of the Czech Republic, Praha, Czech Republic
- ¹²⁷Czech Technical University in Prague, Praha, Czech Republic
- ¹²⁸Faculty of Mathematics and Physics, Charles University in Prague, Praha, Czech Republic
- ¹²⁹State Research Center Institute for High Energy Physics, Protvino, Russia
- ¹³⁰Particle Physics Department, Rutherford Appleton Laboratory, Didcot, United Kingdom
- ¹³¹Physics Department, University of Regina, Regina, SK, Canada
- ¹³²Ritsumeikan University, Kusatsu, Shiga, Japan
- ^{133a}INFN Sezione di Roma, Roma, Italy
- ^{133b}Dipartimento di Fisica, Sapienza Università di Roma, Roma, Italy
- ^{134a}INFN Sezione di Roma Tor Vergata, Roma, Italy
- ^{134b}Dipartimento di Fisica, Università di Roma Tor Vergata, Roma, Italy
- ^{135a}INFN Sezione di Roma Tre, Roma, Italy
- ^{135b}Dipartimento di Matematica e Fisica, Università Roma Tre, Roma, Italy
- ^{136a}Faculté des Sciences Ain Chock, Réseau Universitaire de Physique des Hautes Energies - Université Hassan II, Casablanca, Morocco
- ^{136b}Centre National de l'Energie des Sciences Techniques Nucleaires, Rabat, Morocco
- ^{136c}Faculté des Sciences Semlalia, Université Cadi Ayyad, LPHEA-Marrakech, Morocco
- ^{136d}Faculté des Sciences, Université Mohamed Premier and LPTPM, Oujda, Morocco
- ^{136e}Faculté des sciences, Université Mohammed V-Agdal, Rabat, Morocco
- ¹³⁷DSM/IRFU (Institut de Recherches sur les Lois Fondamentales de l'Univers), CEA Saclay (Commissariat à l'Energie Atomique et aux Energies Alternatives), Gif-sur-Yvette, France

- ¹³⁸*Santa Cruz Institute for Particle Physics, University of California Santa Cruz, Santa Cruz, California, USA*
- ¹³⁹*Department of Physics, University of Washington, Seattle, Washington, USA*
- ¹⁴⁰*Department of Physics and Astronomy, University of Sheffield, Sheffield, United Kingdom*
- ¹⁴¹*Department of Physics, Shinshu University, Nagano, Japan*
- ¹⁴²*Fachbereich Physik, Universität Siegen, Siegen, Germany*
- ¹⁴³*Department of Physics, Simon Fraser University, Burnaby, BC, Canada*
- ¹⁴⁴*SLAC National Accelerator Laboratory, Stanford, California, USA*
- ^{145a}*Faculty of Mathematics, Physics & Informatics, Comenius University, Bratislava, Slovak Republic*
- ^{145b}*Department of Subnuclear Physics, Institute of Experimental Physics of the Slovak Academy of Sciences, Kosice, Slovak Republic*
- ^{146a}*Department of Physics, University of Cape Town, Cape Town, South Africa*
- ^{146b}*Department of Physics, University of Johannesburg, Johannesburg, South Africa*
- ^{146c}*School of Physics, University of the Witwatersrand, Johannesburg, South Africa*
- ^{147a}*Department of Physics, Stockholm University, Stockholm, Sweden*
- ^{147b}*The Oskar Klein Centre, Stockholm, Sweden*
- ¹⁴⁸*Physics Department, Royal Institute of Technology, Stockholm, Sweden*
- ¹⁴⁹*Departments of Physics & Astronomy and Chemistry, Stony Brook University, Stony Brook, New York, USA*
- ¹⁵⁰*Department of Physics and Astronomy, University of Sussex, Brighton, United Kingdom*
- ¹⁵¹*School of Physics, University of Sydney, Sydney, Australia*
- ¹⁵²*Institute of Physics, Academia Sinica, Taipei, Taiwan*
- ¹⁵³*Department of Physics, Technion: Israel Institute of Technology, Haifa, Israel*
- ¹⁵⁴*Raymond and Beverly Sackler School of Physics and Astronomy, Tel Aviv University, Tel Aviv, Israel*
- ¹⁵⁵*Department of Physics, Aristotle University of Thessaloniki, Thessaloniki, Greece*
- ¹⁵⁶*International Center for Elementary Particle Physics and Department of Physics, The University of Tokyo, Tokyo, Japan*
- ¹⁵⁷*Graduate School of Science and Technology, Tokyo Metropolitan University, Tokyo, Japan*
- ¹⁵⁸*Department of Physics, Tokyo Institute of Technology, Tokyo, Japan*
- ¹⁵⁹*Department of Physics, University of Toronto, Toronto, ON, Canada*
- ^{160a}*TRIUMF, Vancouver, BC, Canada*
- ^{160b}*Department of Physics and Astronomy, York University, Toronto, ON, Canada*
- ¹⁶¹*Faculty of Pure and Applied Sciences, University of Tsukuba, Tsukuba, Japan*
- ¹⁶²*Department of Physics and Astronomy, Tufts University, Medford, Massachusetts, USA*
- ¹⁶³*Centro de Investigaciones, Universidad Antonio Narino, Bogota, Colombia*
- ¹⁶⁴*Department of Physics and Astronomy, University of California Irvine, Irvine, California, USA*
- ^{165a}*INFN Gruppo Collegato di Udine, Sezione di Trieste, Udine, Italy*
- ^{165b}*ICTP, Trieste, Italy*
- ^{165c}*Dipartimento di Chimica, Fisica e Ambiente, Università di Udine, Udine, Italy*
- ¹⁶⁶*Department of Physics, University of Illinois, Urbana, Illinois, USA*
- ¹⁶⁷*Department of Physics and Astronomy, University of Uppsala, Uppsala, Sweden*
- ¹⁶⁸*Instituto de Física Corpuscular (IFIC) and Departamento de Física Atómica, Molecular y Nuclear and Departamento de Ingeniería Electrónica and Instituto de Microelectrónica de Barcelona (IMB-CNM), University of Valencia and CSIC, Valencia, Spain*
- ¹⁶⁹*Department of Physics, University of British Columbia, Vancouver, BC, Canada*
- ¹⁷⁰*Department of Physics and Astronomy, University of Victoria, Victoria, BC, Canada*
- ¹⁷¹*Department of Physics, University of Warwick, Coventry, United Kingdom*
- ¹⁷²*Waseda University, Tokyo, Japan*
- ¹⁷³*Department of Particle Physics, The Weizmann Institute of Science, Rehovot, Israel*
- ¹⁷⁴*Department of Physics, University of Wisconsin, Madison, Wisconsin, USA*
- ¹⁷⁵*Fakultät für Physik und Astronomie, Julius-Maximilians-Universität, Würzburg, Germany*
- ¹⁷⁶*Fachbereich C Physik, Bergische Universität Wuppertal, Wuppertal, Germany*
- ¹⁷⁷*Department of Physics, Yale University, New Haven, Connecticut, USA*
- ¹⁷⁸*Yerevan Physics Institute, Yerevan, Armenia*
- ¹⁷⁹*Centre de Calcul de l'Institut National de Physique Nucléaire et de Physique des Particules (IN2P3), Villeurbanne, France*

^aDeceased.^bAlso at Department of Physics, King's College London, London, United Kingdom.^cAlso at Institute of Physics, Azerbaijan Academy of Sciences, Baku, Azerbaijan.

- ^dAlso at Particle Physics Department, Rutherford Appleton Laboratory, Didcot, United Kingdom.
- ^eAlso at TRIUMF, Vancouver, BC, Canada.
- ^fAlso at Department of Physics, California State University, Fresno, CA, USA.
- ^gAlso at Novosibirsk State University, Novosibirsk, Russia.
- ^hAlso at CPPM, Aix-Marseille Université and CNRS/IN2P3, Marseille, France.
- ⁱAlso at Università di Napoli Parthenope, Napoli, Italy.
- ^jAlso at Institute of Particle Physics (IPP), Canada.
- ^kAlso at Department of Physics, St. Petersburg State Polytechnical University, St. Petersburg, Russia.
- ^lAlso at Department of Financial and Management Engineering, University of the Aegean, Chios, Greece.
- ^mAlso at Louisiana Tech University, Ruston LA, USA.
- ⁿAlso at Institutio Catalana de Recerca i Estudis Avancats, ICREA, Barcelona, Spain.
- ^oAlso at CERN, Geneva, Switzerland.
- ^pAlso at Ochadai Academic Production, Ochanomizu University, Tokyo, Japan.
- ^qAlso at Manhattan College, New York, NY, USA.
- ^rAlso at Institute of Physics, Academia Sinica, Taipei, Taiwan.
- ^sAlso at LAL, Université Paris-Sud and CNRS/IN2P3, Orsay, France.
- ^tAlso at School of Physics and Engineering, Sun Yat-sen University, Guangzhou, China.
- ^uAlso at Academia Sinica Grid Computing, Institute of Physics, Academia Sinica, Taipei, Taiwan.
- ^vAlso at Laboratoire de Physique Nucléaire et de Hautes Energies, UPMC and Université Paris-Diderot and CNRS/IN2P3, Paris, France.
- ^wAlso at School of Physical Sciences, National Institute of Science Education and Research, Bhubaneswar, India.
- ^xAlso at Dipartimento di Fisica, Sapienza Università di Roma, Roma, Italy.
- ^yAlso at Moscow Institute of Physics and Technology State University, Dolgoprudny, Russia.
- ^zAlso at Section de Physique, Université de Genève, Geneva, Switzerland.
- ^{aa}Also at Department of Physics, The University of Texas at Austin, Austin, TX, USA.
- ^{bb}Also at Institute for Particle and Nuclear Physics, Wigner Research Centre for Physics, Budapest, Hungary.
- ^{cc}Also at International School for Advanced Studies (SISSA), Trieste, Italy.
- ^{dd}Also at Department of Physics and Astronomy, University of South Carolina, Columbia, SC, USA.
- ^{ee}Also at Faculty of Physics, M.V. Lomonosov Moscow State University, Moscow, Russia.
- ^{ff}Also at Physics Department, Brookhaven National Laboratory, Upton, NY, USA.
- ^{gg}Also at Moscow Engineering and Physics Institute (MEPhI), Moscow, Russia.
- ^{hh}Also at Department of Physics, Oxford University, Oxford, United Kingdom.
- ⁱⁱAlso at Department of Physics, Nanjing University, Jiangsu, China.
- ^{jj}Also at Institut für Experimentalphysik, Universität Hamburg, Hamburg, Germany.
- ^{kk}Also at Department of Physics, The University of Michigan, Ann Arbor, MI, USA.
- ^{ll}Also at Discipline of Physics, University of KwaZulu-Natal, Durban, South Africa.